5

OPTIMUM RECEIVERS FOR THE ADDITIVE WHITE GAUSSIAN NOISE CHANNEL

In Chapter 4, we described various types of modulation methods that may be used to transmit digital information through a communication channel. As we have observed, the modulator at the transmitter performs the function of mapping the digital sequence into signal waveforms.

This chapter deals with the design and performance characteristics of optimum receivers for the various modulation methods, when the channel corrupts the transmitted signal by the addition of gaussian noise. In Section 5-1, we first treat memoryless modulation signals, followed by modulation signals with memory. We evaluate the probability of error of the various modulation methods in Section 5-2. We treat the optimum receiver for CPM signals and its performance in Section 5-3. In Section 5-4, we derive the optimum receiver when the carrier phase of the signals is unknown at the receiver and is treated as a random variable. Finally, in Section 5-5, we consider the use of regenerative repeaters in signal transmission and carry out a link budget analysis for radio channels.

5-1 OPTIMUM RECEIVER FOR SIGNALS CORRUPTED BY ADDITIVE WHITE GAUSSIAN NOISE

Let us begin by developing a mathematical model for the signal at the input to the receiver. We assume that the transmitter sends digital information by use of M signal waveforms $\{s_m(t), m = 1, 2, \ldots, M\}$. Each waveform is transmitted within the symbol (signaling) interval of duration T. To be specific, we consider the transmission of information over the interval $0 \leq t \leq T$.

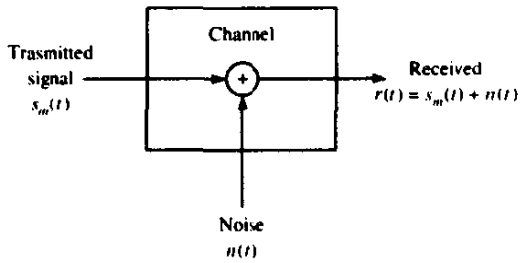

FIGURE 5-1-1 Model for received signal passed through an AWGN channel.

The channel is assumed to corrupt the signal by the addition of white gaussian noise, as illustrated in Fig. 5-1-1. Thus, the received signal in the interval $0 \leq t \leq T$ may be expressed as

$$r(t) = s_m(t) + n(t), \qquad 0 \leq t \leq T \tag{5-1-1}$$

where $n(t)$ denotes a sample function of the additive white gaussian noise (AWGN) process with power spectral density $\Phi_{nn}(f) = \frac{1}{2}N_0$ W/Hz. Based on the observation of $r(t)$ over the signal interval, we wish to design a receiver that is optimum in the sense that it minimizes the probability of making an error.

It is convenient to subdivide the receiver into two parts—the signal demodulator and the detector—as shown in Fig. 5-1-2. The function of the signal demodulator is to convert the received waveform $r(t)$ into an N-dimensional vector $\mathbf{r} = [r_1 \; r_2 \; \ldots \; r_N]$, where N is the dimension of the transmitted signal waveforms. The function of the detector is to decide which of the M possible signal waveforms was transmitted based of the vector $\mathbf{r}$.

Two realizations of the signal demodulator are described in the next two sections. One is based on the use of signal correlators. The second is based on the use of matched filters. The optimum detector that follows the signal demodulator is designed to minimize the probability of error.

5-1-1 Correlation Demodulator

In this section, we describe a correlation demodulator that decomposes the received signal and the noise into N-dimensional vectors. In other words, the signal and the noise are expanded into a series of linearly weighted orthonormal basis functions $\{f_n(t)\}$. It is assumed that the N basis functions $\{f_n(t)\}$ span the signal space, so that every one of the possible transmitted

FIGURE 5-1-2 Receiver configuration.

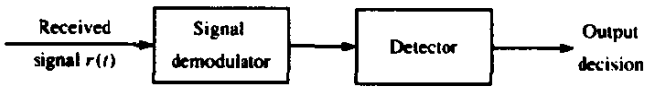

signals of the set $\{s_m(t), 1 \leq m \leq M\}$ can be represented as a weighted linear combination of $\{f_n(t)\}$. In the case of the noise, the functions $\{f_n(t)\}$ do not span the noise space. However, we show below that the noise terms that fall outside the signal space are irrelevant to the detection of the signal.

Suppose the received signal $r(t)$ is passed through a parallel bank of N crosscorrelators which basically compute the projection of $r(t)$ onto the N basis functions $\{f_n(t)\}$, as illustrated in Fig. 5-1-3. Thus, we have

$$\int_0^T r(t)f_k(t)\,dt = \int_0^T [s_m(t) + n(t)]f_k(t)\,dt$$
$$r_k = s_{mk} + n_k, \qquad k = 1, 2, \ldots, N \tag{5-1-2}$$

where

$$s_{mk} = \int_0^T s_m(t)f_k(t)\,dt, \qquad k = 1, 2, \ldots, N$$
$$n_k = \int_0^T n(t)f_k(t)\,dt, \qquad k = 1, 2, \ldots, N \tag{5-1-3}$$

The signal is now represented by the vector $\mathbf{s}_m$ with components s_{mk}, $k = 1, 2, \ldots, N$. Their values depend on which of the M signals was transmitted. The components $\{n_k\}$ are random variables that arise from the presence of the additive noise.

In fact, we can express the received signal $r(t)$ in the interval $0 \leq t \leq T$ as

$$r(t) = \sum_{k=1}^{N} s_{mk}f_k(t) + \sum_{k=1}^{N} n_k f_k(t) + n'(t)$$
$$= \sum_{k=1}^{N} r_k f_k(t) + n'(t) \tag{5-1-4}$$

The term $n'(t)$, defined as

$$n'(t) = n(t) - \sum_{k=1}^{N} n_k f_k(t) \tag{5-1-5}$$

is a zero-mean gaussian noise process that represents the difference between the original noise process $n(t)$ and the part corresponding to the projection of $n(t)$ onto the basis functions $\{f_k(t)\}$. We shall show below that $n'(t)$ is irrelevant to the decision as to which signal was transmitted. Consequently, the decision may be based entirely on the correlator output signal and noise components $r_k = s_{mk} + n_k$, $k = 1, 2, \ldots, N$.

Since the signals $\{s_m(t)\}$ are deterministic, the signal components are deterministic. The noise components $\{n_k\}$ are gaussian. Their mean values are

$$E(n_k) = \int_0^T E[n(t)]f_k(t)\,dt = 0 \tag{5-1-6}$$

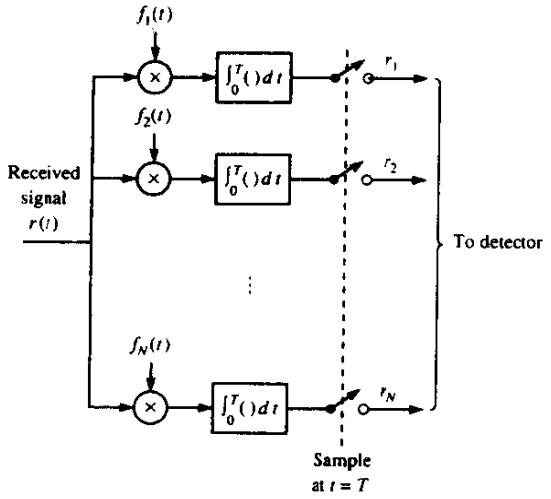

FIGURE 5-1-3 Correlation-type demodulator.

for all n. Their covariances are

$$\begin{aligned} E(n_k n_m) &= \int_0^T \int_0^T E[n(t)n(\tau)]f_k(t)f_m(\tau)\,dt\,d\tau \\ &= \tfrac{1}{2}N_0 \int_0^T \int_0^T \delta(t-\tau)f_k(t)f_m(\tau)\,dt\,d\tau \\ &= \tfrac{1}{2}N_0 \int_0^T f_k(t)f_m(t)\,dt \\ &= \tfrac{1}{2}N_0\delta_{mk} \end{aligned} \tag{5-1-7}$$

where $\delta_{mk} = 1$ when $m = k$ and zero otherwise. Therefore, the N noise components $\{n_k\}$ are zero-mean uncorrelated gaussian random variables with a common variance $\sigma_n^2 = \frac{1}{2}N_0$.

From the above development, it follows that the correlator outputs $\{r_k\}$ conditioned on the mth signal being transmitted are gaussian random variables with mean

$$E(r_k) = E(s_{mk} + n_k) = s_{mk} \tag{5-1-8}$$

and equal variance

$$\sigma_r^2 = \sigma_n^2 = \tfrac{1}{2}N_0 \tag{5-1-9}$$

Since the noise components $\{n_k\}$ are uncorrelated gaussian random variables, they are also statistically independent. As a consequence, the correlator outputs $\{r_k\}$ conditioned on the mth signal being transmitted are statistically independent gaussian variables. Hence, the conditional probability density functions of the random variables $[r_1\ r_2\ \cdots\ r_N] = \mathbf{r}$ are simply

$$p(\mathbf{r} \mid \mathbf{s}_m) = \prod_{k=1}^{N} p(r_k \mid s_{mk}), \qquad m = 1, 2, \ldots, M \tag{5-1-10}$$

where

$$p(r_k \mid s_{mk}) = \frac{1}{\sqrt{\pi N_0}} \exp\left[-\frac{(r_k - s_{mk})^2}{N_0} \right], \quad k = 1, 2, \ldots, N \qquad (5\text{-}1\text{-}11)$$

By substituting (5-1-11) into (5-1-10), we obtain the joint conditional pdfs

$$p(\mathbf{r} \mid \mathbf{s}_m) = \frac{1}{(\pi N_0)^{N/2}} \exp\left[-\sum_{k=1}^{N} \frac{(r_k - s_{mk})^2}{N_0} \right], \quad m = 1, 2, \ldots, M \qquad (5\text{-}1\text{-}12)$$

As a final point we wish to show that the correlator outputs $(r_1, r_2, \ldots, r_N)$ are *sufficient statistics* for reaching a decision on which of the M signals was transmitted, i.e., that no additional relevant information can be extracted from the remaining noise process $n'(t)$. Indeed, $n'(t)$ is uncorrelated with the N correlator outputs $\{r_k\}$, i.e.,

$$\begin{aligned} E[n'(t)r_k] &= E[n'(t)]s_{mk} + E[n'(t)n_k] \\ &= E[n'(t)n_k] \\ &= E\left\{ \left[n(t) - \sum_{j=1}^{N} n_j f_j(t) \right] n_k \right\} \\ &= \int_0^T E[n(t)n(\tau)] f_k(\tau)\, d\tau - \sum_{j=1}^{N} E(n_j n_k) f_j(t) \\ &= \tfrac{1}{2} N_0 f_k(t) - \tfrac{1}{2} N_0 f_k(t) = 0 \end{aligned} \qquad (5\text{-}1\text{-}13)$$

Since $n'(t)$ and $\{r_k\}$ are gaussian and uncorrelated, they are also statistically independent. Consequently, $n'(t)$ does not contain any information that is relevant to the decision as to which signal waveform was transmitted. All the relevant information is contained in the correlator outputs $\{r_k\}$. Hence, $n'(t)$ may be ignored.

Example 5-1-1

Consider an M-ary baseband PAM signal set in which the basic pulse shape $g(t)$ is rectangular as shown in Fig. 5-1-4. The additive noise is a zero-mean white gaussian noise process. Let us determine the basis function $f(t)$ and the output of the correlation-type demodulator. The energy in the rectangular pulse is

$$\mathcal{E}_g = \int_0^T g^2(t)\, dt = \int_0^T a^2\, dt = a^2 T$$

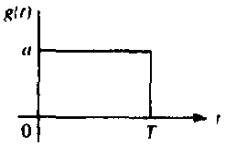

FIGURE 5-1-4 Signal pulse for Example 5-1-1.

Since the PAM signal set has dimension $N = 1$, there is only one basis function $f(t)$. This is given as

$$f(t) = \frac{1}{\sqrt{a^2 T}} g(t)$$

$$= \begin{cases} 1/\sqrt{T} & (0 \leq t \leq T) \\ 0 & \text{(otherwise)} \end{cases}$$

The output of the correlation-type demodulator is

$$r = \int_0^T r(t) f(t)\, dt = \frac{1}{\sqrt{T}} \int_0^T r(t)\, dt$$

It is interesting to note that the correlator becomes a simple integrator when $f(t)$ is rectangular. If we substitute for $r(t)$, we obtain

$$r = \frac{1}{\sqrt{T}} \left\{ \int_0^T [s_m(t) + n(t)] \right\} dt$$

$$= \frac{1}{\sqrt{T}} \left[\int_0^T s_m(t)\, dt + \int_0^T n(t)\, dt \right]$$

$$r = s_m + n$$

where the noise term $E(n) = 0$ and

$$\sigma_n^2 = E\left[\frac{1}{T} \int_0^T \int_0^T n(t) n(\tau)\, dt\, d\tau \right]$$

$$= \frac{1}{T} \int_0^T \int_0^T E[n(t) n(\tau)]\, dt\, d\tau$$

$$= \frac{N_0}{2T} \int_0^T \int_0^T \delta(t - \tau)\, dt\, d\tau = \tfrac{1}{2} N_0$$

The probability density function for the sampled output is

$$p(r \mid s_m) = \frac{1}{\sqrt{\pi N_0}} \exp\left[-\frac{(r - s_m)^2}{N_0} \right]$$

5-1-2 Matched-Filter Demodulator

Instead of using a bank of N correlators to generate the variables $\{r_k\}$, we may use a bank of N linear filters. To be specific, let us suppose that the impulse responses of the N filters are

$$h_k(t) = f_k(T - t), \quad 0 \leq t \leq T \tag{5-1-14}$$

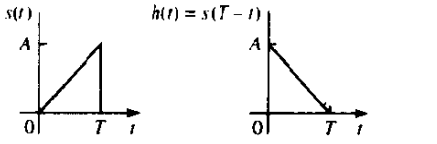

(a) Signal $s(t)$ (b) Impulse response of filter matched to $s(t)$

FIGURE 5-1-5 Signal $s(t)$ and filter matched to $s(t)$.

where $\{f_k(t)\}$ are the N basis functions and $h_k(t) = 0$ outside of the interval $0 \leq t \leq T$. The outputs of these filters are

$$y_k(t) = \int_0^t r(\tau)h_k(t-\tau)\,d\tau$$

$$= \int_0^t r(\tau)f_k(T-t+\tau)\,d\tau, \qquad k = 1, 2, \ldots, N \tag{5-1-15}$$

Now, if we sample the outputs of the filters at $t = T$, we obtain

$$y_k(T) = \int_0^T r(\tau)f_k(\tau)\,d\tau = r_k, \qquad k = 1, 2, \ldots, N \tag{5-1-16}$$

Hence, the sampled outputs of the filters at time $t = T$ are exactly the set of values $\{r_k\}$ obtained from the N linear correlators.

A filter whose impulse response $h(t) = s(T-t)$, where $s(t)$ is assumed to be confined to the time interval $0 \leq t \leq T$, is called the *matched filter* to the signal $s(t)$. An example of a signal and its matched filter are shown in Fig. 5-1-5. The response of $h(t) = s(T-t)$ to the signal $s(t)$ is

$$y(t) = \int_0^t s(\tau)s(T-t+\tau)\,d\tau \tag{5-1-17}$$

which is basically the time-autocorrelation function of the signal $s(t)$. Figure 5-1-6 illustrates $y(t)$ for the triangular signal pulse shown in Fig. 5-1-5. Note that the autocorrelation function $y(t)$ is an even function of t, which attains a peak at $t = T$.

In the case of the demodulator described above, the N matched filters are

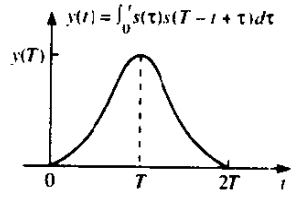

FIGURE 5-1-6 The matched filter output is the autocorrelation function of $s(t)$.

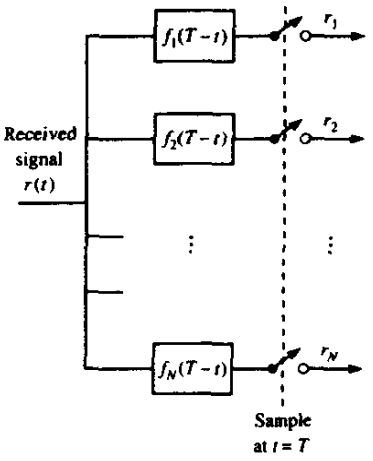

FIGURE 5-1-7 Matched filter demodulator.

matched to the basis functions $\{f_k(t)\}$. Figure 5-1-7 illustrates the matched filter demodulator that generates the observed variables $\{r_k\}$.

Properties of the Matched Filter A matched filter has some interesting properties. Let us prove the most important property, which may be stated as follows: If a signal $s(t)$ is corrupted by AWGN, the filter with impulse response matched to $s(t)$ maximizes the output signal-to-noise ratio (SNR).

To prove this property, let us assume that the received signal $r(t)$ consists of the signal $s(t)$ and AWGN $n(t)$ which has zero-mean and power spectral density $\Phi_{nn}(f) = \frac{1}{2}N_0$ W/Hz. Suppose the signal $r(t)$ is passed through a filter with impulse response $h(t)$, $0 \leq t \leq T$, and its output is sampled at time $t = T$. The filter response to the signal and noise components is

$$\begin{aligned} y(t) &= \int_0^t r(\tau)h(t-\tau)\,d\tau \\ &= \int_0^t s(\tau)h(t-\tau)\,d\tau + \int_0^t n(\tau)h(t-\tau)\,d\tau \end{aligned} \tag{5-1-18}$$

At the sampling instant $t = T$, the signal and noise components are

$$\begin{aligned} y(T) &= \int_0^T s(\tau)h(T-\tau)\,d\tau + \int_0^T n(\tau)h(t-\tau)\,d\tau \\ &= y_s(T) + y_n(T) \end{aligned} \tag{5-1-19}$$

where $y_s(T)$ represents the signal component and $y_n(T)$ the noise component. The problem is to select the filter impulse response that maximizes the output signal-to-noise ratio (SNR_0) defined as

$$\text{SNR}_0 = \frac{y_s^2(T)}{E[y_n^2(T)]} \tag{5-1-20}$$

The denominator in (5-1-20) is simply the variance of the noise term at the output of the filter. Let us evaluate $E[y_n^2(T)]$. We have

$$\begin{aligned} E[y_n^2(T)] &= \int_0^T \int_0^T E[n(\tau)n(t)]h(T-\tau)h(T-t)\,dt\,d\tau \\ &= \tfrac{1}{2}N_0 \int_0^T \int_0^T \delta(t-\tau)h(T-\tau)h(T-t)\,dt\,d\tau \\ &= \tfrac{1}{2}N_0 \int_0^T h^2(T-t)\,dt \end{aligned} \tag{5-1-21}$$

Note that the variance depends on the power spectral density of the noise and the energy in the impulse response $h(t)$.

By substituting for $y_s(T)$ and $E[y_n^2(T)]$ into (5-1-20), we obtain the expression for the output SNR as

$$\text{SNR}_0 = \frac{[\int_0^T s(\tau)h(T-\tau)\,d\tau]^2}{\frac{1}{2}N_0 \int_0^T h^2(T-t)\,dt} = \frac{[\int_0^T h(\tau)s(T-\tau)\,d\tau]^2}{\frac{1}{2}N_0 \int_0^T h^2(T-t)\,dt} \tag{5-1-22}$$

Since the denominator of the SNR depends on the energy in $h(t)$, the maximum output SNR over $h(t)$ is obtained by maximizing the numerator subject to the constraint that the demoninator is held constant. The maximization of the numerator is most easily performed by use of the Cauchy–Schwarz inequality, which states, in general, that if $g_1(t)$ and $g_2(t)$ are finite-energy signals then

$$\left[\int_{-\infty}^{\infty} g_1(t)g_2(t)\,dt\right]^2 \leq \int_{-\infty}^{\infty} g_1^2(t)\,dt \int_{-\infty}^{\infty} g_2^2(t)\,dt \tag{5-1-23}$$

with equality when $g_1(t) = Cg_2(t)$ for any arbitrary constant C. If we set $g_1(t) = h(t)$ and $g_2(t) = s(T-t)$, it is clear that the SNR is maximized when $h(t) = Cs(T-t)$, i.e., $h(t)$ is matched to the signal $s(t)$. The scale factor C^2 drops out of the expression for the SNR, since it appears in both the numerator and the denominator.

The output (maximum) SNR obtained with the matched filter is

$$\begin{aligned} \text{SNR}_0 &= \frac{2}{N_0}\int_0^T s^2(t)\,dt \\ &= 2\mathscr{E}/N_0 \end{aligned} \tag{5-1-24}$$

Note that the output SNR from the matched filter depends on the energy of the waveform $s(t)$ but not on the detailed characteristics of $s(t)$. This is another interesting property of the matched filter.

Frequency-Domain Interpretation of the Matched Filter The matched filter has an interesting frequency-domain interpretation. Since $h(t) = s(T-t)$,

the Fourier transform of this relationship is

$$\begin{aligned} H(f) &= \int_0^T s(T-t)e^{-j2\pi ft}\,dt \\ &= \left[\int_0^T s(\tau)e^{j2\pi f\tau}\,d\tau\right]e^{-j2\pi fT} \\ &= S^*(f)e^{-j2\pi fT} \end{aligned} \tag{5-1-25}$$

We observe that the matched filter has a frequency response that is the complex conjugate of the transmitted signal spectrum multiplied by the phase factor $e^{-j2\pi fT}$, which represents the sampling delay of T. In other words, $|H(f)| = |S(f)|$, so that the magnitude response of the matched filter is identical to the transmitted signal spectrum. On the other hand, the phase of $H(f)$ is the negative of the phase of $S(f)$.

Now, if the signal $s(t)$ with spectrum $S(f)$ is passed through the matched filter, the filter output has a spectrum $Y(f) = |S(f)|^2 e^{-j2\pi fT}$. Hence, the output waveform is

$$\begin{aligned} y_s(t) &= \int_{-\infty}^{\infty} Y(f)e^{j2\pi ft}\,df \\ &= \int_{-\infty}^{\infty} |S(f)|^2 e^{-j2\pi fT}e^{j2\pi ft}\,df \end{aligned} \tag{5-1-26}$$

By sampling the output of the matched filter at $t = T$, we obtain

$$y_s(T) = \int_{-\infty}^{\infty} |S(f)|^2\,df = \int_0^T s^2(t)\,dt = \mathscr{E} \tag{5-1-27}$$

where the last step follows from Parseval's relation.

The noise at the output of the matched filter has a power spectral density

$$\Phi_0(f) = \tfrac{1}{2}|H(f)|^2 N_0 \tag{5-1-28}$$

Hence, the total noise power at the output of the matched filter is

$$\begin{aligned} P_n &= \int_{-\infty}^{\infty} \Phi_0(f)\,df \\ &= \tfrac{1}{2}N_0 \int_{-\infty}^{\infty} |H(f)|^2\,df = \tfrac{1}{2}N_0 \int_{-\infty}^{\infty} |S(f)|^2\,df = \tfrac{1}{2}\mathscr{E}N_0 \end{aligned} \tag{5-1-29}$$

The output SNR is simply the ratio of the signal power P_s, given by

$$P_s = y_s^2(T) \tag{5-1-30}$$

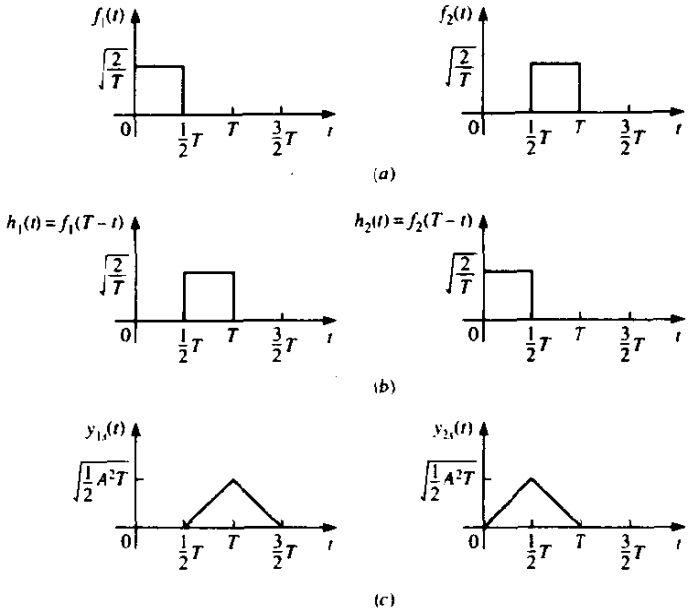

FIGURE 5-1-8 Basis functions and matched filter responses for Example 5-1-2.

to the noise power P_n. Hence,

$$\text{SNR}_0 = \frac{P_s}{P_n} = \frac{\mathscr{E}^2}{\frac{1}{2}\mathscr{E}N_0} = \frac{2\mathscr{E}}{N_0} \tag{5-1-31}$$

which agrees with the result given by (5-1-24).

Example 5-1-2

Consider the $M = 4$ biorthogonal signals shown in Fig. 5-1-8 for transmitting information over an AWGN channel. The noise is assumed to have zero mean and power spectral density $\frac{1}{2}N_0$. Let us determine the basis functions for this signal set, the impulse responses of the matched-filter demodulators, and the output waveforms of the matched-filter demodulators when the transmitted signal is $s_1(t)$.

The $M = 4$ biorthogonal signals have dimension $N = 2$. Hence, two basis functions are needed to represent the signals. From Fig. 5-1-8, we choose $f_1(t)$ and $f_2(t)$ as

$$\begin{aligned} f_1(t) &= \begin{cases} \sqrt{2/T} & (0 \leq t \leq \frac{1}{2}T) \\ 0 & \text{(otherwise)} \end{cases} \\ f_2(t) &= \begin{cases} \sqrt{2/T} & (\frac{1}{2}T \leq t \leq T) \\ 0 & \text{(otherwise)} \end{cases} \end{aligned} \tag{5-1-32}$$

These waveforms are illustrated in Fig. 5-1-8(a). The impulse responses of the two matched filters are

$$h_1(t) = f_1(T-t) = \begin{cases} \sqrt{2/T} & (\tfrac{1}{2}T \le t \le T) \\ 0 & \text{(otherwise)} \end{cases}$$
$$h_2(t) = f_2(T-t) = \begin{cases} \sqrt{2/T} & (0 \le t \le \tfrac{1}{2}T) \\ 0 & \text{(otherwise)} \end{cases} \tag{5-1-33}$$

and are illustrated in Fig. 5-1-8(b).

If $s_1(t)$ is transmitted, the (noise-free) responses of the two matched filters are as shown in Fig. 5-1-8(c). Since $y_1(t)$ and $y_2(t)$ are sampled at $t = T$, we observe that $y_{1s}(T) = \sqrt{\frac{1}{2}A^2T}$ and $y_{2s}(T) = 0$. Note that $\frac{1}{2}A^2T = \mathscr{E}$, the signal energy. Hence, the received vector formed from the two matched filter outputs at the sampling instant $t = T$ is

$$\mathbf{r} = [r_1 \quad r_2] = [\sqrt{\mathscr{E}} + n_1 \quad n_2] \tag{5-1-34}$$

where $n_1 = y_{1n}(T)$ and $n_2 = y_{2n}(T)$ are the noise components at the outputs of the matched filters, given by

$$y_{kn}(T) = \int_0^T n(t) f_k(t)\, dt, \qquad k = 1, 2 \tag{5-1-35}$$

Clearly, $E(n_k) = E[y_{kn}(T)] = 0$. Their variance is

$$\begin{aligned} \sigma_n^2 = E[y_{kn}^2(T)] &= \int_0^T \int_0^T E[n(t)n(\tau)] f_k(t) f_k(\tau)\, dt\, d\tau \\ &= \tfrac{1}{2}N_0 \int_0^T \int_0^T \delta(t-\tau) f_k(\tau) f_k(t)\, dt\, d\tau \\ &= \tfrac{1}{2}N_0 \int_0^T f_k^2(t)\, dt = \tfrac{1}{2}N_0 \end{aligned} \tag{5-1-36}$$

Observe that the SNR_0 for the first matched filter is

$$\text{SNR}_0 = \frac{(\sqrt{\mathscr{E}})^2}{\frac{1}{2}N_0} = \frac{2\mathscr{E}}{N_0} \tag{5-1-37}$$

which agrees with our previous result. Also note that the four possible outputs of the two matched filters, corresponding to the four possible transmitted signals in Fig. 5-1-8 are $(r_1, r_2) = (\sqrt{\mathscr{E}} + n_1, n_2)$, $(n_1, \sqrt{\mathscr{E}} + n_2)$, $(-\sqrt{\mathscr{E}} + n_1, n_2)$ and $(n_1, -\sqrt{\mathscr{E}} + n_2)$.

5-1-3 The Optimum Detector

We have demonstrated that, for a signal transmitted over an AWGN channel, either a correlation demodulator or a matched filter demodulator produces the vector $\mathbf{r} = [r_1 \; r_2 \; \cdots \; r_N]$, which contains all the relevant information in the received signal waveform. In this section, we describe the optimum decision

rule based on the observation vector $\mathbf{r}$. For this development, we assume that there is no memory in signals transmitted in successive signal intervals.

We wish to design a signal detector that makes a decision on the transmitted signal in each signal interval based on the observation of the vector $\mathbf{r}$ in each interval such that the probability of a correct decision is maximized. With this goal in mind, we consider a decision rule based on the computation of the *posterior probabilities* defined as

$$P(\text{signal } \mathbf{s}_m \text{ was transmitted} \mid \mathbf{r}), \quad m = 1, 2, \ldots, M$$

which we abbreviate as $P(\mathbf{s}_m \mid \mathbf{r})$. The decision criterion is based on selecting the signal corresponding to the maximum of the set of posterior probabilities $\{P(\mathbf{s}_m \mid \mathbf{r})\}$. Later, we show that this criterion maximizes the probability of a correct decision and, hence, minimizes the probability of error. This decision criterion is called the *maximum a posteriori probability* (MAP) criterion.

Using Bayes' rule, the posterior probabilities may be expressed as

$$P(\mathbf{s}_m \mid \mathbf{r}) = \frac{p(\mathbf{r} \mid \mathbf{s}_m)P(\mathbf{s}_m)}{p(\mathbf{r})} \tag{5-1-38}$$

where $p(\mathbf{r} \mid \mathbf{s}_m)$ is the conditional pdf of the observed vector given $\mathbf{s}_m$, and $P(\mathbf{s}_m)$ is the *a priori probability* of the mth signal being transmitted. The denominator of (5-1-38) may be expressed as

$$p(\mathbf{r}) = \sum_{m=1}^{M} p(\mathbf{r} \mid \mathbf{s}_m)P(\mathbf{s}_m) \tag{5-1-39}$$

From (5-1-38) and (5-1-39), we observe that the computation of the posterior probabilities $P(\mathbf{s}_m \mid \mathbf{r})$ requires knowledge of the *a priori probabilities* $P(\mathbf{s}_m)$ and the conditional pdfs $p(\mathbf{r} \mid \mathbf{s}_m)$ for $m = 1, 2, \ldots, M$.

Some simplification occurs in the MAP criterion when the M signals are equally probable a priori, i.e., $P(\mathbf{s}_m) = 1/M$ for all M. Furthermore, we note that the denominator in (5-1-38) is independent of which signal is transmitted. Consequently, the decision rule based on finding the signal that maximizes $P(\mathbf{s}_m \mid \mathbf{r})$ is equivalent to finding the signal that maximizes $p(\mathbf{r} \mid \mathbf{s}_m)$.

The conditional pdf $p(\mathbf{r} \mid \mathbf{s}_m)$ or any monotonic function of it is usually called the *likelihood function*. The decision criterion based on the maximum of $p(\mathbf{r} \mid \mathbf{s}_m)$ over the M signals is called the *maximum-likelihood* (ML) *criterion*. We observe that a detector based on the MAP criterion and one that is based on the ML criterion make the same decisions as long as the a priori probabilities $P(\mathbf{s}_m)$ are all equal, i.e., the signals $\{\mathbf{s}_m\}$ are equiprobable.

In the case of an AWGN channel, the likelihood function $p(\mathbf{r} \mid \mathbf{s}_m)$ is given by (5-1-12). To simplify the computations, we may work with the natural logarithm of $p(\mathbf{r} \mid \mathbf{s}_m)$, which is a monotonic function. Thus,

$$\ln p(\mathbf{r} \mid \mathbf{s}_m) = -\tfrac{1}{2}N \ln (\pi N_0) - \frac{1}{N_0} \sum_{k=1}^{N} (r_k - s_{mk})^2 \tag{5-1-40}$$

The maximum of $\ln p(\mathbf{r} \mid \mathbf{s}_m)$ over $\mathbf{s}_m$ is equivalent to finding the signal $\mathbf{s}_m$ that minimizes the Euclidean distance

$$D(\mathbf{r}, \mathbf{s}_m) = \sum_{k=1}^{N} (r_k - s_{mk})^2 \tag{5-1-41}$$

We call $D(\mathbf{r}, \mathbf{s}_m)$, $m = 1, 2, \ldots, M$, the *distance metrics*. Hence, for the AWGN channel, the decision rule based on the ML criterion reduces to finding the signal $\mathbf{s}_m$ that is closest in distance to the received signal vector $\mathbf{r}$. We shall refer to this decision rule as *minimum distance detection*.

Another interpretation of the optimum decision rule based on the ML criterion is obtained by expanding the distance metrics in (5-1-41) as

$$\begin{aligned} D(\mathbf{r}, \mathbf{s}_m) &= \sum_{n=1}^{N} r_n^2 - 2 \sum_{n=1}^{N} r_n s_{mn} + \sum_{n=1}^{N} s_{mn}^2 \\ &= |\mathbf{r}|^2 - 2\mathbf{r} \cdot \mathbf{s}_m + |\mathbf{s}_m|^2, \qquad m = 1, 2, \ldots, M \end{aligned} \tag{5-1-42}$$

The term $|\mathbf{r}|^2$ is common to all decision metrics, and, hence, it may be ignored in the computations of the metrics. The result is a set of modified distance metrics

$$D'(\mathbf{r}, \mathbf{s}_m) = -2\mathbf{r} \cdot \mathbf{s}_m + |\mathbf{s}_m|^2 \tag{5-1-43}$$

Note that selecting the signal $\mathbf{s}_m$ that minimizes $D'(\mathbf{r}, \mathbf{s}_m)$ is equivalent to selecting the signal that maximizes the metric $C(\mathbf{r}, \mathbf{s}_m) = -D'(\mathbf{r}, \mathbf{s}_m)$, i.e.,

$$C(\mathbf{r}, \mathbf{s}_m) = 2\mathbf{r} \cdot \mathbf{s}_m - |\mathbf{s}_m|^2 \tag{5-1-44}$$

The term $\mathbf{r} \cdot \mathbf{s}_m$ represents the projection of the received signal vector onto each of the M possible transmitted signal vectors. The value of each of these projections is a measure of the correlation between the received vector and the mth signal. For this reason, we call $C(\mathbf{r}, \mathbf{s}_m)$, $m = 1, 2, \ldots, M$, the *correlation metrics* for deciding which of the M signals was transmitted. Finally, the terms $|\mathbf{s}_m|^2 = \mathcal{E}_m$, $m = 1, 2, \ldots, M$, may be viewed as bias terms that serve as compensation for signal sets that have unequal energies, such as PAM. If all signals have the same energy, $|\mathbf{s}_m|^2$ may also be ignored in the computation of the correlation metrics $C(\mathbf{r}, \mathbf{s}_m)$ and the distance metrics $D(\mathbf{r}, \mathbf{s}_m)$ or $D'(\mathbf{r}, \mathbf{s}_m)$.

It is easy to show (see Problem 5-5) that the correlation metrics $C(\mathbf{r}, \mathbf{s}_m)$ can also be expressed as

$$C(\mathbf{r}, \mathbf{s}_m) = 2 \int_0^T r(t) s_m(t)\, dt - \mathcal{E}_m, \qquad m = 0, 1, \ldots, M \tag{5-1-45}$$

Therefore, these metrics can be generated by a demodulator that cross-correlates the received signal $r(t)$ with each of the M possible transmitted signals and adjusts each correlator output for the bias in the case of unequal signal energies. Equivalently, the received signal may be passed through a bank of M filters matched to the possible transmitted signals $\{s_m(t)\}$ and

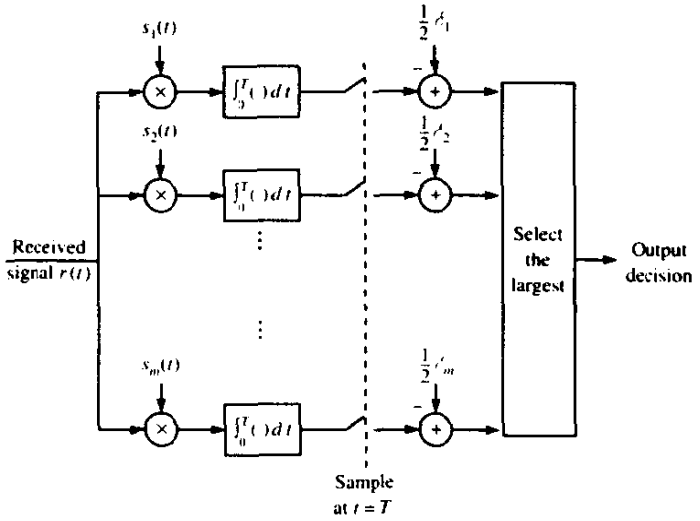

FIGURE 5-1-9 An alternative realization of the optimum AWGN receiver.

sampled at $t = T$, the end of the symbol interval. Consequently, the optimum receiver (demodulator and detector) can be implemented in the alternative configuration illustrated in Fig. 5-1-9.

In summary, we have demonstrated that the optimum ML detector computes a set of M distances $D(\mathbf{r}, \mathbf{s}_m)$ or $D'(\mathbf{r}, \mathbf{s}_m)$ and selects the signal corresponding to the smallest (distance) metric. Equivalently, the optimum ML detector computes a set of M correlation metrics $C(\mathbf{r}, \mathbf{s}_m)$ and selects the signal corresponding to the largest correlation metric.

The above development for the optimum detector treated the important case in which all signals are equally probable. In this case, the MAP criterion is equivalent to the ML criterion. However, when the signals are not equally probable, the optimum MAP detector bases its decision on the probabilities $P(\mathbf{s}_m \mid \mathbf{r})$, $m = 1, 2, \ldots, M$, given by (5-1-38) or, equivalently, on the *metrics*,

$$PM(\mathbf{r}, \mathbf{s}_m) = p(\mathbf{r} \mid \mathbf{s}_m)P(\mathbf{s}_m)$$

The following example illustrates this computation for binary PAM signals.

Example 5-1-3

Consider the case of binary PAM signals in which the two possible signal points are $s_1 = -s_2 = \sqrt{\mathscr{E}_b}$, where $\mathscr{E}_b$ is the energy per bit. The prior probabilities are $P(s_1) = p$ and $P(s_2) = 1 - p$. Let us determine the metrics for the optimum MAP detector when the transmitted signal is corrupted with AWGN.

The received signal vector (one-dimensional) for binary PAM is

$$r = \pm\sqrt{\mathscr{E}_b} + y_n(T) \tag{5-1-46}$$

where $y_n(T)$ is a zero-mean Gaussian random variable with variance $\sigma_n^2 = \frac{1}{2}N_0$. Consequently, the conditional pdfs $p(r \mid s_m)$ for the two signals are

$$p(r \mid s_1) = \frac{1}{\sqrt{2\pi}\,\sigma_n} \exp\left[-\frac{(r - \sqrt{\mathscr{E}_b})^2}{2\sigma_n^2}\right] \tag{5-1-47}$$

$$p(r \mid s_2) = \frac{1}{\sqrt{2\pi}\,\sigma_n} \exp\left[-\frac{(r + \sqrt{\mathscr{E}_b})^2}{2\sigma_n^2}\right] \tag{5-1-48}$$

Then the metrics $PM(\mathbf{r}, \mathbf{s}_1)$ and $PM(\mathbf{r}, \mathbf{s}_2)$ are

$$\begin{aligned} PM(\mathbf{r}, \mathbf{s}_1) &= pp(r \mid s_1) \\ &= \frac{p}{\sqrt{2\pi}\,\sigma_n} \exp\left[-\frac{(r - \sqrt{\mathscr{E}_b})^2}{2\sigma_n^2}\right] \end{aligned} \tag{5-1-49}$$

$$PM(\mathbf{r}, \mathbf{s}_2) = \frac{1-p}{\sqrt{2\pi}\,\sigma_n} \exp\left[-\frac{(r + \sqrt{\mathscr{E}_b})^2}{2\sigma_n^2}\right] \tag{5-1-50}$$

If $PM(\mathbf{r}, \mathbf{s}_1) > PM(\mathbf{r}, \mathbf{s}_2)$, we select s_1 as the transmitted signal; otherwise, we select s_2. This decision rule may be expressed as

$$\frac{PM(\mathbf{r}, \mathbf{s}_1)}{PM(\mathbf{r}, \mathbf{s}_2)} \underset{s_2}{\overset{s_1}{\gtrless}} 1 \tag{5-1-51}$$

But

$$\frac{PM(\mathbf{r}, \mathbf{s}_1)}{PM(\mathbf{r}, \mathbf{s}_2)} = \frac{p}{1-p} \exp\left[\frac{(r + \sqrt{\mathscr{E}_b})^2 - (r - \sqrt{\mathscr{E}_b})^2}{2\sigma_n^2}\right] \tag{5-1-52}$$

so that (5-1-51) may be expressed as

$$\frac{(r + \sqrt{\mathscr{E}_b})^2 - (r - \sqrt{\mathscr{E}_b})^2}{2\sigma_n^2} \underset{s_2}{\overset{s_1}{\gtrless}} \ln \frac{1-p}{p} \tag{5-1-53}$$

or equivalently,

$$\sqrt{\mathscr{E}_b}\, r \underset{s_2}{\overset{s_1}{\gtrless}} \tfrac{1}{2}\sigma_n^2 \ln \frac{1-p}{p} = \tfrac{1}{4}N_0 \ln \frac{1-p}{p} \tag{5-1-54}$$

This is the final form for the optimum detector. It computes the correlation metric $C(\mathbf{r}, \mathbf{s}_1) = r\sqrt{\mathscr{E}_b}$ and compares it with threshold $\frac{1}{4}N_0 \ln[(1-p)/p]$. Figure 5-1-10 illustrates the two signal points s_1 and s_2. The threshold, denoted by τ_h, divides the real line into two regions, say R_1 and R_2, where R_1 consists of the set of points that are greater than τ_h and

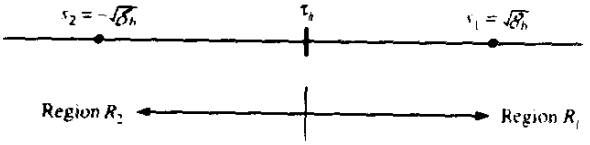

FIGURE 5-1-10 Signal space representation illustrating the operation of the optimum detector for binary (PAM) modulation.

R_2 consists of the set of points that are less than τ_h. If $r\sqrt{\mathscr{E}_b} > \tau_h$, the decision is made that s_1 was transmitted, and if $r\sqrt{\mathscr{E}_b} < \tau_h$, the decision is made that s_2 was transmitted. The threshold τ_h depends on N_0 and p. If $p = \frac{1}{2}$, $\tau_h = 0$. If $p > \frac{1}{2}$, the signal point s_1 is more probable and, hence, $\tau_h < 0$. In this case, the region R_1 is larger than R_2, so that s_1 is more likely to be selected than s_2. If $p < \frac{1}{2}$, the opposite is the case. Thus, the average probability of error is minimized.

It is interesting to note that in the case of unequal prior probabilities, it is necessary to know not only the values of the prior probabilities but also the value of the power spectral density N_0 in order to compute the threshold. When $p = \frac{1}{2}$, the threshold is zero, and knowledge of N_0 is not required by the detector.

We conclude this section with the proof that the decision rule based on the maximum-likelihood criterion minimizes the probability of error when the M signals are equally probable a priori. Let us denote by R_m the region in the N-dimensional space for which we decide that signal $s_m(t)$ was transmitted when the vector $\mathbf{r} = [r_1 \; r_2 \; \cdots \; r_N]$ is received. The probability of a decision error given that $s_m(t)$ was transmitted is

$$P(e \mid \mathbf{s}_m) = \int_{R_m^c} p(\mathbf{r} \mid \mathbf{s}_m)\, d\mathbf{r} \tag{5-1-55}$$

where R_m^c is the complement of R_m. The average probability of error is

$$\begin{aligned} P(e) &= \sum_{m=1}^{M} \frac{1}{M} P(e \mid \mathbf{s}_m) \\ &= \sum_{m=1}^{M} \frac{1}{M} \int_{R_m^c} p(\mathbf{r} \mid \mathbf{s}_m)\, d\mathbf{r} \\ &= \sum_{m=1}^{M} \frac{1}{M} \left[1 - \int_{R_m} p(\mathbf{r} \mid \mathbf{s}_m)\, d\mathbf{r} \right] \end{aligned} \tag{5-1-56}$$

Note that $P(e)$ is minimized by selecting the signal $\mathbf{s}_m$ if $p(\mathbf{r} \mid \mathbf{s}_m)$ is larger than $p(\mathbf{r} \mid \mathbf{s}_k)$ for all $m \neq k$.

When the M signals are not equally probable, the above proof can be generalized to show that the MAP criterion minimizes the average probability of error.

5-1-4 The Maximum-Likelihood Sequence Detector

When the signal has no memory, the symbol-by-symbol detector described in the preceding section is optimum in the sense of minimizing the probability of a symbol error. On the other hand, when the transmitted signal has memory, i.e., the signals transmitted in successive symbol intervals are interdependent, the optimum detector is a detector that bases its decisions on observation of a

sequence of received signals over successive signal intervals. Below, we describe two different types of detection algorithms. In this section, we describe a *maximum-likelihood* sequence detection algorithm that searches for the minimum euclidean distance path through the trellis that characterizes the memory in the transmitted signal. In the following section, we describe a maximum a posteriori probability algorithm that makes decisions on a symbol-by-symbol basis, but each symbol decision is based on an observation of a sequence of received signal vectors.

To develop the maximum likelihood sequence detection algorithm, let us consider, as an example, the NRZI signal described in Section 4-3-2. Its memory is characterized by the trellis shown in Fig. 4-3-14. The signal transmitted in each signal interval is binary PAM. Hence, there are two possible transmitted signals corresponding to the signal points $s_1 = -s_2 = \sqrt{\mathscr{E}_b}$, where $\mathscr{E}_b$ is the energy per bit. The output of the matched-filter or correlation demodulator for binary PAM in the kth signal interval may be expressed as

$$r_k = \pm\sqrt{\mathscr{E}_b} + n_k \tag{5-1-57}$$

where n_k is a zero-mean gaussian random variable with variance $\sigma_n^2 = N_0/2$. Consequently, the conditional pdfs for the two possible transmitted signals are

$$\begin{aligned} p(r_k \mid s_1) &= \frac{1}{\sqrt{2\pi}\,\sigma_n} \exp\left[-\frac{(r_k - \sqrt{\mathscr{E}_b})^2}{2\sigma_n^2}\right] \\ p(r_k \mid s_2) &= \frac{1}{\sqrt{2\pi}\,\sigma_n} \exp\left[-\frac{(r_k + \sqrt{\mathscr{E}_b})^2}{2\sigma_n^2}\right] \end{aligned} \tag{5-1-58}$$

Now, suppose we observe the sequence of matched-filter outputs $r_1, r_2, \ldots, r_K$. Since the channel noise is assumed to be white and gaussian, and $f(t - iT)$, $f(t - jT)$ for $i \neq j$ are orthogonal, it follows that $E(n_k n_j) = 0$, $k \neq j$. Hence, the noise sequence $n_1, n_2, \ldots, n_K$ is also white. Consequently, for any given transmitted sequence $\mathbf{s}^{(m)}$, the joint pdf of $r_1, r_2, \ldots, r_K$ may be expressed as a product of K marginal pdfs, i.e.,

$$\begin{aligned} p(r_1, r_2, \ldots, r_K \mid \mathbf{s}^{(m)}) &= \prod_{k=1}^{K} p(r_k \mid s_k^{(m)}) \\ &= \prod_{k=1}^{K} \frac{1}{\sqrt{2\pi}\,\sigma_n} \exp\left[-\frac{(r_k - s_k^{(m)})^2}{2\sigma_n^2}\right] \\ &= \left(\frac{1}{\sqrt{2\pi}\,\sigma_n}\right)^K \exp\left[-\sum_{k=1}^{K} \frac{(r_k - s_k^{(m)})^2}{2\sigma_n^2}\right] \end{aligned} \tag{5-1-59}$$

where either $s_k = \sqrt{\mathscr{E}_b}$ or $s_k = -\sqrt{\mathscr{E}_b}$. Then, given the received sequence $r_1, r_2, \ldots, r_K$ at the output of the matched filter or correlation demodulator, the detector determines the sequence $\mathbf{s}^{(m)} = \{s_1^{(m)}, s_2^{(m)}, \ldots, s_K^{(m)}\}$ that maximizes the conditional pdf $p(r_1, r_2, \ldots, r_K \mid \mathbf{s}^{(m)})$. Such a detector is called the *maximum-likelihood* (ML) *sequence detector.*

By taking the logarithm of (5-1-59) and neglecting the terms that are

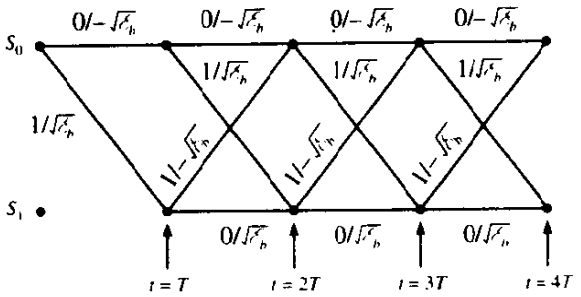

FIGURE 5-1-11 Trellis for NRZI signal.

independent of $(r_1, r_2, \ldots, r_K)$, we find that an equivalent ML sequence detector selects the sequence $\mathbf{s}^{(m)}$ that minimizes the *euclidean distance metric*

$$D(\mathbf{r}, \mathbf{s}^{(m)}) = \sum_{k=1}^{K} (r_k - s_k^{(m)})^2 \tag{5-1-60}$$

In searching through the trellis for the sequence that minimizes the euclidean distance $D(\mathbf{r}, \mathbf{s}^{(m)})$, it may appear that we must compute the distance $D(\mathbf{r}, \mathbf{s}^{(m)})$ for every possible sequence. For the NRZI example, which employs binary modulation, the total number of sequences is 2^K, where K is the number of outputs obtained from the demodulator. However, this is not the case. We may reduce the number of sequences in the trellis search by using the *Viterbi algorithm* to eliminate sequences as new data is received from the demodulator.

The Viterbi algorithm is a sequential trellis search algorithm for performing ML sequence detection. It is described in Chapter 8 as a decoding algorithm for convolutional codes. We describe it below in the context of the NRZI signal. We assume that the search process begins initially at state S_0. The corresponding trellis is shown in Fig. 5-1-11.

At time $t = T$, we receive $r_1 = s_1^{(m)} + n$ from the demodulator, and at $t = 2T$, we receive $r_2 = s_2^{(m)} + n_2$. Since the signal memory is one bit, which we denote by $L = 1$, we observe that the trellis reaches its regular (steady state) form after two transitions. Thus, upon receipt of r_2 at $t = 2T$ (and thereafter), we observe that there are two signal paths entering each of the nodes and two signal paths leaving each node. The two paths entering node S_0 at $t = 2T$ correspond to the information bits (0, 0) and (1, 1) or, equivalently, to the signal points $(-\sqrt{\mathcal{E}_b}, -\sqrt{\mathcal{E}_b})$ and $(\sqrt{\mathcal{E}_b}, -\sqrt{\mathcal{E}_b})$, respectively. The two paths entering node S_1 at $t = 2T$ correspond to the information bits (0, 1) and (1, 0) or, equivalently, to the signal points $(-\sqrt{\mathcal{E}_b}, \sqrt{\mathcal{E}_b})$ and $(\sqrt{\mathcal{E}_b}, \sqrt{\mathcal{E}_b})$, respectively.

For the two paths entering node S_0, we compute the two Euclidean distance metrics

$$\begin{aligned} D_0(0, 0) &= (r_1 + \sqrt{\mathcal{E}_b})^2 + (r_2 + \sqrt{\mathcal{E}_b})^2 \\ D_0(1, 1) &= (r_1 - \sqrt{\mathcal{E}_b})^2 + (r_2 + \sqrt{\mathcal{E}_b})^2 \end{aligned} \tag{5-1-61}$$

by using the outputs r_1 and r_2 from the demodulator. The Viterbi algorithm compares these two metrics and discards the path having the larger (greater-distance) metric.† The other path with the lower metric is saved and is called the *survivor* at $t = 2T$. The elimination of one of the two paths may be done without compromising the optimality of the trellis search, because any extension of the path with the larger distance beyond $t = 2T$ will always have a larger metric than the survivor that is extended along the same path beyond $t = 2T$.

Similarly, for the two paths entering node S_1 at $t = 2T$, we compute the two Euclidean distance metrics

$$\begin{aligned} D_1(0, 1) &= (r_1 + \sqrt{\mathscr{E}_b})^2 + (r_2 - \sqrt{\mathscr{E}_b})^2 \\ D_1(1, 0) &= (r_1 - \sqrt{\mathscr{E}_b})^2 + (r_2 - \sqrt{\mathscr{E}_b})^2 \end{aligned} \tag{5-1-62}$$

by using the outputs r_1 and r_2 from the demodulator. The two metrics are compared and the signal path with the larger metric is eliminated. Thus, at $t = 2T$, we are left with two survivor paths, one at node S_0 and the other at node S_1, and their corresponding metrics. The signal paths at nodes S_0 and S_1 are then extended along the two survivor paths.

Upon receipt of r_3 at $t = 3T$, we compute the metrics of the two paths entering state S_0. Suppose the survivors at $t = 2T$ are the paths (0, 0) at S_0 and (0, 1) at S_1. Then, the two metrics for the paths entering S_0 at $t = 3T$ are

$$\begin{aligned} D_0(0, 0, 0) &= D_0(0, 0) + (r_3 + \sqrt{\mathscr{E}_b})^2 \\ D_0(0, 1, 1) &= D_1(0, 1) + (r_3 + \sqrt{\mathscr{E}_b})^2 \end{aligned} \tag{5-1-63}$$

These two metrics are compared and the path with the larger (greater-distance) metric is eliminated. Similarly, the metrics for the two paths entering S_1 at $t = 3T$ are

$$\begin{aligned} D_1(0, 0, 1) &= D_0(0, 0) + (r_3 - \sqrt{\mathscr{E}_b})^2 \\ D_1(0, 1, 0) &= D_1(0, 1) + (r_3 - \sqrt{\mathscr{E}_b})^2 \end{aligned} \tag{5-1-64}$$

These two metrics are compared and the path with the larger (greater-distance) metric is eliminated.

This process is continued as each new signal sample is received from the demodulator. Thus, the Viterbi algorithm computes two metrics for the two signal paths entering a node at each stage of the trellis search and eliminates one of the two paths at each node. The two survivor paths are then extended forward to the next state. Therefore, the number of paths searched in the trellis is reduced by a factor of two at each stage.

It is relatively easy to generalize the trellis search performed by the Viterbi algorithm for M-ary modulation. For example, delay modulation employs

† Note that, for NRZI, the reception of r_2 from the demodulator neither increases nor decreases the relative difference between the two metrics, $D_0(0, 0)$ and $D_0(1, 1)$. At this point, one may ponder on the implication of this observation. In any case, we continue with the description of the ML sequence detector based on the Viterbi algorithm.

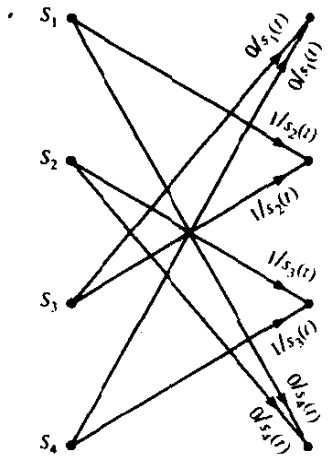

FIGURE 5-1-12 One stage of trellis diagram for delay modulation.

$M = 4$ signals and is characterized by the four-state trellis shown in Fig. 5-1-12. We observe that each state has two signal paths entering and two signal paths leaving each node. The memory of the signal is $L = 1$. Hence, the Viterbi algorithm will have four survivors at each stage and their corresponding metrics. Two metrics corresponding to the two entering paths are computed at each node, and one of the two signal paths entering the node is eliminated at each state of the trellis. Thus, the Viterbi algorithm minimizes the number of trellis paths searched in performing ML sequence detection.

From the description of the Viterbi algorithm given above, it is unclear as to how decisions are made on the individual detected information symbols given the surviving sequences. If we have advanced to some stage, say K, where $K \gg L$ in the trellis, and we compare the surviving sequences, we shall find that with probability approaching one all surviving sequences will be identical in bit (or symbol) positions $K - 5L$ and less. In a practical implementation of the Viterbi algorithm, decisions on each information bit (or symbol) are forced after a delay of $5L$ bits (or symbols), and hence, the surviving sequences are truncated to the $5L$ most recent bits (or symbols). Thus, a variable delay in bit or symbol detection is avoided. The loss in performance resulting from the suboptimum detection procedure is negligible if the delay is at least $5L$.

Example 5-1-4

Consider the decision rule for detecting the data sequence in an NRZI signal with a Viterbi algorithm having a delay of $5L$ bits. The trellis for the NRZI signal is shown in Fig. 5-1-11. In this case, $L = 1$, hence the delay in bit detection is set to five bits. Hence, at $t = 6T$, we shall have two surviving sequences, one for each of the two states and the corresponding metrics $\mu_6(b_1, b_2, b_3, b_4, b_5, b_6)$ and $\mu_6(b_1', b_2', b_3', b_4', b_5', b_6')$. At this stage, with probability nearly equal to one, the bit b_1 will be the same as b_1'; that is,

both surviving sequences will have a common first branch. If $b_1 \neq b_1'$, we may select the bit (b_1 or b_1') corresponding to the smaller of the two metrics. Then the first bit is dropped from the two surviving sequences. At $t = 7T$, the two metrics $\mu_7(b_2, b_3, b_4, b_5, b_6, b_7)$ and $\mu_7(b_2', b_3', b_4', b_5', b_6', b_7')$ will be used to determine the decision on bit b_2. This process continues at each stage of the search through the trellis for the minimum distance sequence. Thus the detection delay is fixed at five bits.†

5-1-5 A Symbol-by-Symbol Detector for Signals with Memory

In contrast to the maximum-likelihood sequence detector for detecting the transmitted information, we now describe a detector that makes symbol-by-symbol decisions based on the computation of the maximum a posteriori probability (MAP) for each detected symbol. Hence, this detector is optimum in the sense that it minimizes the probability of a symbol error. The detection algorithm that is presented below is due to Abend and Fritchman (1970), who developed it as a detection algorithm for channels with intersymbol interference, i.e., channels with memory.

We illustrate the algorithm in the context of detecting a PAM signal with M possible levels. Suppose that it is desired to detect the information symbol transmitted in the kth signal interval, and let $r_1, r_2, \ldots, r_{k+D}$ be the observed received sequence, where D is the delay parameter which is chosen to exceed the signal memory, i.e., $D \geq L$, where L is the inherent memory in the signal. On the basis of the received sequence, we compute the posterior probabilities

$$P(s^{(k)} = A_m \mid r_{k+D}, r_{k+D-1}, \ldots, r_1) \tag{5-1-65}$$

for the M possible symbol values and choose the symbol with the largest probability. Since

$$P(s^{(k)} = A_m \mid r_{k+D}, \ldots, r_1) = \frac{p(r_{k+D}, \ldots, r_1 \mid s^{(k)} = A_m) P(s^{(k)} = A_m)}{p(r_{k+D}, r_{k+D-1}, \ldots, r_1)} \tag{5-1-66}$$

and since the denominator is common for all M probabilities, the maximum a posteriori probability (MAP) criterion is equivalent to choosing the value of $s^{(k)}$ that maximizes the numerator of (5-1-66). Thus, the criterion for deciding on the transmitted symbol $s^{(k)}$ is

$$\tilde{s}^{(k)} = \arg \left\{ \max_{s^{(k)}} p(r_{k+D}, \ldots, r_1 \mid s^{(k)} = A_m) P(s^{(k)} = A_m) \right\} \tag{5-1-67}$$

† One may have observed by now that the ML sequence detector and the symbol-by-symbol detector that ignores the memory in the NRZI signal reach the same decisions. Hence, there is no need for a decision delay. Nevertheless, the procedure described above applies in general.

When the symbols are equally probable, the probability $P(s^{(k)} = A_m)$ may be dropped from the computation.

The algorithm for computing the probabilities in (5-1-67) recursively begins with the first symbol $s^{(1)}$. We have

$$\begin{aligned}\tilde{s}^{(1)} &= \arg\left\{\max_{s^{(1)}} p(r_{k+D}, \ldots, r_1 \mid s^{(1)} = A_m)P(s^{(1)} = A_m)\right\} \\ &= \arg\left\{\max_{s^{(1)}} \sum_{s^{(1+D)}} \cdots \sum_{s^{(2)}} p(r_{1+D}, \ldots, r_1 \mid s^{(1+D)}, \ldots, s^{(1)})P(s^{(1+D)}, \ldots, s^{(1)})\right\} \\ &= \arg\left\{\max_{s^{(1)}} \sum_{s^{(1+D)}} \cdots \sum_{s^{(2)}} p_1(s^{(1+D)}, \ldots, s^{(2)}, s^{(1)})\right\} \qquad (5\text{-}1\text{-}68)\end{aligned}$$

where $\tilde{s}^{(1)}$ denotes the decision on $s^{(1)}$ and, for mathematical convenience, we have defined

$$p_1(s^{(1+D)}, \ldots, s^{(2)}, s^{(1)}) \equiv p(r_{1+D}, \ldots, r_1 \mid s^{(1+D)}, \ldots, s^{(1)})P(s^{(1+D)}, \ldots, s^{(1)}) \qquad (5\text{-}1\text{-}69)$$

The joint probability $P(s^{(1+D)}, \ldots, s^{(2)}, s^{(1)})$ may be omitted if the symbols are equally probable and statistically independent. As a consequence of the statistical independence of the additive noise sequence, we have

$$\begin{aligned}&p(r_{1+D}, \ldots, r_1 \mid s^{(1+D)}, \ldots, s^{(1)}) \\ &\quad = p(r_{1+D} \mid s^{(1+D)}, \ldots, s^{(1+D-L)})p(r_D \mid s^{(D)}, \ldots, s^{(D-L)}) \cdots \\ &\qquad\qquad p(r_2 \mid s^{(2)}, s^{(1)})p(r_1 \mid s^{(1)}) \qquad (5\text{-}1\text{-}70)\end{aligned}$$

where we assume that $s^{(k)} = 0$ for $k \leq 0$.

For detection of the symbol $s^{(2)}$, we have

$$\begin{aligned}\tilde{s}^{(2)} &= \arg\left\{\max_{s^{(2)}} p(r_{2+D}, \ldots, r_1 \mid s^{(2)} = A_m)P(s^{(2)} = A_m)\right\} \\ &= \arg\left\{\max_{s^{(2)}} \sum_{s^{(2+D)}} \cdots \sum_{s^{(3)}} p(r_{2+D}, \ldots, r_1 \mid s^{(2+D)}, \ldots, s^{(2)})P(s^{(2+D)}, \ldots, s^{(2)})\right\} \qquad (5\text{-}1\text{-}71)\end{aligned}$$

The joint conditional probability in the multiple summation can be expressed as

$$\begin{aligned}&p(r_{2+D}, \ldots, r_1 \mid s^{(2+D)}, \ldots, s^{(2)}) \\ &\quad = p(r_{2+D} \mid s^{(2+D)}, \ldots, s^{(2+D-L)})p(r_{1+D} \ldots, r_1 \mid s^{(1+D)}, \ldots, s^{(2)}) \qquad (5\text{-}1\text{-}72)\end{aligned}$$

Furthermore, the joint probability

$$p(r_{1+D}, \ldots, r_1 \mid s^{(1+D)}, \ldots, s^{(2)})P(s^{(1+D)}, \ldots, s^{(2)})$$

can be obtained from the probabilities computed previously in the detection of $s^{(1)}$. That is,

$$\begin{aligned} &p(r_{1+D}, \ldots, r_1 \mid s^{(1+D)}, \ldots, s^{(2)}) \\ &\quad = \sum_{s^{(1)}} p(r_{1+D}, \ldots, r_1 \mid s^{(1+D)}, \ldots, s^{(1)})P(s^{(1+D)}, \ldots, s^{(1)}) \\ &\quad = \sum_{s^{(1)}} p_1(s^{(1+D)}, \ldots, s^{(2)}, s^{(1)}) \end{aligned} \tag{5-1-73}$$

Thus, by combining (5-1-73) and (5-1-72) and then substituting into (5-1-71), we obtain

$$\tilde{s}^{(2)} = \arg\left\{\max_{s^{(2)}} \sum_{s^{(2+D)}} \cdots \sum_{s^{(3)}} p_2(s^{(2+D)}, \ldots, s^{(3)}, s^{(2)})\right\} \tag{5-1-74}$$

where, by definition,

$$\begin{aligned} &p_2(s^{(2+D)}, \ldots, s^{(3)}, s^{(2)}) \\ &\quad = p(r_{2+D} \mid s^{(2+D)}, \ldots, s^{(2+D-L)})P(s^{(2+D)}) \sum_{s^{(1)}} p_1(s^{(1+D)}, \ldots, s^{(2)}, s^{(1)}) \end{aligned} \tag{5-1-75}$$

In general, the recursive algorithm for detecting the symbol $s^{(k)}$ is as follows: upon reception of $r_{k+D}, \ldots, r_2, r_1$, we compute

$$\begin{aligned} \tilde{s}^{(k)} &= \arg\left\{\max_{s^{(k)}} p(r_{k+D}, \ldots, r_1 \mid s^{(k)})P(s^{(k)})\right\} \\ &= \arg\left\{\max_{s^{(k)}} \sum_{s^{(k+D)}} \cdots \sum_{s^{(k+1)}} p_k(s^{(k+D)}, \ldots, s^{(k+1)}, s^{(k)})\right\} \end{aligned} \tag{5-1-76}$$

where, by definition,

$$\begin{aligned} &p_k(s^{(k+D)}, \ldots, s^{(k-1)}, s^{(k)}) \\ &\quad = p(r_{k+D} \mid s^{(k+D)}, \ldots, s^{(k+D-L)})P(s^{(k+D)}) \sum_{s^{(k-1)}} p_{k-1}(s^{(k-1+D)}, \ldots, s^{(k-1)}) \end{aligned} \tag{5-1-77}$$

Thus, the recursive nature of the algorithm is established by the relations (5-1-76) and (5-1-77).

The major problem with the algorithm is its computational complexity. In particular, the averaging performed over the symbols $s^{(k+D)}, \ldots, s^{(k+1)}, s^{(k)}$ in (5-1-76) involves a large amount of computation per received signal, especially if the number M of amplitude levels $\{A_m\}$ is large. On the other hand, if M is small and the memory L is relatively short, this algorithm is easily implemented.

5-2 PERFORMANCE OF THE OPTIMUM RECEIVER FOR MEMORYLESS MODULATION

In this section, we evaluate the probability of error for the memoryless modulation signals described in Section 4-3-1. First, we consider binary PAM signals and then M-ary signals of various types.

5-2-1 Probability of Error for Binary Modulation

Let us consider binary PAM signals where the two signal waveforms are $s_1(t) = g(t)$ and $s_2(t) = -g(t)$, and $g(t)$ is an arbitrary pulse that is nonzero in the interval $0 \leq t \leq T_b$ and zero elsewhere.

Since $s_1(t) = -s_2(t)$, these signals are said to be *antipodal.* The energy in the pulse $g(t)$ is $\mathcal{E}_b$. As indicated in Section 4-3-1, PAM signals are one-dimensional, and, hence, their geometric representation is simply the one-dimensional vector $s_1 = \sqrt{\mathcal{E}_b}$, $s_2 = -\sqrt{\mathcal{E}_b}$. Figure 5-2-1 illustrates the two signal points.

Let us assume that the two signals are equally likely and that signal $s_1(t)$ was transmitted. Then, the received signal from the (matched filter or correlation) demodulator is

$$r = s_1 + n = \sqrt{\mathcal{E}_b} + n \tag{5-2-1}$$

where n represents the additive gaussian noise component, which has zero mean and variance $\sigma_n^2 = \frac{1}{2}N_0$. In this case, the decision rule based on the correlation metric given by (5-1-44) compares r with the threshold zero. If $r > 0$, the decision is made in favor of $s_1(t)$, and if $r < 0$, the decision is made that $s_2(t)$ was transmitted. Clearly, the two conditional pdfs of r are

$$p(r \mid s_1) = \frac{1}{\sqrt{\pi N_0}} e^{-(r - \sqrt{\mathcal{E}_b})^2/N_0} \tag{5-2-2}$$

$$p(r \mid s_2) = \frac{1}{\sqrt{\pi N_0}} e^{-(r + \sqrt{\mathcal{E}_b})^2/N_0} \tag{5-2-3}$$

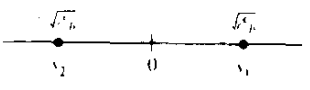

FIGURE 5-2-1 Signal points for binary antipodal signals.

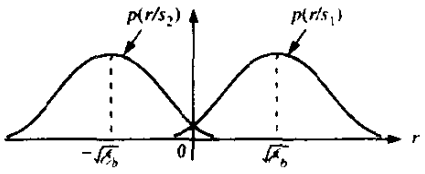

FIGURE 5-2-2 Conditional pdfs of two signals.

These two conditional pdfs are shown in Fig. 5-2-2.

Given that $s_1(t)$ was transmitted, the probability of error is simply the probability that $r < 0$, i.e.,

$$\begin{aligned} P(e \mid s_1) &= \int_{-\infty}^{0} p(r \mid s_1)\, dr \\ &= \frac{1}{\sqrt{\pi N_0}} \int_{-\infty}^{0} \exp\left[-\frac{(r - \sqrt{\mathscr{E}_b})^2}{N_0} \right] dr \\ &= \frac{1}{\sqrt{2\pi}} \int_{-\infty}^{-\sqrt{2\mathscr{E}_b/N_0}} e^{-x^2/2}\, dx \\ &= \frac{1}{\sqrt{2\pi}} \int_{\sqrt{2\mathscr{E}_b/N_0}}^{\infty} e^{-x^2/2}\, dx \\ &= Q\left(\sqrt{\frac{2\mathscr{E}_b}{N_0}} \right) \end{aligned} \tag{5-2-4}$$

where $Q(x)$ is the Q-function defined in (2-1-97). Similarly, if we assume that $s_2(t)$ was transmitted, $r = -\sqrt{\mathscr{E}_b} + n$ and the probability that $r > 0$ is also $P(e \mid s_2) = Q(\sqrt{2\mathscr{E}_b/N_0})$. Since the signals $s_1(t)$ and $s_2(t)$ are equally likely to be transmitted, the average probability of error is

$$\begin{aligned} P_b &= \tfrac{1}{2}P(e \mid s_1) + \tfrac{1}{2}P(e \mid s_2) \\ &= Q\left(\sqrt{\frac{2\mathscr{E}_b}{N_0}} \right) \end{aligned} \tag{5-2-5}$$

We should observe two important characteristics of this performance measure. First, we note that the probability of error depends only on the ratio $\mathscr{E}_b/N_0$ and not on any other detailed characteristics of the signals and the noise. Secondly, we note that $2\mathscr{E}_b/N_0$ is also the output SNR_0 from the matched-filter (and correlation) demodulator. The ratio $\mathscr{E}_b/N_0$ is usually called the *signal-to-noise ratio per bit.*

We also observe that the probability of error may be expressed in terms of the distance between the two signals s_1 and s_2. From Fig. 5-2-1, we observe that the two signals are separated by the distance $d_{12} = 2\sqrt{\mathscr{E}_b}$. By substituting $\mathscr{E}_b = \frac{1}{4}d_{12}^2$ into (5-2-5), we obtain

$$P_b = Q\left(\sqrt{\frac{d_{12}^2}{2N_0}} \right) \tag{5-2-6}$$

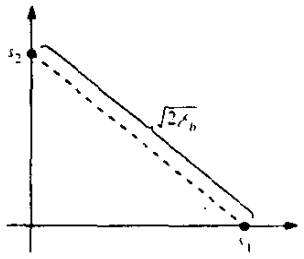

FIGURE 5-2-3 Signal points for binary orthogonal signals

This expression illustrates the dependence of the error probability on the distance between the two signal points.

Next, let us evaluate the error probability for binary orthogonal signals. Recall that the signal vectors $\mathbf{s}_1$ and $\mathbf{s}_1$ are two-dimensional, as shown in Fig. 5-2-3, and may be expressed, according to (4-3-30), as

$$\begin{aligned} \mathbf{s}_1 &= [\sqrt{\mathscr{E}_b} \quad 0] \\ \mathbf{s}_2 &= [0 \quad \sqrt{\mathscr{E}_b}] \end{aligned} \tag{5-2-7}$$

where $\mathscr{E}_b$ denotes the energy for each of the waveforms. Note that the distance between these signal points is $d_{12} = \sqrt{2\mathscr{E}_b}$.

To evaluate the probability of error, let us assume that $\mathbf{s}_1$ was transmitted. Then, the received vector at the output of the demodulator is

$$\mathbf{r} = [\sqrt{\mathscr{E}_b} + n_1 \quad n_2] \tag{5-2-8}$$

We can now substitute for r into the correlation metrics given by (5-1-44) to obtain $C(\mathbf{r}, \mathbf{s}_1)$ and $C(\mathbf{r}, \mathbf{s}_2)$. Then, the probability of error is the probability that $C(\mathbf{r}, \mathbf{s}_2) > C(\mathbf{r}, \mathbf{s}_1)$. Thus,

$$P(e \mid \mathbf{s}_1) = P[C(\mathbf{r}, \mathbf{s}_2) > C(\mathbf{r}_1, \mathbf{s}_1)] = P[n_2 - n_1 > \sqrt{\mathscr{E}_b}] \tag{5-2-9}$$

Since n_1 and n_2 are zero-mean statistically independent gaussian random variables each with variance $\frac{1}{2}N_0$, the random variable $x = n_2 - n_1$ is zero-mean gaussian with variance N_0. Hence,

$$\begin{aligned} P(n_2 - n_1 > \sqrt{\mathscr{E}_b}) &= \frac{1}{\sqrt{2\pi N_0}} \int_{\sqrt{2\mathscr{E}_b}}^{\infty} e^{-x^2/2N_0}\, dx \\ &= \frac{1}{\sqrt{2\pi}} \int_{\sqrt{2\mathscr{E}_b/N_0}}^{\infty} e^{-x^2/2}\, dx \\ &= Q\left(\sqrt{\frac{\mathscr{E}_b}{N_0}}\right) \end{aligned} \tag{5-2-10}$$

Due to symmetry, the same error probability is obtained when we assume that

$\mathbf{s}_2$ is transmitted. Consequently, the average error probability for binary orthogonal signals is

$$P_b = Q\left(\sqrt{\frac{\mathscr{E}_b}{N_0}}\right) = Q(\sqrt{\gamma_b}) \tag{5-2-11}$$

where, by definition, γ_b is the SNR per bit.

If we compare the probability of error for binary antipodal signals with that for binary orthogonal signals, we find that orthogonal signals require a factor of two increase in energy to achieve the same error probability as antipodal signals. Since $10 \log_{10} 2 = 3$ dB, we say that orthogonal signals are 3 dB poorer than antipodal signals. The difference of 3 dB is simply due to the distance between the two signal points, which is $d_{12}^2 = 2\mathscr{E}_b$ for orthogonal signals, whereas $d_{12}^2 = 4\mathscr{E}_b$ for antipodal signals.

The error probability versus $10 \log_{10} \mathscr{E}_b/N_0$ for these two types of signals is shown in Fig. 5-2-4. As observed from this figure, at any given error probability, the $\mathscr{E}_b/N_0$ required for orthogonal signals is 3 dB more than that for antipodal signals.

5-2-2 Probability of Error for M-ary Orthogonal Signals

For equal energy orthogonal signals, the optimum detector selects the signal resulting in the largest cross correlation between the received vector $\mathbf{r}$ and each of the M possible transmitted signal vectors $\{\mathbf{s}_m\}$, i.e.,

$$C(\mathbf{r}, \mathbf{s}_m) = \mathbf{r} \cdot \mathbf{s}_m = \sum_{k=1}^{M} r_k s_{mk}, \qquad m = 1, 2, \ldots, M \tag{5-2-12}$$

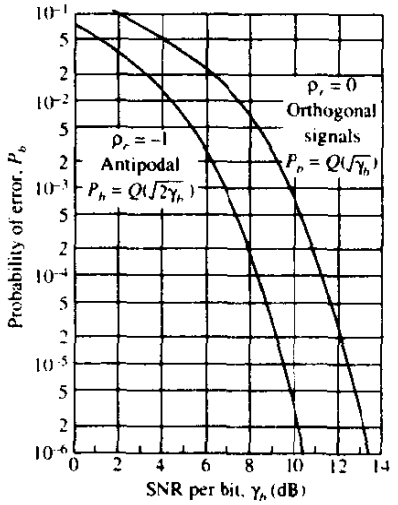

FIGURE 5-2-4 Probability of error for binary signals.

To evaluate the probability of error, let us suppose that the signal $\mathbf{s}_1$ is transmitted. Then the received signal vector is

$$\mathbf{r} = [\sqrt{\mathscr{E}_s} + n_1 \quad n_2 \quad n_3 \quad \dots \quad n_M] \tag{5-2-13}$$

where $n_1, n_2, \dots, n_M$ are zero-mean, mutually statistically independent gaussian random variables with equal variance $\sigma_n^2 = \frac{1}{2}N_0$. In this case, the outputs from the bank of M correlators are

$$\begin{aligned} C(\mathbf{r}, \mathbf{s}_1) &= \sqrt{\mathscr{E}_s}(\sqrt{\mathscr{E}_s} + n_1) \\ C(\mathbf{r}, \mathbf{s}_2) &= \sqrt{\mathscr{E}_s} n_2 \\ &\vdots \qquad\quad \vdots \\ C(\mathbf{r}, \mathbf{s}_M) &= \sqrt{\mathscr{E}_s} n_M \end{aligned} \tag{5-2-14}$$

Note that the scale factor $\mathscr{E}_s$ may be elminated from the correlator outputs by dividing each output by $\sqrt{\mathscr{E}_s}$. Then, with this normalization, the pdf of the first correlator output ($r_1 = \sqrt{\mathscr{E}_s} + n_1$) is

$$p_{r_1}(x_1) = \frac{1}{\sqrt{\pi N_0}} \exp\left[-\frac{(x_1 - \sqrt{\mathscr{E}_s})^2}{N_0}\right] \tag{5-2-15}$$

and the pdfs of the other $M - 1$ correlator outputs are

$$p_{r_m}(x_m) = \frac{1}{\sqrt{\pi N_0}} e^{-x_m^2/N_0}, \qquad m = 2, 3, \dots, M \tag{5-2-16}$$

It is mathematically convenient to first derive the probability that the detector makes a correct decision. This is the probability that r_1 is larger than each of the other $M - 1$ correlator outputs $n_2, n_3, \dots n_M$. This probability may be expressed as

$$P_c = \int_{-\infty}^{\infty} P(n_2 < r_1, n_3 < r_1, \dots, n_M < r_1 \mid r_1) p(r_1)\, dr_1 \tag{5-2-17}$$

where $P(n_2 < r_1, n_3 < r_1, \dots, n_M < r_1 \mid r_1)$ denotes the joint probability that $n_2, n_3, \dots, n_M$ are all less than r_1, conditioned on any given r_1. Then this joint probability is averaged over all r_1. Since the $\{r_m\}$ are statistically independent, the joint probability factors into a product of $M - 1$ marginal probabilities of the form

$$\begin{aligned} P(n_m < r_1 \mid r_1) &= \int_{-\infty}^{r_1} p_{r_m}(x_m)\, dx_m, \qquad m = 2, 3, \dots, M \\ &= \frac{1}{\sqrt{2\pi}} \int_{-\infty}^{r_1\sqrt{2/N_0}} e^{-x^2/2}\, dx \end{aligned} \tag{5-2-18}$$

These probabilities are identical for $m = 2, 3, \dots, M$, and, hence, the joint

probability under consideration is simply the result in (5-2-18) raised to the $(M-1)$th power. Thus, the probability of a correct decision is

$$P_c = \int_{-\infty}^{\infty} \left(\frac{1}{\sqrt{2\pi}} \int_{-\infty}^{r_1\sqrt{2/N_0}} e^{-x^2/2}\, dx \right)^{M-1} p(r_1)\, dr_1 \tag{5-2-19}$$

and the probability of a (k-bit) symbol error is

$$P_M = 1 - P_c \tag{5-2-20}$$

where

$$P_M = \frac{1}{\sqrt{2\pi}} \int_{-\infty}^{\infty} \left[1 - \left(\frac{1}{\sqrt{2\pi}} \int_{-\infty}^{y} e^{-x^2/2}\, dx \right)^{M-1} \right] \exp\left[-\tfrac{1}{2}\left(y - \sqrt{\frac{2\mathscr{E}_s}{N_0}} \right)^2 \right] dy \tag{5-2-21}$$

The same expression for the probability of error is obtained when any one of the other $M-1$ signals is transmitted. Since all the M signals are equally likely, the expression for P_M given in (5-2-21) is the average probability of a symbol error. This expression can be evaluated numerically.

In comparing the performance of various digital modulation methods, it is desirable to have the probability of error expressed in terms of the SNR per bit, $\mathscr{E}_b/N_0$, instead of the SNR per symbol, $\mathscr{E}_s/N_0$. With $M = 2^k$, each symbol conveys k bits of information, and hence $\mathscr{E}_s = k\mathscr{E}_b$. Thus, (5-2-21) may be expressed in terms of $\mathscr{E}_b/N_0$ by substituting for $\mathscr{E}_s$.

Sometimes, it is also desirable to convert the probability of a symbol error into an equivalent probability of a binary digit error. For equiprobable orthogonal signals, all symbol errors are equiprobable and occur with probability

$$\frac{P_M}{M-1} = \frac{P_M}{2^k - 1} \tag{5-2-22}$$

Furthermore, there are $\binom{k}{n}$ ways in which n bits out of k may be in error. Hence, the average number of bit errors per k-bit symbol is

$$\sum_{n=1}^{k} \binom{k}{n} \frac{P_M}{2^k - 1} = k \frac{2^{k-1}}{2^k - 1} P_M \tag{5-2-23}$$

and the average bit error probability is just the result in (5-2-23) divided by k, the number of bits per symbol. Thus,

$$P_b = \frac{2^{k-1}}{2^k - 1} P_M \approx \frac{P_M}{2}, \qquad k \gg 1 \tag{5-2-24}$$

The graphs of the probability of a binary digit error as a function of the

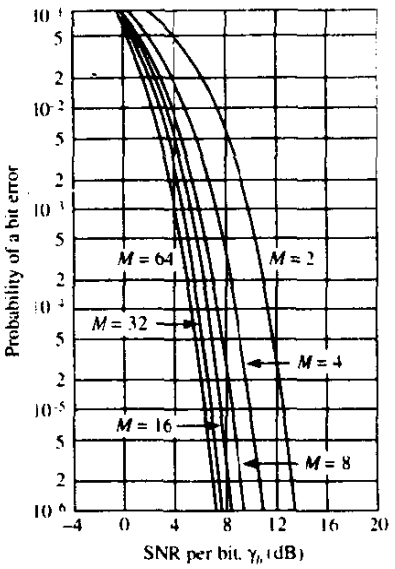

FIGURE 5-2-5 Probability of bit error for coherent detection of orthogonal signals.

SNR per bit, $\mathscr{E}_b/N_0$, are shown in Fig. 5-2-5 for $M = 2, 4, 8, 16, 32$ and 64. This figure illustrates that, by increasing the number M of waveforms, one can reduce the SNR per bit required to achieve a given probability of a bit error. For example, to achieve a $P_b = 10^{-5}$, the required SNR per bit is a little more than 12 dB for $M = 2$, but if M is increased to 64 signal waveforms ($k = 6$ bits/symbol), the required SNR per bit is approximately 6 dB. Thus, a savings of over 6 dB (a factor-of-four reduction) is realized in transmitter power (or energy) required to achieve a $P_b = 10^{-5}$ by increasing M from $M = 2$ to $M = 64$.

What is the minimum required $\mathscr{E}_b/N_0$ to achieve an arbitrarily small probability of error as $M \to \infty$? This question is answered below.

A Union Bound on the Probability of Error Let us investigate the effect of increasing M on the probability of error for orthogonal signals. To simplify the mathematical development, we first derive an upper bound on the probability of a symbol error that is much simpler than the exact form given in (5-2-21).

Recall that the probability of error for binary orthogonal signals is given by (5-2-11). Now, if we view the detector for M orthogonal signals as one that makes $M - 1$ binary decisions between the correlator output $C(\mathbf{r}, \mathbf{s}_1)$ that contains the signal and the other $M - 1$ correlator outputs $C(\mathbf{r}, \mathbf{s}_m)$, $m = 2, 3, \ldots, M$, the probability of error is upper-bounded by the *union bound* of the $M - 1$ events. That is, if E_i represents the event that $C(\mathbf{r}, \mathbf{s}_i) > C(\mathbf{r}, \mathbf{s}_1)$ for $i \neq 1$ then we have $P_M = P(\bigcup_{i=1}^{M} E_i) \leq \sum_{i=1}^{M} P(E_i)$. Hence,

$$P_M \leq (M-1)P_2 = (M-1)Q(\sqrt{\mathscr{E}_s/N_0}) < MQ(\sqrt{\mathscr{E}_s/N_0}) \qquad (5\text{-}2\text{-}25)$$

This bound can be simplified further by upper-bounding $Q(\sqrt{\mathscr{E}_s/N_0})$. We have

$$Q(\sqrt{\mathscr{E}_s/N_0}) < e^{-\mathscr{E}_s/2N_0} \tag{5-2-26}$$

Thus,

$$\begin{aligned} P_M &< Me^{-\mathscr{E}_s/2N_0} = 2^k e^{-k\mathscr{E}_b/2N_0} \\ P_M &< e^{-k(\mathscr{E}_b/N_0 - 2\ln 2)/2} \end{aligned} \tag{5-2-27}$$

As $k \to \infty$, or equivalently, as $M \to \infty$, the probability of error approaches zero exponentially, provided that $\mathscr{E}_b/N_0$ is greater than $2 \ln 2$, i.e.,

$$\frac{\mathscr{E}_b}{N_0} > 2 \ln 2 = 1.39 \quad (1.42 \text{ dB}) \tag{5-2-28}$$

The simple upper bound on the probability of error given by (5-2-27) implies that, as long as SNR > 1.42 dB, we can achieve an arbitrarily low P_M. However, this union bound is not a very tight upper bound at a sufficiently low SNR due to the fact that the upper bound for the Q function in (5-2-26) is loose. In fact, by more elaborate bounding techniques, it is shown in Chapter 7 that the upper bound in (5-2-27) is sufficiently tight for $\mathscr{E}_b/N_0 > 4 \ln 2$. For $\mathscr{E}_b/N_0 < 4 \ln 2$, a tighter upper bound on P_M is

$$P_M < 2e^{-k(\sqrt{\mathscr{E}_b/N_0} - \sqrt{\ln 2})^2} \tag{5-2-29}$$

Consequently, $P_M \to 0$ as $k \to \infty$, provided that

$$\frac{\mathscr{E}_b}{N_0} > \ln 2 = 0.693 \quad (-1.6 \text{ dB}) \tag{5-2-30}$$

Hence, -1.6 dB is the minimum required SNR per bit to achieve an arbitrarily small probability of error in the limit as $k \to \infty$ ($M \to \infty$). This minimum SNR per bit (-1.6 dB) is called the *Shannon limit* for an additive white Gaussian noise channel.

5-2-3 Probability of Error for M-ary Biorthogonal Signals

As indicated in Section 4-3, a set of $M = 2^k$ biorthogonal signals are constructed from $\frac{1}{2}M$ orthogonal signals by including the negatives of the orthogonal signals. Thus, we achieve a reduction in the complexity of the demodulator for the biorthogonal signals relative to that for orthogonal signals, since the former is implemented with $\frac{1}{2}M$ cross-correlators or matched filters, whereas the latter requires M matched filters or cross-correlators.

To evaluate the probability of error for the optimum detector, let us assume that the signal $s_1(t)$ corresponding to the vector $\mathbf{s}_1 = [\sqrt{\mathscr{E}_s}\ 0\ 0\ \ldots\ 0]$ was transmitted. Then, the received signal vector is

$$\mathbf{r} = [\sqrt{\mathscr{E}_s} + n_1 \quad n_2 \quad \ldots \quad n_{M/2}] \tag{5-2-31}$$

where the $\{n_m\}$ are zero-mean, mutually statistically independent and identically distributed gaussian random variables with variance $\sigma_n^2 = \frac{1}{2}N_0$. The

magnitude of the cross-correlators

$$C(\mathbf{r}, \mathbf{s}_m) = \mathbf{r} \cdot \mathbf{s}_m = \sum_{k=1}^{M/2} r_k s_{mk}, \qquad m = 1, 2, \ldots, \tfrac{1}{2}M \tag{5-2-32}$$

while the sign of this largest term is used to decide whether $s_m(t)$ or $-s_m(t)$ was transmitted. According to this decision rule, the probability of a correct decision is equal to the probability that $r_1 = \sqrt{\mathcal{E}_s} + n_1 > 0$ and r_1 exceeds $|r_m| = |n_m|$ for $m = 2, 3, \ldots, \frac{1}{2}M$. But

is similar to that for orthogonal signals (see Fig. 5-2-5). However, in this case, the probability of error for $M = 4$ is greater than that for $M = 2$. This is due to the fact that we have plotted the symbol error probability P_M in Fig. 5-2-6. If we plotted the equivalent bit error probability, we should find that the graphs for $M = 2$ and $M = 4$ coincide. As in the case of orthogonal signals, as $M \to \infty$ (or $k \to \infty$), the minimum required $\mathscr{E}_b/N_0$ to achieve arbitrarily small probability of error is -1.6 dB, the Shannon limit.

5-2-4 Probability of Error for Simplex Signals

Next we consider the probability of error for M simplex signals. Recall from Section 4-3 that simplex signals are a set of M equally correlated signals with mutual cross-correlation coefficient $\rho_{mn} = -1/(M-1)$. These signals have the same minimum separation of $\sqrt{2\mathscr{E}_s}$ between adjacent signal points in M-dimensional space as orthogonal signals. They achieve this mutual separation with a transmitted energy of $\mathscr{E}_s(M-1)/M$, which is less than that required for orthogonal signals by a factor of $(M-1)/M$. Consequently, the probability of error for simplex signals is identical to the probability of error for orthogonal signals, but this performance is achieved with a saving of

$$10 \log (1 - \rho) = 10 \log \frac{M}{M-1} \text{ dB} \tag{5-2-35}$$

in SNR. For $M = 2$, the saving is 3 db. However, as M is increased, the saving in SNR approaches 0 dB.

5-2-5 Probability of Error for M-ary Binary-Coded Signals

We have shown in Section 4-3 that binary-coded signal waveforms are represented by the signal vectors

$$\mathbf{s}_m = [s_{m1} \quad s_{m2} \quad \cdots \quad s_{mN}], \qquad m = 1, 2, \ldots, M$$

where $s_{mj} = \pm\sqrt{\mathscr{E}/N}$ for all m and j. N is the block length of the code, and is also the dimension of the M signal waveforms.

If $d_{\min}^{(e)}$ is the minimum euclidean distance of the M signal waveforms then the probability of a symbol error is upper-bounded as

$$\begin{aligned} P_m &< (M-1)P_b = (M-1)Q\left(\sqrt{\frac{(d_{\min}^{(e)})^2}{2N_0}}\right) \\ &< 2^k \exp\left[-\frac{(d_{\min}^{(e)})^2}{4N_0}\right] \end{aligned} \tag{5-2-36}$$

The value of the minimum euclidean distance will depend on the selection of the code words, i.e., the design of the code.

5-2-6 Probability of Error for M-ary PAM

Recall that M-ary PAM signals are represented geometrically as M one-dimensional signal points with value

$$s_m = \sqrt{\tfrac{1}{2}\mathscr{E}_g} A_m, \qquad m = 1, 2, \ldots, M \tag{5-2-37}$$

where $\mathscr{E}_g$ is the energy of the basic signal pulse $g(t)$. The amplitude values may be expressed as

$$A_m = (2m - 1 - M)d, \qquad m = 1, 2, \ldots, M \tag{5-3-38}$$

where the euclidean distance between adjacent signal points is $d\sqrt{2\mathscr{E}_g}$.

$$\mathscr{E}_{av} = \frac{1}{M}\sum_{m=1}^{M} \mathscr{E}_m = \frac{d^2\mathscr{E}_g}{2M}\sum_{m=1}^{M}(2m - 1 - M)^2$$

$$= \frac{d^2\mathscr{E}_g}{2M}[\tfrac{1}{3}M(M^2 - 1)] = \tfrac{1}{6}(M^2 - 1)\, d^2\mathscr{E}_g \tag{5-2-39}$$

Equivalently, we may characterize these signals in terms of their average power, which is

$$P_{av} = \frac{\mathscr{E}_{av}}{T} = \tfrac{1}{6}(M^2 - 1)\frac{d^2\mathscr{E}_g}{T} \tag{5-2-40}$$

The average probability of error for M-ary PAM can be determined from the decision rule that maximizes the correlation metrics given by (5-1-44). Equivalently, the detector compares the demodulator output r with a set of $M - 1$ thresholds, which are placed at the midpoints of successive amplitude levels, as shown in Fig. 5-2-7. Thus, a decision is made in favor of the amplitude level that is closest to r.

The placing of the thresholds as shown in Fig. 5-2-7 helps in evaluating the probability of error. We note that if the mth amplitude level is transmitted, the demodulator output is

$$r = s_m + n = \sqrt{\tfrac{1}{2}\mathscr{E}_g} A_m + n \tag{5-2-41}$$

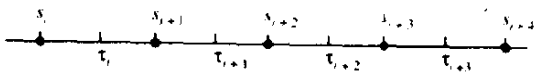

FIGURE 5-2-7 Placement of thresholds at midpoints of successive amplitude levels.

where the noise variable n has zero mean and variance $\sigma_n^2 = \frac{1}{2}N_0$. On the basis that all amplitude levels are equally likely a priori, the average probability of a symbol error is simply the probability that the noise variable n exceeds in magnitude one-half of the distance between levels. However, when either one of the two outside levels $\pm(M-1)$ is transmitted, an error can occur in one direction only. Thus, we have

$$\begin{aligned} P_M &= \frac{M-1}{M} P(|r - s_m| > d\sqrt{\tfrac{1}{2}\mathscr{E}_g}) \\ &= \frac{M-1}{M} \frac{2}{\sqrt{\pi N_0}} \int_{d\sqrt{\mathscr{E}_g/2}}^{\infty} e^{-x^2/N_0}\, dx \\ &= \frac{M-1}{M} \frac{2}{\sqrt{2\pi}} \int_{\sqrt{d^2\mathscr{E}_g/N_0}}^{\infty} e^{-x^2/2}\, dx \\ &= \frac{2(M-1)}{M} Q\left(\sqrt{\frac{d^2\mathscr{E}_g}{N_0}}\right) \end{aligned} \tag{5-2-42}$$

The error probability in (5-2-42) can also be expressed in terms of the average transmitted power. From (5-2-40), we note that

$$d^2\mathscr{E}_g = \frac{6}{M^2-1} P_{\text{av}} T \tag{5-2-43}$$

By substituting for $d^2\mathscr{E}_g$ in (5-2-42), we obtain the average probability of a symbol error for PAM in terms of the average power as

$$P_M = \frac{2(M-1)}{M} Q\left(\sqrt{\frac{6P_{\text{av}}T}{(M^2-1)N_0}}\right) \tag{5-2-44}$$

or, equivalently,

$$P_M = \frac{2(M-1)}{M} Q\left(\sqrt{\frac{6\mathscr{E}_{\text{av}}}{(M^2-1)N_0}}\right) \tag{5-2-45}$$

where $\mathscr{E}_{\text{av}} = P_{\text{av}}T$ is the average energy.

In plotting the probability of a symbol error for M-ary signals such as M-ary PAM, it is customary to use the SNR per bit as the basic parameter. Since $T = kT_b$ and $k = \log_2 M$, (5-2-45) may be expressed as

$$P_M = \frac{2(M-1)}{M} Q\left(\sqrt{\frac{(6\log_2 M)\mathscr{E}_{b\,\text{av}}}{(M^2-1)N_0}}\right) \tag{5-2-46}$$

where $\mathscr{E}_{b\text{av}} = P_{\text{av}}T_b$ is the average bit energy and $\mathscr{E}_{b\text{av}}/N_0$ is the average SNR

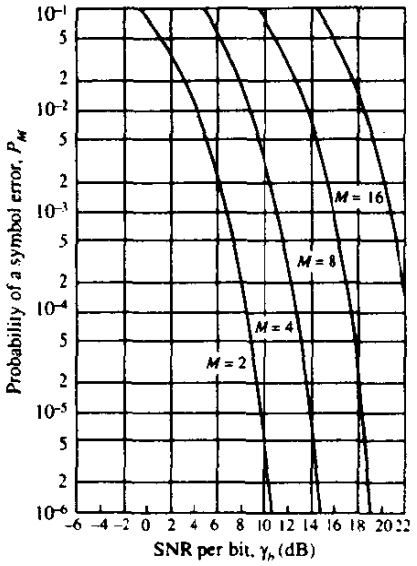

FIGURE 5-2-8 Probability of a symbol error for PAM.

per bit. Figure 5-2-8 illustrates the probability of a symbol error as a function of $10\log_{10} \mathscr{E}_{b\,\mathrm{av}}/N_0$, with M as a parameter. Note that the case $M = 2$ corresponds to the error probability for binary antipodal signals. Also observe that the SNR per bit increases by over 4 dB for every factor-of-two increase in M. For large M, the additional SNR per bit required to increase M by a factor of two approaches 6 dB.

5-2-7 Probability of Error For M-ary PSK

Recall from Section 4-3 that digital phase-modulated signal waveforms may be expressed as

$$\mathbf{s}_m(t) = g(t)\cos\left[2\pi f_c t + \frac{2\pi}{M}(m-1)\right], \quad 1 \leq m \leq M, \quad 0 \leq t \leq T \tag{5-2-47}$$

and have the vector representation

$$\mathbf{s}_m = \left[\sqrt{\mathscr{E}_s}\cos\frac{2\pi}{M}(m-1) \quad \sqrt{\mathscr{E}_s}\sin\frac{2\pi}{M}(m-1)\right] \tag{5-2-48}$$

where $\mathscr{E}_s = \frac{1}{2}\mathscr{E}_g$ is the energy in each of the waveforms and $g(t)$ is the pulse shape of the transmitted signal. Since the signal waveforms have equal energy, the optimum detector for the AWGN channel given by (5-1-44) computes the correlation metrics

$$C(\mathbf{r}, \mathbf{s}_m) = \mathbf{r}\cdot\mathbf{s}_m, \quad m = 1, 2, \ldots, M \tag{5-2-49}$$

In other words, the received signal vector $\mathbf{r} = [r_1 \quad r_2]$ is projected onto each of

the M possible signal vectors and a decision is made in favor of the signal with the largest projection.

The correlation detector described above is equivalent to a phase detector that computes the phase of the received signal from $\mathbf{r}$ and selects the signal vector $\mathbf{s}_m$ whose phase is closest to $\mathbf{r}$. Since the phase of $\mathbf{r}$ is

$$\Theta_r = \tan^{-1}\frac{r_2}{r_1} \tag{5-2-50}$$

we will determine the pdf of Θ_r, from which we shall compute the probability of error.

Let us consider the case in which the transmitted signal phase is $\Theta_r = 0$, corresponding to the signal $s_1(t)$. Hence, the transmitted signal vector is

$$s_0 = [\sqrt{\mathscr{E}_s} \quad 0] \tag{5-2-51}$$

and the received signal vector has components

$$\begin{aligned} r_1 &= \sqrt{\mathscr{E}_s} + n_1 \\ r_2 &= n_2 \end{aligned} \tag{5-2-52}$$

Because n_1 and n_2 are jointly gaussian random variables, it follows that r_1 and r_2 are jointly gaussian random variables with $E(r_1) = \sqrt{\mathscr{E}_s}$, $E(r_2) = 0$, and $\sigma_{r_1}^2 = \sigma_{r_2}^2 = \frac{1}{2}N_0 = \sigma_r^2$. Consequently,

$$p_r(r_1, r_2) = \frac{1}{2\pi\sigma_r^2}\exp\left[-\frac{(r_1 - \sqrt{\mathscr{E}_s})^2 + r_2^2}{2\sigma_r^2}\right] \tag{5-2-53}$$

The pdf of the phase Θ_r is obtained by a change in variables from (r_1, r_2) to

$$\begin{aligned} V &= \sqrt{r_1^2 + r_2^2} \\ \Theta_r &= \tan^{-1}(r_2/r_1) \end{aligned} \tag{5-2-54}$$

This yields the joint pdf

$$p_{V,\Theta_r}(V, \Theta_r) = \frac{V}{2\pi\sigma_r^2}\exp\left(-\frac{V^2 + \mathscr{E}_s - 2\sqrt{\mathscr{E}_s}\,V\cos\Theta_r}{2\sigma_r^2}\right)$$

Integration of $p_{V,\Theta_r}(V, \Theta_r)$ over the range of V yields $p_{\Theta_r}(\Theta_r)$. That is,

$$\begin{aligned} p_{\Theta_r}(\Theta_r) &= \int_0^\infty p_{V,\Theta_r}(V, \Theta_r)\,dV \\ &= \frac{1}{2\pi}e^{-2\gamma_s\sin^2\Theta_r}\int_0^\infty Ve^{-(V-\sqrt{4\gamma_s}\cos\Theta_r)^2/2}\,dV \end{aligned} \tag{5-2-55}$$

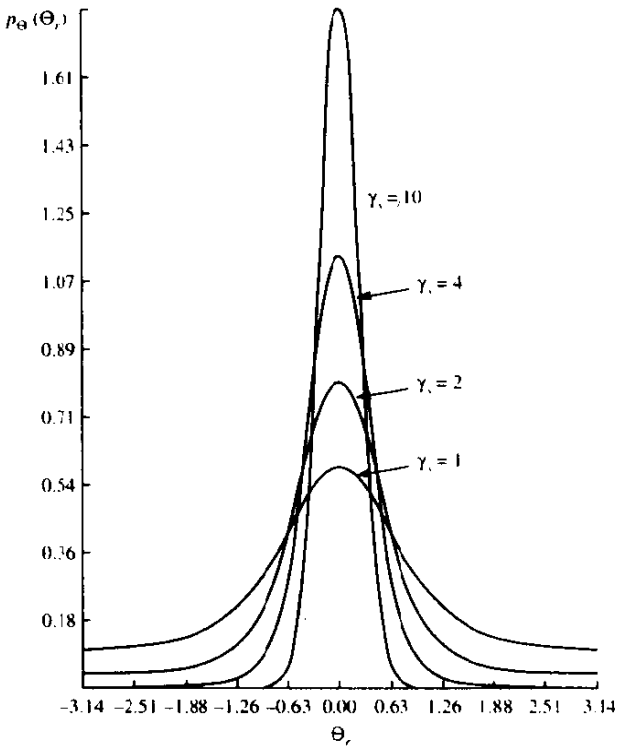

FIGURE 5-2-9 Probability density function $p_{\Theta_r}(\Theta_r)$ for $\gamma_s = 1, 2, 4$ and 10.

where for convenience, we have defined the symbol SNR as $\gamma_s = \mathscr{E}_s/N_0$. Figure 5-2-9 illustrates $f_{\Theta_r}(\Theta_r)$ for several values of the SNR parameter γ_s when the transmitted phase is zero. Note that $f_{\Theta_r}(\Theta_r)$ becomes narrower and more peaked about $\Theta_r = 0$ as the SNR γ_s increases.

When $s_1(t)$ is transmitted, a decision error is made if the noise causes the phase to fall outside the range $-\pi/M \leq \Theta_r \leq \pi/M$. Hence, the probability of a symbol error is

$$P_M = 1 - \int_{-\pi/M}^{\pi/M} p_{\Theta_r}(\Theta_r)\, d\Theta_r \tag{5-2-56}$$

In general, the integral of $p_{\Theta_r}(\Theta)$ does not reduce to a simple form and must be evaluated numerically, except for $M = 2$ and $M = 4$.

For binary phase modulation, the two signals $s_1(t)$ and $s_2(t)$ are antipodal, and, hence, the error probability is

$$P_2 = Q\left(\sqrt{\frac{2\mathscr{E}_b}{N_0}}\right) \tag{5-2-57}$$

When $M = 4$, we have in effect two binary phase-modulation signals in phase

quadrature. Since there is no crosstalk or interference between the signals on the two quadrature carriers, the bit error probability is identical to that in (5-2-57). On the other hand, the symbol error probability for $M = 4$ is determined by noting that

$$P_c = (1 - P_2)^2 = \left[1 - Q\left(\sqrt{\frac{2\mathscr{E}_b}{N_0}}\right)\right]^2 \tag{5-2-58}$$

where P_c is the probability of a correct decision for the 2-bit symbol. The result (5-2-58) follows from the statistical independence of the noise on the quadrature carriers. Therefore, the symbol error probability for $M = 4$ is

$$\begin{aligned} P_4 &= 1 - P_c \\ &= 2Q\left(\sqrt{\frac{2\mathscr{E}_b}{N_0}}\right)\left[1 - \tfrac{1}{2}Q\left(\sqrt{\frac{2\mathscr{E}_b}{N_0}}\right)\right] \end{aligned} \tag{5-2-59}$$

For $M > 4$, the symbol error probability P_M is obtained by numerically integrating (5-2-55). Figure 5-2-10 illustrates this error probability as a function of the SNR per bit for $M = 2$, 4, 8, 16, and 32. The graphs clearly illustrate the penalty in SNR per bit as M increases beyond $M = 4$. For example, at $P_M = 10^{-5}$, the difference between $M = 4$ and $M = 8$ is approximately 4 dB, and the difference between $M = 8$ and $M = 16$ is approximately 5 dB. For large values of M, doubling the number of phases requires an additional 6 dB/bit to achieve the same performance.

An approximation to the error probability for large values of M and for

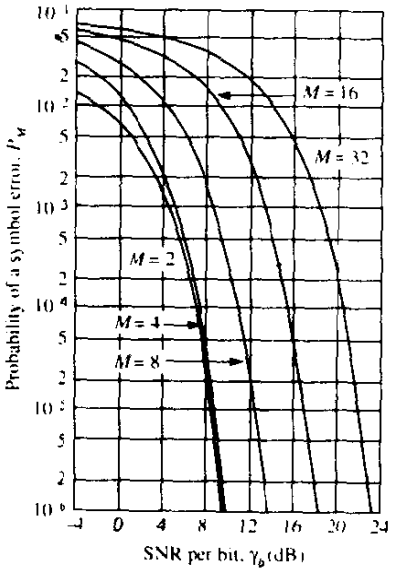

FIGURE 5-2-10 Probability of a symbol error for PSK signals.

large SNR may be obtained by first approximating $p_{\Theta_r}(\Theta)$. For $\mathcal{E}_s/N_0 \gg 1$ and $|\Theta_r| \leq \frac{1}{2}\pi$, $p_{\Theta_r}(\Theta_r)$ is well approximated as

$$p_{\Theta_r}(\Theta_r) \approx \sqrt{\frac{2\gamma_s}{\pi}} \cos \Theta_r e^{-2\gamma_s \sin^2 \Theta_r} \tag{5-2-60}$$

By substituting for $p_{\Theta_r}(\Theta_r)$ in (5-2-56) and performing the change in variable from Θ_r to $u = \sqrt{2\gamma_s} \sin \Theta_r$, we find that

$$\begin{aligned} P_M &\approx 1 - \int_{-\pi/M}^{\pi/M} \sqrt{\frac{2\gamma_s}{\pi}} \cos \Theta_r e^{-2\gamma_s \sin^2 \Theta_r} \, d\Theta_r \\ &\approx \frac{2}{\sqrt{\pi}} \int_{\sqrt{2\gamma_s} \sin(\pi/M)}^{\infty} e^{-u^2/2} \, du \\ &= 2Q\left(\sqrt{2\gamma_s} \sin \frac{\pi}{M}\right) = 2Q\left(\sqrt{2k\gamma_b} \sin \frac{\pi}{M}\right) \end{aligned} \tag{5-2-61}$$

where $k = \log_2 M$ and $\gamma_s = k\gamma_b$. Note that this approximation to the error probability is good for all values of M. For example, when $M = 2$ and $M = 4$, we have $P_2 = P_4 = 2Q(\sqrt{2\gamma_s})$, which compares favorably (a factor-of-two difference) with the exact probability given by (5-2-57).

The equivalent bit error probability for M-ary PSK is rather tedious to derive due to its dependence on the mapping of k-bit symbols into the corresponding signal phases. When a Gray code is used in the mapping, two k-bit symbols corresponding to adjacent signal phases differ in only a single bit. Since the most probable errors due to noise result in the erroneous selection of an adjacent phase to the true phase, most k-bit symbol errors contain only a single-bit error. Hence, the equivalent bit error probability for M-ary PSK is well approximated as

$$P_b \approx \frac{1}{k} P_M \tag{5-2-62}$$

Our treatment of the demodulation of PSK signals assumed that the demodulator had a perfect estimate of the carrier phase available. In practice, however, the carrier phase is extracted from the received signal by performing some nonlinear operation that introduces a phase ambiguity. For example, in binary PSK, the signal is often squared in order to remove the modulation, and the double-frequency component that is generated is filtered and divided by 2 in frequency in order to extract an estimate of the carrier frequency and phase ϕ. These operations result in a phase ambiguity of 180° in the carrier phase. Similarly, in four-phase PSK, the received signal is raised to the fourth power in order to remove the digital modulation, and the resulting fourth harmonic of the carrier frequency is filtered and divided by 4 in order to extract the carrier component. These operations yield a carrier frequency component containing the estimate of the carrier phase ϕ, but there are phase ambiguities of ±90° and 180° in the phase estimate. Consequently, we do not have an absolute estimate of the carrier phase for demodulation.

The phase ambiguity problem resulting from the estimation of the carrier phase ϕ can be overcome by encoding the information in phase differences between successive signal transmissions as opposed to absolute phase encoding. For example, in binary PSK, the information bit 1 may be transmitted by shifting the phase of the carrier by 180° relative to the previous carrier phase, while the information bit 0 is transmitted by a zero phase shift relative to the phase in the previous signaling interval. In four-phase PSK, the relative phase shifts between successive intervals are 0, 90°, 180°, and −90°, corresponding to the information bits 00, 01, 11, and 10, respectively. The generalization to $M > 4$ phases is straightforward. The PSK signals resulting from the encoding process are said to be *differentially encoded.* The encoding is performed by a relatively simple logic circuit preceding the modulator.

Demodulation of the differentially encoded PSK signal is performed as described above, by ignoring the phase ambiguities. Thus, the received signal is demodulated and detected to one of the M possible transmitted phases in each signaling interval. Following the detector is a relatively simple phase comparator that compares the phases of the demodulated signal over two consecutive intervals in order to extract the information.

Coherent demodulation of differently encoded PSK results in a higher probability of error than the error probability derived for absolute phase encoding. With differentially encoded PSK, an error in the demodulated phase of the signal in any given interval will usually result in decoding errors over two consecutive signaling intervals. This is especially the case for error probabilities below 0.1. Therefore, the probability of error in differentially encoded M-ary PSK is approximately twice the probability of error for M-ary PSK with absolute phase encoding. However, this factor-of-two increase in the error probability translates into a relatively small loss in SNR.

5-2-8 Differential PSK (DPSK) and its Performance

A differentially encoded phase-modulated signal also allows another type of demodulation that does not require the estimation of the carrier phase.† Instead, the received signal in any given signaling interval is compared to the phase of the received signal from the preceding signaling interval. To elaborate, suppose that we demodulate the differentially encoded signal by multiplying $r(t)$ by $\cos 2\pi f_c t$ and $\sin 2\pi f_c t$ and integrating the two products over the interval T. At the kth signaling interval, the demodulator output is

$$\mathbf{r}_k = [\sqrt{\mathscr{E}_s}\cos(\theta_k - \phi) + n_{k1} \quad \sqrt{\mathscr{E}_s}\sin(\theta_k - \phi) + n_{k2}]$$

or, equivalently,

$$r_k = \sqrt{\mathscr{E}_s}e^{j(\theta_k - \phi)} + n_k \tag{5-2-63}$$

† Because no phase estimation is required, DPSK is often considered to be a noncoherent communication technique. We take the view that DPSK represents a form of digital phase modulation in the extreme case where the phase estimate is derived only from the previous symbol interval.

where θ_k is the phase angle of the transmitted signal at the kth signaling interval, ϕ is the carrier phase, and $n_k = n_{k_1} + jn_{k_2}$ is the noise vector. Similarly, the received signal vector at the output of the demodulator in the preceding signaling interval is

$$r_{k-1} = \sqrt{\mathscr{E}_s} e^{j(\theta_{k-1} - \phi)} + n_{k-1} \tag{5-2-64}$$

The decision variable for the phase detector is the phase difference between these two complex numbers. Equivalently, we can project r_k onto r_{k-1} and use the phase of the resulting complex number; that is,

$$r_k r_{k-1}^* = \mathscr{E}_s e^{j(\theta_k - \theta_{k-1})} + \sqrt{\mathscr{E}_s} e^{j(\theta_k - \phi)} n_{k-1}^* + \sqrt{\mathscr{E}_s} e^{-j(\theta_{k-1} - \phi)} n_k + n_k n_{k-1}^* \tag{5-2-65}$$

which, in the absence of noise, yields the phase difference $\theta_k - \theta_{k-1}$. Thus, the mean value of $r_k r_{k-1}^*$ is independent of the carrier phase. Differentially encoded PSK signaling that is demodulated and detected as described above is called *differential PSK* (DPSK).

The demodulation and detection of DSPK using matched filters is illustrated in Figure 5-2-11. If the pulse $g(t)$ is rectangular, the matched filters may be replaced by integrate-and-dump filters.

Let us now consider the evaluation of the error probability performance of a DPSK demodulator and detector. The derivation of the exact value of the probability of error for M-ary DPSK is extremely difficult, except for $M = 2$. The major difficulty is encountered in the determination of the pdf for the phase of the random variable $r_k r_{k-1}^*$, given by (5-2-65). However, an approximation to the performance of DPSK is easily obtained, as we now demonstrate.

Without loss of generality, suppose the phase difference $\theta_k - \theta_{k-1} = 0$. Furthermore, the exponential factors $e^{-j(\theta_{k-1} - \phi)}$ and $e^{j(\theta_k - \phi)}$ in (5-2-65) can be absorbed into the gaussian noise components n_{k-1} and n_k, without changing their statistical properties. Therefore, $r_k r_{k-1}^*$ in (5-2-65) can be expressed as

$$r_k r_{k-1}^* = \mathscr{E}_s + \sqrt{\mathscr{E}_s}(n_k + n_{k-1}^*) + n_k n_{k-1}^* \tag{5-2-66}$$

The complication in determining the pdf of the phase is the term $n_k n_{k-1}^*$. However, at SNRs of practial interest, the term $n_k n_{k-1}^*$ is small relative to the dominant noise term $\sqrt{\mathscr{E}_s}(n_k + n_{k-1}^*)$. If we neglect the term $n_k n_{k-1}^*$ and we

FIGURE 5-2-11 Block diagram of DPSK demodulator.

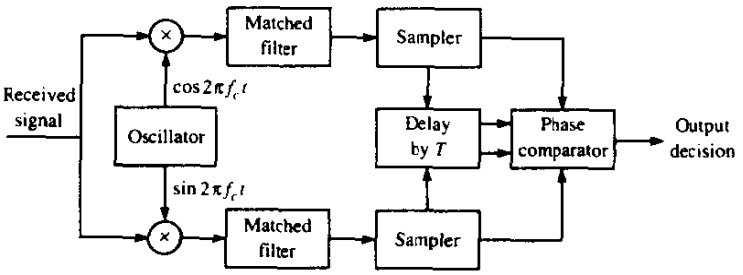

also normalize $r_k r_{k-1}^*$ by dividing through by $\sqrt{\mathscr{E}_s}$, the new set of decision metrics becomes

$$\begin{aligned} x &= \sqrt{\mathscr{E}_s} + \text{Re}\,(n_k + n_{k-1}^*) \\ y &= \text{Im}\,(n_k + n_{k-1}^*) \end{aligned} \tag{5-2-67}$$

The variables x and y are uncorrelated gaussian random variables with identical variances $\sigma_n^2 = N_0$. The phase is

$$\Theta_r = \tan^{-1}\frac{y}{x} \tag{5-2-68}$$

At this stage, we have a problem that is identical to the one we solved previously for phase-coherent demodulation. The only difference is that the noise variance is now twice as large as in the case of PSK. Thus we conclude that the performance of DPSK is 3 dB poorer than that for PSK. This result is relatively good for $M \geq 4$, but it is pessimistic for $M = 2$ in the sense that the loss in binary DPSK relative to binary PSK is less than 3 db at large SNR. This is demonstrated below.

In binary DPSK, the two possible transmitted phase differences are 0 and π rad. As a consequence, only the real part of $r_k r_{k-1}^*$ is needed for recovering the information. Using (5-2-67), we express the real part as

$$\text{Re}\,(r_k r_{k-1}^*) = \tfrac{1}{2}(r_k r_{k-1}^* + r_k^* r_{k-1})$$

Because the phase difference between the two successive signaling intervals is zero, an error is made if $\text{Re}\,(r_k r_{k-1}^*) < 0$. The probability that $r_k r_{k-1}^* + r_k^* r_{k-1} < 0$ is a special case of a derivation, given in Appendix B concerned with the probability that a general quadratic form in complex-valued gaussian random variables is less than zero. The general form for this probability is given by (B-21) of Appendix B, and it depends entirely on the first and second moments of the complex-valued gaussian random variables r_k and r_{k-1}. Upon evaluating the moments and the parameters that are functions of the moments, we obtain the probability of error for binary DPSK in the form

$$P_b = \tfrac{1}{2}e^{-\mathscr{E}_b/N_0} \tag{5-2-69}$$

where $\mathscr{E}_b/N_0$ is the SNR per bit.

The graph is shown in Fig. 5-2-12. Also shown in that illustration is the probability of error for binary, coherent PSK. We observe that at error probabilities of $P_b \leq 10^{-3}$ the difference in SNR between binary PSK and binary DPSK is less than 3 dB. In fact, at $P_b \leq 10^{-5}$, the difference in SNR is less than 1 dB.

The probability of a binary digit error for four-phase DPSK with Gray coding can be expressed in terms of well-known functions, but its derivation is quite involved. We simply state the result at this point and refer the interested reader to Appendix C for the details of derivation. It is expressed in the form

$$P_b = Q_1(a, b) - \tfrac{1}{2}I_0(ab)\exp\left[-\tfrac{1}{2}(a^2 + b^2)\right] \tag{5-2-70}$$

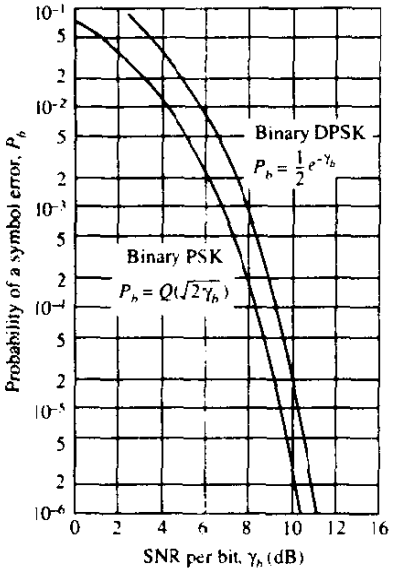

FIGURE 5-2-12 Probability of error for binary PSK and DPSK.

where $Q_1(a, b)$ is the Markum Q function defined by (2-1-122) and (2-1-123), $I_0(x)$ is the modified Bessel function of order zero, defined by (2-1-120), and the parameters a and b are defined as

$$a = \sqrt{2\gamma_b(1 - \sqrt{\tfrac{1}{2}})}$$
$$b = \sqrt{2\gamma_b(1 + \sqrt{\tfrac{1}{2}})} \tag{5-2-71}$$

Figure 5-2-13 illustrates the probability of a binary digit error for two- and

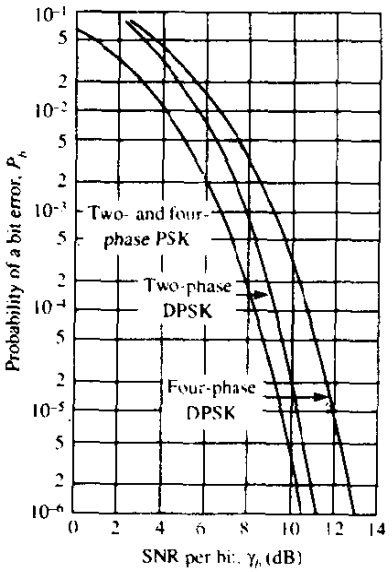

FIGURE 5-2-13 Probability of bit error for binary and four-phase PSK and DPSK.

four-phase DPSK and coherent PSK signaling obtained from evaluating the exact formulas derived in this section. Since binary DPSK is only slightly inferior to binary PSK at large SNR, and DPSK does not require an elaborate method for estimating the carrier phase, it is often used in digital communications systems. On the other hand, four-phase DPSK is approximately 2.3 dB poorer in performance than four-phase PSK at large SNR. Consequently the choice between these two four-phase systems is not as clear cut. One must weigh the 2.3 dB loss against the reduction in implementation complexity.

5-2-9 Probability of Error for QAM

Recall from Section 4-3 that QAM signal waveforms may be expressed as

$$s_m(t) = A_{mc}g(t)\cos 2\pi f_c t - A_{ms}g(t)\sin 2\pi f_c t, \quad 0 \leq t \leq T \qquad (5\text{-}2\text{-}72)$$

where A_{mc} and A_{ms} are the information-bearing signal amplitudes of the quadrature carriers and $g(t)$ is the signal pulse. The vector representation of these waveforms is

$$\mathbf{s}_m = [A_{mc}\sqrt{\tfrac{1}{2}\mathscr{E}_g} \quad A_{ms}\sqrt{\tfrac{1}{2}\mathscr{E}_g}] \qquad (5\text{-}2\text{-}73)$$

To determine the probability of error for QAM, we must specify the signal point constellation. We begin with QAM signal sets that have $M = 4$ points. Figure 5-2-14 illustrates two four-point signal sets. The first is a four-phase modulated signal and the second is a QAM signal with two amplitude levels, labeled A_1 and A_2, and four phases. Because the probability of error is dominated by the minimum distance between pairs of signal points, let us impose the condition that $d_{\min}^{(e)} = 2A$ for both signal constellations and let us evaluate the average transmitter power, based on the premise that all signal points are equally probable. For the four-phase signal, we have

$$P_{\text{av}} = \tfrac{1}{4}(4)2A^2 = 2A^2 \qquad (5\text{-}2\text{-}74)$$

For the two-amplitude, four-phase QAM, we place the points on circles of radii A and $\sqrt{3}A$. Thus, $d_{\min}^{(e)} = 2A$, and

$$P_{\text{av}} = \tfrac{1}{4}[2(3A^2) + 2A^2] = 2A^2 \qquad (5\text{-}2\text{-}75)$$

which is the same average power as the $M = 4$-phase signal constellation. Hence, for all practical purposes, the error rate performance of the two signal

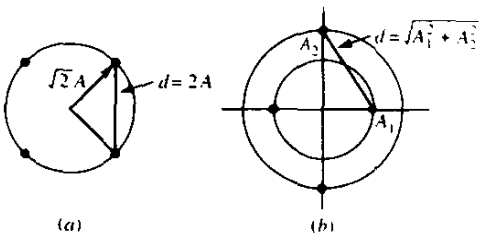

FIGURE 5-2-14 Two four-point signal constellations.

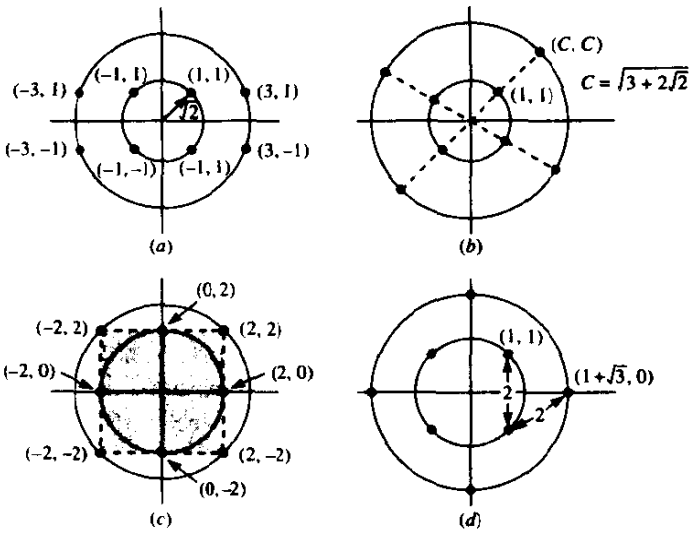

FIGURE 5-2-15 Four eight-point QAM signal constellations.

sets is the same. In other words, there is no advantage of the two-amplitude QAM signal set over $M = 4$-phase modulation.

Next, let us consider $M = 8$ QAM. In this case, there are many possible signal constellations. We shall consider the four signal constellations shown in Fig. 5-2-15, all of which consist of two amplitudes and have a minimum distance between signal points of $2A$. The coordinates (A_{mc}, A_{ms}) for each signal point, normalized by A, are given in the figure. Assuming that the signal points are equally probable, the average transmitted signal power is

$$P_{\text{av}} = \frac{1}{M}\sum_{m=1}^{M}(A_{mc}^2 + A_{ms}^2)$$

$$= \frac{A^2}{M}\sum_{m=1}^{M}(a_{mc}^2 + a_{mc}^2) \tag{5-2-76}$$

where (a_{mc}, a_{ms}) are the coordinates of the signal points, normalized by A.

The two signal sets (a) and (c) in Fig. 5-2-15 contain signal points that fall on a rectangular grid and have $P_{\text{av}} = 6A^2$. The signal set (b) requires an average transmitted power $P_{\text{av}} = 6.83A^2$, and (d) requires $P_{\text{av}} = 4.73A^2$. Therefore, the fourth signal set requires approximately 1 dB less power than the first two and 1.6 dB less power than the third to achieve the same probability of error. This signal constellation is known to be the best eight-point QAM constellation because it requires the least power for a given minimum distance between signal points.

For $M \geq 16$, there are many more possibilities for selecting the QAM signal points in the two-dimensional space. For example, we may choose a circular multiamplitude constellation for $M = 16$, as shown in Fig. 4-3-4. In this case,

the signal points at a given amplitude level are phase-rotated by $\frac{1}{4}\pi$ relative to the signal points at adjacent amplitude levels. This 16-QAM constellation is a generalization of the optimum 8-QAM constellation. However, the circular 16-QAM constallation is not the best 16-point QAM signal constellation for the AWGN channel.

Rectangular QAM signal constellations have the distinct advantage of being easily generated as two PAM signals impressed on phase-quadrature carriers. In addition, they are easily demodulated. Although they are not the best M-ary QAM signal constellations for $M \geq 16$, the average transmitted power required to achieve a given minimum distance is only slightly greater than the average power required for the best M-ary QAM signal constellation. For these reasons, rectangular M-ary QAM signals are most frequently used in practice.

For rectangular signal constellations in which $M = 2^k$, where k is even, the QAM signal constellation is equivalent to two PAM signals on quadrature carriers, each having $\sqrt{M} = 2^{k/2}$ signal points. Since the signals in the phase-quadrature components can be perfectly separated at the demodulator, the probability of error for QAM is easily determined from the probability of error for PAM. Specifically, the probability of a correct decision for the M-ary QAM system is

$$P_c = (1 - P_{\sqrt{M}})^2 \tag{5-2-77}$$

where $P_{\sqrt{M}}$ is the probability of error of a $\sqrt{M}$ − ary PAM with one-half the average power in each quadrature signal of the equivalent QAM system. By appropriately modifying the probability of error for M-ary PAM, we obtain

$$P_{\sqrt{M}} = 2\left(1 - \frac{1}{\sqrt{M}}\right)Q\left(\sqrt{\frac{3}{M-1}\frac{\mathscr{E}_{av}}{N_0}}\right) \tag{5-2-78}$$

where $\mathscr{E}_{av}/N_0$ is the average SNR per symbol. Therefore, the probability of a symbol error for the M-ary QAM is

$$P_M = 1 - (1 - P_{\sqrt{M}})^2 \tag{5-2-79}$$

Note that this result is exact for $M = 2^k$ when k is even. On the other hand, when k is odd, there is no equivalent $\sqrt{M}$ − ary PAM system. This is no problem, however, because it is rather easy to determine the error rate for a rectangular signal set. If we employ the optimum detector that bases its decisions on the optimum distance metrics given by (5-1-43), it is relatively straightforward to show that the symbol error probability is tightly upper-bounded as

$$\begin{aligned} P_M &\leq 1 - \left[1 - 2Q\left(\sqrt{\frac{3\mathscr{E}_{av}}{(M-1)N_0}}\right)\right]^2 \\ &\leq 4Q\left(\sqrt{\frac{3k\mathscr{E}_{b\,av}}{(M-1)N_0}}\right) \end{aligned} \tag{5-2-80}$$

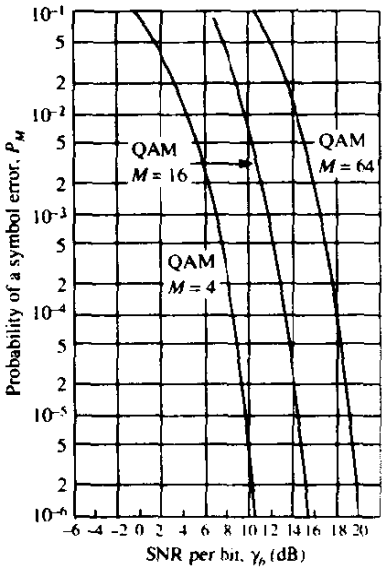

FIGURE 5-2-16 Probability of a symbol error for QAM.

for any $k \geq 1$, where $\mathscr{E}_{b\,\mathrm{av}}/N_0$ is the average SNR per bit. The probability of a symbol error is plotted in Fig. 5-2-16 as a function of the average SNR per bit.

For non-rectangular QAM signal constellations, we may upper-bound the error probability by use of a union bound. An obvious upper bound is

$$P_M < (M-1)Q(\sqrt{[d_{\min}^{(e)}]^2/2N_0})$$

where $d_{\min}^{(e)}$ in the minimum euclidean distance between signal points. This bound may be loose when M is large. In such a case, we may approximate P_M by replacing $M-1$ by M_n, where M_n is the largest number of neighboring points that are at distance $d_{\min}^{(e)}$ from any constellation point.

It is interesting to compare the performance of QAM with that of PSK for any given signal size M, since both types of signals are two-dimensional. Recall that for M-ary PSK, the probability of a symbol error is approximated as

$$P_M \approx 2Q\left(\sqrt{2\gamma_s}\sin\frac{\pi}{M}\right) \tag{5-2-81}$$

where γ_s is the SNR per symbol. For M-ary QAM, we may use the expression (5-2-78). Since the error probability is dominated by the argument of the Q function, we may simply compare the arguments of Q for the two signal formats. Thus, the ratio of these two arguments is

$$\mathscr{R}_M = \frac{3/(M-1)}{2\sin^2(\pi/M)} \tag{5-2-82}$$

For example, when $M = 4$, we have $\mathscr{R}_M = 1$. Hence, 4-PSK and 4-QAM yield comparable performance for the same SNR per symbol. On the other hand,

TABLE 5-2-1 SNR ADVANTAGE OF M-ARY QAM OVER M-ARY PSK

M	$10 \log_{10} \mathcal{R}_M$
8	1.65
16	4.20
32	7.02
64	9.95

when $M > 4$ we find that $\mathcal{R}_M > 1$, so that M-ary QAM yields better performance than M-ary PSK. Table 5-2-1 illustrates the SNR advantage of QAM over PSK for several values of M. For example, we observe that 32-QAM has a 7 dB SNR advantage over 32-PSK.

5-2-10 Comparison of Digital Modulation Methods

The digital modulation methods described in this chapter can be compared in a number of ways. For example, one can compare them on the basis of the SNR required to achieve a specified probability of error. However, such a comparison would not be very meaningful, unless it were made on the basis of some constraint, such as a fixed data rate of transmission or, equivalently, on the basis of a fixed bandwidth. With this goal in mind, let us consider the bandwidth requirements for several modulation methods.

For multiphase signals, the channel bandwidth required is simply the bandwidth of the equivalent lowpass signal pulse $g(t)$, which depends on its detailed characteristics. For our purposes, we assume that $g(t)$ is a pulse of duration T and that its bandwidth W is approximately equal to the reciprocal of T. Thus, $W = 1/T$ and, since $T = k/R = (\log_2 M)/R$, it follows that

$$W = \frac{R}{\log_2 M} \tag{5-2-83}$$

Therefore, as M is increased, the channel bandwidth required, when the bit rate R is fixed, decreases. The bandwidth efficiency is measured by the bit rate to bandwidth ratio, which is

$$\frac{R}{W} = \log_2 M \tag{5-2-84}$$

The bandwidth-efficient method for transmitting PAM is single-sideband. Then, the channel bandwidth required to transmit the signal is approximately equal to $1/2T$ and, since $T = k/R = (\log_2 M)/R$, it follows that

$$\frac{R}{W} = 2 \log_2 M \tag{5-2-85}$$

This is a factor of two better than PSK.

In the case of QAM, we have two orthogonal carriers, with each carrier having a PAM signal. Thus, we double the rate relative to PAM. However, the QAM signal must be transmitted via double sideband. Consequently, QAM and PAM have the same bandwidth efficiency when the bandwidth is referenced to the bandpass signal.

Orthogonal signals have totally different bandwidth requirements. If the $M = 2^k$ orthogonal signals are constructed by means of orthogonal carriers with minimum frequency separation of $1/2T$ for orthogonality, the bandwidth required for transmission of $k = \log_2 M$ information bits is

$$W = \frac{M}{2T} = \frac{M}{2(k/R)} = \frac{M}{2\log_2 M} R \tag{5-2-86}$$

In this case, the bandwidth increases as M increases. Similar relationships obtain for simplex and biorthogonal signals. In the case of biothogonal signals, the required bandwidth is one half of that for orthogonal signals.

A compact and meaningful comparison of these modulation methods is one based on the normalized data rate R/W (bits per second per hertz of bandwidth) versus the SNR per bit ($\mathscr{E}_b/N_0$) required to achieve a given error probability. Figure 5-2-17 illustrates the graph of R/W versus SNR per bit for PAM, QAM, PSK, and orthogonal signals, for the case in which the error probability is $P_M = 10^{-5}$. We observe that in the case of PAM, QAM, and PSK, increasing M results in a higher bit rate-to-bandwidth ratio R/W. However, the cost of achieving the higher data rate is an increase in the SNR per bit. Consequently, these modulation methods are appropriate for communication channels that are bandwidth limited, where we desire a bit rate-to-bandwidth ratio $R/W > 1$ and where there is sufficiently high SNR to support increases in M. Telephone channels and digital microwave radio channels are examples of such bandlimited channels.

In contrast, M-ary orthogonal signals yield a bit rate-to-bandwidth ratio of $R/W \leq 1$. As M increases, R/W decreases due to an increase in the required channel bandwidth. However, the SNR per bit required to achieve a given error probability (in this case, $P_M = 10^{-5}$) decreases as M increases. Consequently, M-ary orthogonal signals are appropriate for power-limited channels that have sufficiently large bandwidth to accommodate a large number of signals. In this case, as $M \to \infty$, the error probability can be made as small as desired, provided that $\mathscr{E}_b/N_0 > 0.693$ (-1.6 dB). This is the minimum SNR per bit required to achieve reliable transmission in the limit as the channel bandwidth $W \to \infty$ and the corresponding bit rate-to-bandwidth ratio $R/W \to 0$.

Also shown in Fig. 5-2-17 is the graph for the normalized capacity of the bandlimited AWGN channel, which is due to Shannon (1948). The ratio C/W, where C ($= R$) is the capacity in bits/s, represents the highest achievable bit rate-to-bandwidth ratio on this channel. Hence, it serves as the upper bound

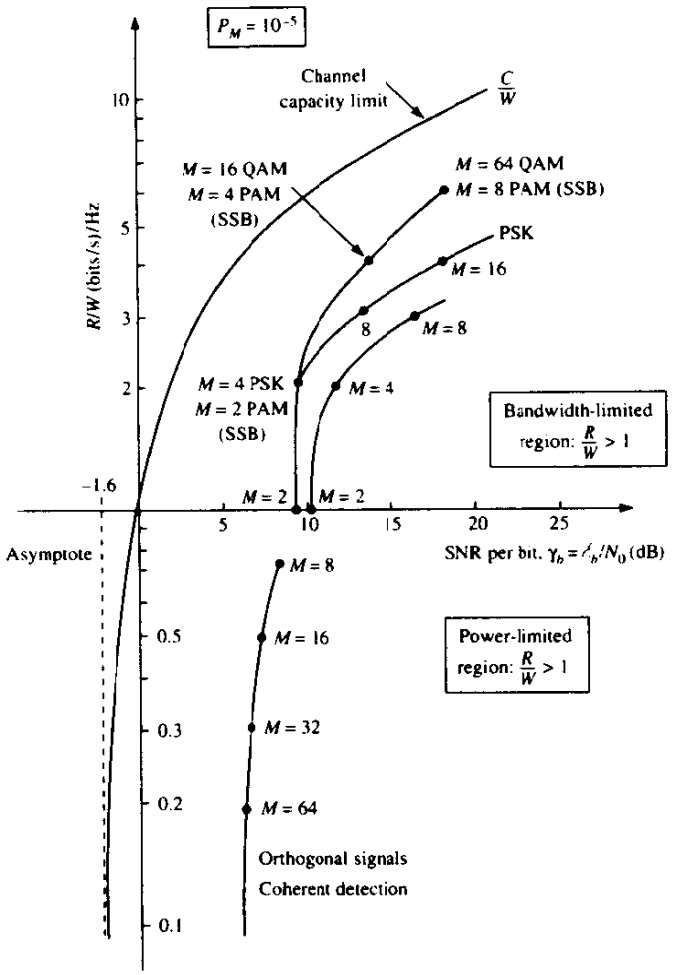

FIGURE 5-2-17 Comparison of several modulation methods at 10^{-5} symbol error probability.

on the bandwidth efficiency of any type of modulation. This bound is derived in Chapter 7 and discussed in greater detail there.

5-3 OPTIMUM RECEIVER FOR CPM SIGNALS

We recall from Section 4-3 that CPM is a modulation method with memory. The memory results from the continuity of the transmitted carrier phase from one signal interval to the next. The transmitted CPM signal may be expressed as

$$s(t) = \sqrt{\frac{2\mathcal{E}}{T}} \cos\left[2\pi f_c t + \phi(t; \mathbf{I})\right] \tag{5-3-1}$$

where $\phi(t; \mathbf{I})$ is the carrier phase. The filtered received signal for an additive gaussian noise channel is

$$r(t) = s(t) + n(t) \tag{5-3-2}$$

where

$$n(t) = n_c(t) \cos 2\pi f_c t - n_s(t) \sin 2\pi f_c t \tag{5-3-3}$$

5-3-1 Optimum Demodulation and Detection of CPM

The optimum receiver for this signal consists of a correlator followed by a maximum-likelihood sequence detector that searches the paths through the state trellis for the minimum euclidean distance path. The Viterbi algorithm is an efficient method for performing this search. Let us establish the general state trellis structure for CPM and then describe the metric computations.

Recall that the carrier phase for a CPM signal with a fixed modulation index h may be expressed as

$$\begin{aligned}\phi(t; \mathbf{I}) &= 2\pi h \sum_{k=-\infty}^{n} I_k q(t - kT) \\ &= \pi h \sum_{k=-\infty}^{n-L} I_k + 2\pi h \sum_{k=n-L+1}^{n} I_k q(t - kT) \\ &= \theta_n + \theta(t; \mathbf{I}), \quad nT \leq t \leq (n+1)T\end{aligned} \tag{5-3-4}$$

where we have assumed that $q(t) = 0$ for $t < 0$, $q(t) = \frac{1}{2}$ for $t \geq LT$, and

$$q(t) = \int_0^t g(\tau)\, d\tau \tag{5-3-5}$$

The signal pulse $g(t) = 0$ for $t < 0$ and $t \geq LT$. For $L = 1$, we have a full response CPM, and for $L > 1$, where L is a positive integer, we have a partial response CPM signal.

Now, when h is rational, i.e., $h = m/p$ where m and p are relatively prime positive integers, the CPM scheme can be represented by a trellis. In this case, there are *p phase states*

$$\Theta_s = \left\{0, \frac{\pi m}{p}, \frac{2\pi m}{p}, \ldots, \frac{(p-1)\pi m}{p}\right\} \tag{5-3-6}$$

when m is even, and $2p$ phase states

$$\Theta_s = \left\{0, \frac{\pi m}{p}, \ldots, \frac{(2p-1)\pi m}{p}\right\} \tag{5-3-7}$$

when m is odd. If $L = 1$, these are the only states in the trellis. On the other hand, if $L > 1$, we have an additional number of states due to the partial

response character of the signal pulse $g(t)$. These additional states can be identified by expressing $\theta(t, \mathbf{I})$ given by (5-3-4) as

$$\theta(t; \mathbf{I}) = 2\pi h \sum_{k=n-L+1}^{n-1} I_k q(t - kT) + 2\pi h I_n q(t - nT) \tag{5-3-8}$$

The first term on the right-hand side of (5-3-8) depends on the information symbols $(I_{n-1}, I_{n-2}, \ldots, I_{n-L+1})$, which is called the *correlative state vector*, and represents the phase term corresponding to signal pulses that have not reached their final value. The second term in (5-3-8) represents the phase contribution due to the most recent symbol I_n. Hence, the state of the CPM signal (or the modulator) at time $t = nT$ may be expressed as the combined *phase state* and *correlative state*, denoted as

$$S_n = \{\theta_n, I_{n-1}, I_{n-2}, \ldots, I_{n-L+1}\} \tag{5-3-9}$$

for a partial response signal pulse of length LT, where $L > 1$. In this case, the number of states is

$$N_s = \begin{cases} pM^{L-1} & (\text{even } m) \\ 2pM^{L-1} & (\text{odd } m) \end{cases} \tag{5-3-10}$$

when $h = m/p$.

Now, suppose the state of the modulator at $t = nT$ is S_n. The effect of the new symbol in the time interval $nT \leq t \leq (n+1)T$ is to change the state from S_n to S_{n+1}. Hence, at $t = (n+1)T$, the state becomes

$$S_{n+1} = (\theta_{n+1}, I_n, I_{n+1}, \ldots, I_{n-L+2})$$

where

$$\theta_{n+1} = \theta_n + \pi h I_{n-L+1}$$

Example 5-3-1

Consider a binary CPM scheme with a modulation index $h = 3/4$ and a partial response pulse with $L = 2$. Let us determine the states S_n of the CPM scheme and sketch the phase tree and state trellis.

First, we note that there are $2p = 8$ phase states, namely,

$$\Theta_s = \{0, \pm\tfrac{1}{4}\pi, \pm\tfrac{1}{2}\pi, \pm\tfrac{3}{4}\pi, \pi\}$$

For each of these phase states, there are two states that result from the memory of the CPM scheme. Hence, the total number of states is $N_s = 16$, namely,

$$(0, 1),\ (0, -1),\ (\pi, 1),\ (\pi, -1),\ (\tfrac{1}{4}\pi, 1),\ (\tfrac{1}{4}\pi, -1),\ (\tfrac{1}{2}\pi, 1),\ (\tfrac{1}{2}\pi, -1),$$
$$(\tfrac{3}{4}\pi, 1),\ (\tfrac{3}{4}\pi, -1),\ (-\tfrac{1}{4}\pi, 1),\ (-\tfrac{1}{4}\pi, -1),\ (-\tfrac{1}{2}\pi, 1),\ (-\tfrac{1}{2}\pi, -1),$$
$$(-\tfrac{3}{4}\pi, 1),\ (-\tfrac{3}{4}\pi, -1)$$

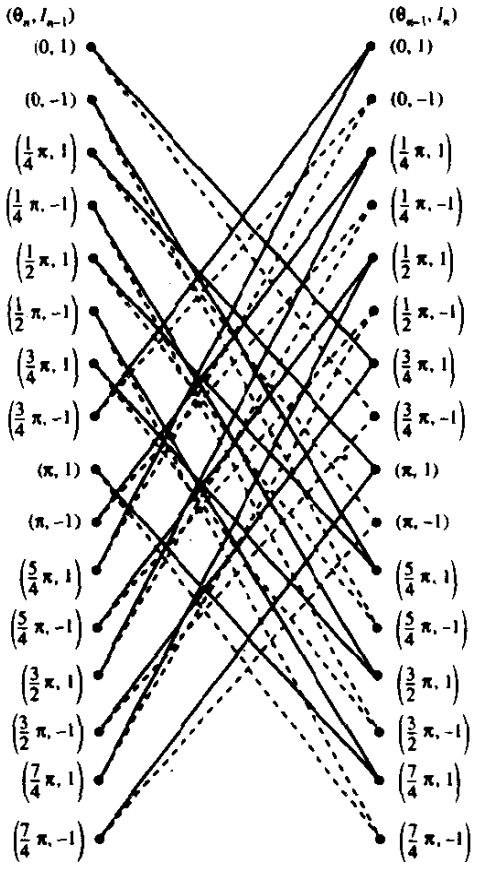

FIGURE 5-3-1 State trellis for partial response ($L = 2$) CPM with $h = \frac{3}{4}$.

If the system is in phase state $\theta_n = -\frac{1}{4}\pi$ and $I_{n-1} = -1$ then

$$\theta_{n+1} = \theta_n + \pi h I_{n-1}$$
$$= -\tfrac{1}{4}\pi - \tfrac{3}{4}\pi = -\pi$$

The state trellis is illustrated in Fig. 5-3-1. A path through the state trellis corresponding to the sequence $(1, -1, -1, -1, 1, 1)$ is illustrated in Fig. 5-3-2.

In order to sketch the phase tree, we must know the signal pulse shape $g(t)$. Figure 5-3-3 illustrates the phase tree when $g(t)$ is a rectangular pulse of duration $2T$, with initial state $(0, 1)$.

Having established the state trellis representation of CPM, let us now consider the metric computations performed in the Viterbi algorithm.

Metric Computations By referring back to the mathematical development

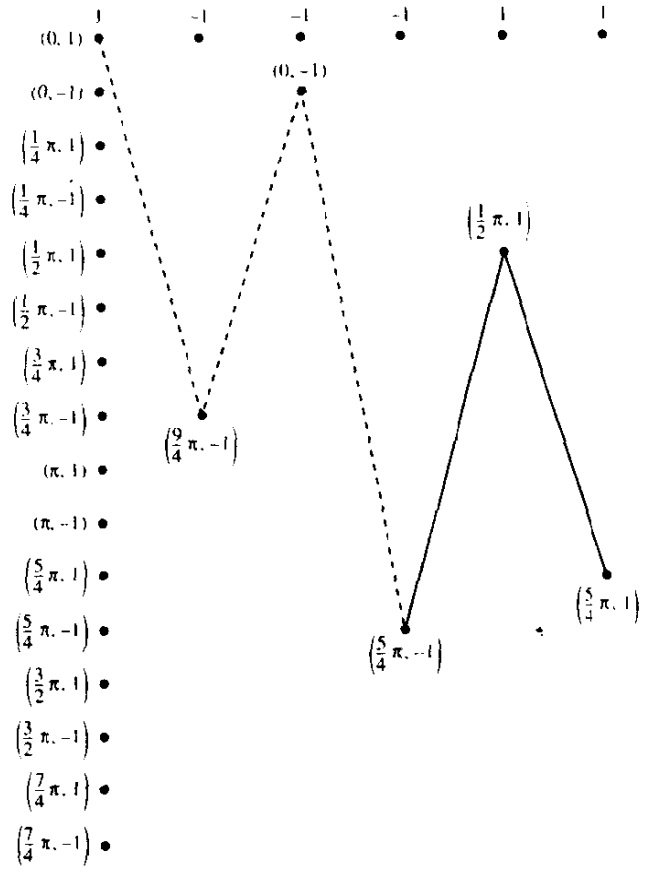

FIGURE 5-3-2 A single signal path through the trellis.

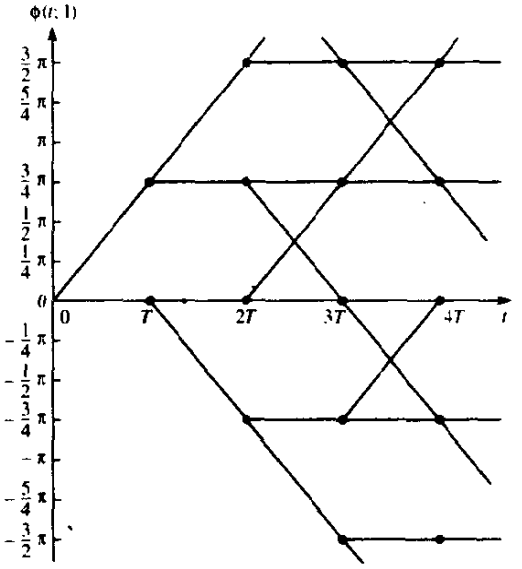

FIGURE 5-3-3 Phase tree for $L = 2$ partial response CPM with $h = \frac{3}{4}$.

for the derivation of the maximum likelihood demodulator given in Section 5-1-4, it is easy to show that the logarithm of the probability of the observed signal $r(t)$ conditioned on a particular sequence of transmitted symbols $\mathbf{I}$ is proportional to the cross-correlation metric

$$CM_n(\mathbf{I}) = \int_{-\infty}^{(n+1)T} r(t)\cos\left[\omega_c t + \phi(t;\mathbf{I})\right] dt$$

$$= CM_{n-1}(\mathbf{I}) + \int_{nT}^{(n+1)T} r(t)\cos\left[\omega_c t + \theta(t;\mathbf{I}) + \theta_n\right] dt \quad (5\text{-}3\text{-}11)$$

The term $CM_{n-1}(\mathbf{I})$ represents the metrics for the surviving sequences up to time nT, and the term

$$v_n(\mathbf{I};\theta_n) = \int_{nT}^{(n+1)T} r(t)\cos\left[\omega_c t + \theta(t;\mathbf{I}) + \theta_n\right] dt \quad (5\text{-}3\text{-}12)$$

represents the additonal increments to the metrics contributed by the signal in the time interval $nT \leq t \leq (n+1)T$. Note that there are M^L possible sequences $\mathbf{I} = (I_n, I_{n-1}, \ldots, I_{n-L+1})$ of symbols and p (or $2p$) possible phase states $\{\theta_n\}$. Therefore, there are pM^L (or $2pM^L$) different values of $v_n(\mathbf{I}, \theta_n)$, computed in each signal interval, and each value is used to increment the metrics corresponding to the pM^{L-1} surviving sequences from the previous signaling interval. A general block diagram that illustrates the computations of $v_n(\mathbf{I};\theta_n)$ for the Viterbi decoder is shown in Fig. 5-3-4.

Note that the number of surviving sequences at each state of the Viterbi decoding process is pM^{L-1} (or $2pM^{L-1}$). For each surviving sequence, we have M new increments of $v_n(\mathbf{I};\Theta_n)$ that are added to the existing metrics to yield pM^L (or $2pM^L$) sequences with pM^L (or $2pM^L$) metrics. However, this number is then reduced back to pM^{L-1} (or $2pM^{L-1}$) survivors with corresponding metrics by selecting the most probable sequence of the M sequences merging at each node of the trellis and discarding the other $M-1$ sequences.

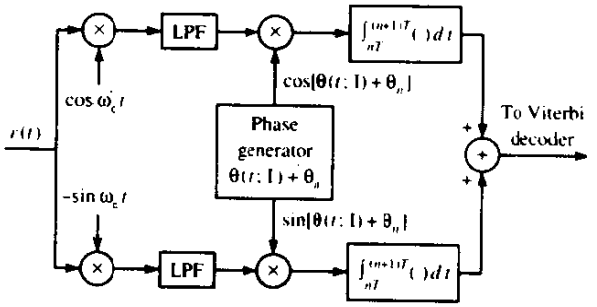

FIGURE 5-3-4 Computation of metric increments $v_n(\mathbf{I};\theta_n)$.

5-3-2 Performance of CPM Signals

In evaluating the performance of CPM signals achieved with MLSE, we must determine the minimum euclidean distance of paths through the trellis that separate at the node at $t = 0$ and re-emerge at a later time at the same node. The distance between two paths through the trellis is related to the corresponding signals as we now demonstrate.

Suppose that we have two signals $s_i(t)$ and $s_j(t)$ corresponding to two phase trajectories $\phi(t; \mathbf{I}_i)$ and $\phi(t; \mathbf{I}_j)$. The sequences $\mathbf{I}_i$ and $\mathbf{I}_j$ must be different in their first symbol. Then, the euclidean distance between the two signals over an interval of length NT, where $1/T$ is the symbol rate, is defined as

$$\begin{aligned} d_{ij}^2 &= \int_0^{NT} [s_i(t) - s_j(t)]^2 \, dt \\ &= \int_0^{NT} s_i^2(t) \, dt + \int_0^{NT} s_j^2(t) \, dt - 2 \int_0^{NT} s_i(t) s_j(t) \, dt \\ &= 2N\mathscr{E} - 2 \frac{2\mathscr{E}}{T} \int_0^{NT} \cos [\omega_c t + \phi(t; \mathbf{I}_i)] \cos [\omega_c t + \phi(t; \mathbf{I}_j)] \, dt \\ &= 2N\mathscr{E} - \frac{2\mathscr{E}}{T} \int_0^{NT} \cos [\phi(t; \mathbf{I}_i) - \phi(t; \mathbf{I}_j)] \, dt \\ &= \frac{2\mathscr{E}}{T} \int_0^{NT} \{1 - \cos [\phi(t; \mathbf{I}_i) - \phi(t; \mathbf{I}_j)]\} \, dt \end{aligned} \tag{5-3-13}$$

Hence the euclidean distance is related to the phase difference between the paths in the state trellis according to (5-3-13).

It is desirable to express the distance d_{ij}^2 in terms of the bit energy. Since $\mathscr{E} = \mathscr{E}_b \log_2 M$, (5-3-13) may be expressed as

$$d_{ij}^2 = 2\mathscr{E}_b \delta_{ij}^2 \tag{5-3-14}$$

where δ_{ij}^2 is defined as

$$\delta_{ij}^2 = \frac{\log_2 M}{T} \int_0^{NT} \{1 - \cos [\phi(t; \mathbf{I}_i) - \phi(t; \mathbf{I}_j)]\} \, dt \tag{5-3-15}$$

Furthermore, we observe that $\phi(t; \mathbf{I}_i) - \phi(t; \mathbf{I}_j) = \phi(t; \mathbf{I}_i - \mathbf{I}_j)$, so that, with $\boldsymbol{\xi} = \mathbf{I}_i - \mathbf{I}_j$, (5-3-15) may be written as

$$\delta_{ij}^2 = \frac{\log_2 M}{T} \int_0^{NT} [1 - \cos \phi(t; \boldsymbol{\xi})] \, dt \tag{5-3-16}$$

where any element of $\boldsymbol{\xi}$ can take the values $0, \pm 2, \pm 4, \pm \ldots \pm 2(M-1)$, except that $\boldsymbol{\xi}_0 \neq 0$.

The error rate performance for CPM is dominated by the term corresponding to the minimum euclidean distance, and it may be expressed as

$$P_M = K_{\delta_{\min}} Q\left(\sqrt{\frac{\mathcal{E}_b}{N_0}\,\delta_{\min}^2}\right) \tag{5-3-17}$$

where

$$\begin{aligned}\delta_{\min}^2 &= \lim_{N\to\infty} \min_{i,j} \delta_{ij}^2 \\ &= \lim_{N\to\infty} \min_{i,j} \left\{\frac{\log_2 M}{T}\int_0^{NT} [1-\cos\phi(t;\mathbf{I}_i-\mathbf{I}_j)]\,dt\right\}\end{aligned} \tag{5-3-18}$$

We note that for conventional binary PSK with no memory, $N = 1$ and $\delta_{\min}^2 = \delta_{12}^2 = 2$. Hence, (5-3-17) agrees with our previous result.

Since $\delta_{\min}^2$ characterizes the performance of CPM with MLSE, we can investigate the effect on $\delta_{\min}^2$ resulting from varying the alphabet size M, the modulation index h, and the length of the transmitted pulse in partial response CPM.

First, we consider full response ($L = 1$) CPM. If we take $M = 2$ as a beginning, we note that the sequences

$$\begin{aligned}\mathbf{I}_i &= +1, -1, I_2, I_3 \\ \mathbf{I}_j &= -1, +1, I_2, I_3\end{aligned} \tag{5-3-19}$$

which differ for $k = 0, 1$ and agree for $k \geq 2$, result in two phase trajectories that merge after the second symbol. This corresponds to the difference sequence

$$\boldsymbol{\xi} = \{2, -2, 0, 0, \ldots\} \tag{5-3-20}$$

The euclidean distance for this sequence is easily calculated from (5-3-16), and provides an upper bound on $\delta_{\min}^2$. This upper bound for $M = 2$ is

$$d_B^2(h) = 2\left(1 - \frac{\sin 2\pi h}{2\pi h}\right), \qquad M = 2 \tag{5-3-21}$$

For example, where $h = \frac{1}{2}$, which corresponds to MSK, we have $d_B^2(\frac{1}{2}) = 2$, so that $\delta_{\min}^2(\frac{1}{2}) \leq 2$.

For $M > 2$ and full response CPM, it is also easily seen that phase trajectories merge at $t = 2T$. Hence, an upper bound on $\delta_{\min}^2$ can be obtained by considering the phase difference sequence $\xi = \{\alpha, -\alpha, 0, 0, \ldots\}$ where $\alpha = \pm 2, \pm 4, \ldots, \pm 2(M-1)$. This sequence yields the upper bound

$$d_B^2(h) = \min_{1\leq k\leq M-1} \left\{(2\log_2 M)\left(1 - \frac{\sin 2k\pi h}{2k\pi h}\right)\right\} \tag{5-3-22}$$

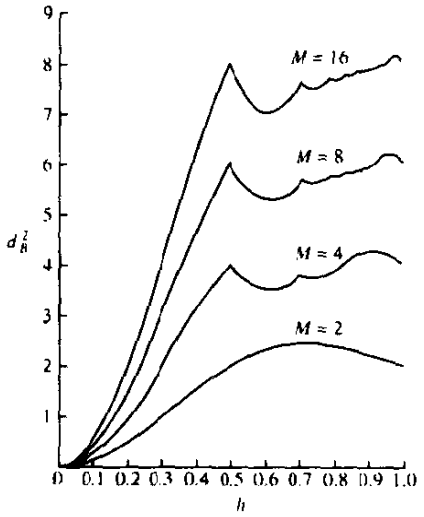

FIGURE 5-3-5 The upper bound d_B^2 as a function of the modulation index h for full response CPM with rectangular pulses. [*From Aulin and Sundberg (1984). © 1984, John Wiley Ltd. Reprinted with permission of the publisher.*]

The graphs of $d_B^2(h)$ versus h for $M = 2, 4, 8, 16$ are shown in Fig. 5-3-5. It is apparent from these graphs that large gains in performance can be achieved by increasing the alphabet size M. It must be remembered, however, that $\delta_{min}^2(h) \leq d_B^2(h)$. That is, the upper bound may not be achievable for all values of h.

The minimum euclidean distance $\delta_{\min}^2(h)$ has been determined, by evaluating (5-3-16), for a variety of CPM signals by Aulin and Sundberg (1981). For example, Fig. 5-3-6 illustrates the dependence of the euclidean distance for binary CPFSK as a function of the modulation index h, with the number N of

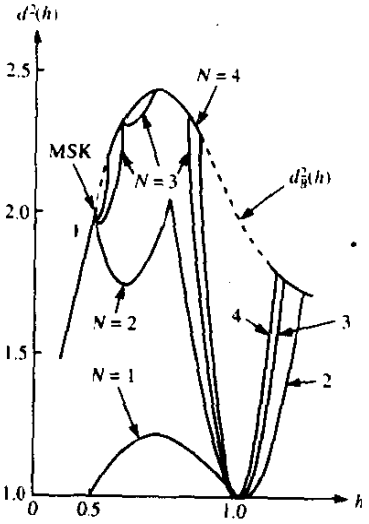

FIGURE 5-3-6 Squared minimum euclidean distance as a function of the modulation index for binary CPFSK. The upper bound is d_B^2. [*From Aulin and Sundberg (1981). © 1981 IEEE.*].

bit observation (decision) intervals ($N = 1, 2, 3, 4$) as a parameter. Also shown is the upper bound $d_B^2(h)$ given by (5-3-21). In particular, we note that when $h = \frac{1}{2}$, $\delta_{\min}^2(\frac{1}{2}) = 2$, which is the same squared distance as PSK (binary or quaternary) with $N = 1$. On the other hand, the required observation interval for MSK is $N = 2$ intervals, for which we have $\delta_{\min}^2(\frac{1}{2}) = 2$. Hence, the performance of MSK with MLSE is comparable to (binary or quaternary) PSK as we have previously observed.

We also note from Fig. 5-3-6 that the optimum modulation index for binary CPFSK is $h = 0.715$ when the observation interval is $N = 3$. This yields $\delta_{\min}^2(0.715) = 2.43$, or a gain of 0.85 dB relative to MSK.

Figure 5-3-7 illustrates the euclidean distance as a function of h for $M = 4$ CPFSK, with the length of the observation interval N as a parameter. Also shown (as a dashed line where it is not reached) is the upper bound d_B^2 evaluated from (5-3-22). Note that $\delta_{\min}^2$ achieves the upper bound for several values of h for some N. In particular, note that the maximum value of d_B^2, which occurs at $h \approx 0.9$, is approximately reached for $N = 8$ observed symbol intervals. The true maximum is achieved at $h = 0.914$ with $N = 9$. For this case, $\delta_{\min}^2(0.914) = 4.2$, which represents a 3.2 dB gain over MSK. Also note that the euclidean distance contains minima at $h = \frac{1}{3}, \frac{1}{2}, \frac{2}{3}, 1$, etc. These values of h are called *weak modulation indices* and should be avoided. Similar results are available for larger values of M, and may be found in the paper by Aulin and Sundberg (1981) and the text by Anderson *et al.* (1986).

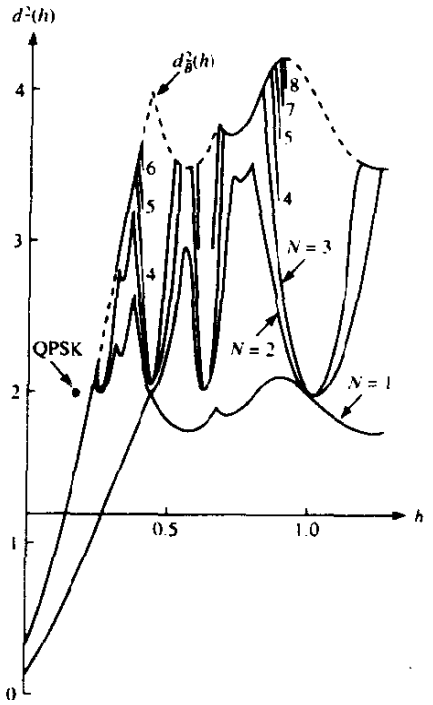

FIGURE 5-3-7 Squared minimum euclidean distance as a function of the modulation index for quaternary CPFSK. The upper bound is d_B^2. [*From Aulin and Sundberg (1981). © 1981 IEEE.*]

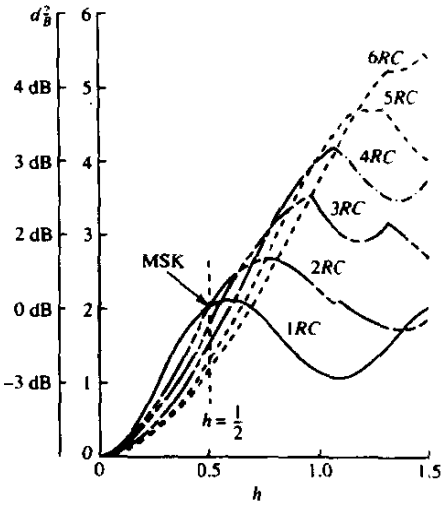

FIGURE 5-3-8 Upper bound d_B^2 on the minimum distance for partial response (raised cosine pulse) binary CPM. [*From Sundberg (1986). © 1986 IEEE.*]

Large performance gains can also be achieved with MLSE of CPM by using partial response signals. For example, the distance bound $d_B^2(h)$ for partial response, raised cosine pulses given by

$$g(t) = \begin{cases} \dfrac{1}{2LT}\left(1 - \cos\dfrac{2\pi t}{2LT}\right) & (0 \leq t \leq LT) \\ 0 & (\text{otherwise}) \end{cases} \tag{5-3-23}$$

is shown in Fig. 5-3-8 for $M = 2$. Here, note that, as L increases, d_B^2 also achieves higher values. Clearly, the performance of CPM improves as the correlative memory L increases, but h must also be increased in order to achieve the larger values of d_B^2. Since a larger modulation index implies a larger bandwidth (for fixed L), while a larger memory length L (for fixed h) implies a smaller bandwidth, it is better to compare the euclidean distance as a function of the normalized bandwidth $2WT_b$, where W is the 99% power bandwidth and T_b is the bit interval. Figure 5-3-9 illustrates this type of comparison with MSK used as a point of reference (0 dB). Note from this figure that there are several decibels to be gained by using partial response signals and higher signaling alphabets. The major price to be paid for this performance gain is the added exponentially increasing complexity in the implementation of the Viterbi decoder.

The performance results shown in Fig. 5-3-9 illustrate that 3–4 dB gain relative to MSK can be easily obtained with relatively no increase in bandwidth by the use of raised cosine partial response CPM and $M = 4$. Although these results are for raised cosine signal pulses, similar gains can be achieved with other partial response pulse shapes. We emphasize that this gain in SNR is achieved by introducing memory into the signal modulation and exploiting the memory in the demodulation of the signal. No redundancy through coding has

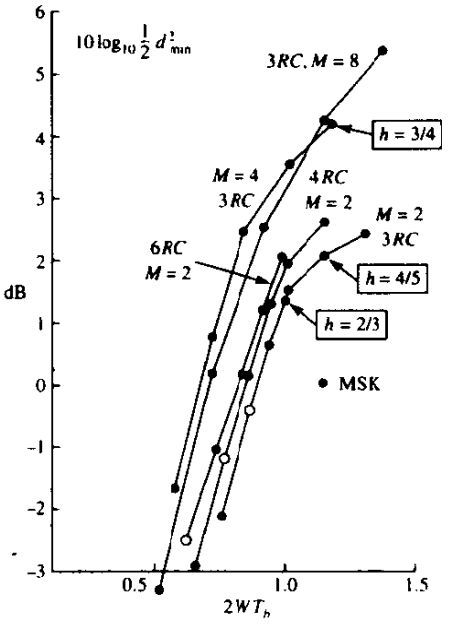

FIGURE 5-3-9 Power bandwidth tradeoff for partial response CPM signals with raised cosine pulses. W is the 99 percent in-band power bandwidth. [*From Sundberg (1986). © 1986 IEEE.*]

been introduced. In effect, the code has been built into the modulation and the trellis-type (Viterbi) decoding exploits the phase constraints in the CPM signal.

Additional gains in performance can be achieved by introducing additional redundancy through coding and increasing the alphabet size as a means of maintaining a fixed bandwidth. In particular, trellis-coded CPM using relatively simple convolution codes has been thoroughly investigated and many results are available in the technical literature. The Viterbi decoder for the convolutionally encoded CPM signal now exploits the memory inherent in the code and in the CPM signal. Performance gains of the order of 4–6 dB, relative to uncoded MSK with the same bandwidth, have been demonstrated by combining convolutional coding with CPM. Extensive numerical results for coded CPM are given by Lindell (1985).

Multi-h CPM By varying the modulation index from one signaling interval to another, it is possible to increase the minimum euclidean distance $\delta^2_{\min}$ between pairs of phase trajectories and, thus, improve the performance gain over constant-h CPM. Usually, multi-h CPM employs a fixed number H of modulation indices that are varied cyclically in successive signaling intervals. Thus, the phase of the signal varies piecewise linearly.

Significant gains in SNR are achievable by using only a small number of different values of h. For example, with full response ($L = 1$) CPM and $H = 2$, it is possible to obtain a gain of 3 dB relative to binary or quaternary PSK. By increasing H to $H = 4$, a gain of 4.5 dB relative to PSK can be obtained. The performance gain can also be increased with an increase in the signal alphabet.

Table 5-3-1 lists the performance gains achieved with $M = 2, 4,$ and 8 for several values of H. The upper bounds on the minimum euclidean distance are also shown in Fig. 5-3-10 for several values of M and H. Note that the major gain in performance is obtained when H is increased from $H = 1$ to $H = 2$. For $H > 2$, the additional gain is relatively small for small values of $\{h_i\}$. On the other hand, significant performance gains are achieved by increasing the alphabet size M.

The results shown above hold for full response CPM. One can also extend the use of multi-h CPM to partial response in an attempt to further improve performance. It is anticipated that such schemes will yield some additional performance gains, but numerical results on partial response, multi-h CPM are limited. The interested reader is referred to the paper by Aulin and Sundberg (1982b).

Multiamplitude CPM Multiamplitude CPM (MACPM) is basically a combined amplitude and phase digital modulation scheme that allows us to increase the signaling alphabet relative to CPM in another dimension and, thus, to achieve higher data rates on a band-limited channel. Simultaneously, the combination of multiple amplitude in conjunction with CPM results in a bandwidth-efficient modulation technique.

We have already observed the spectral characteristics of MACPM in Section 4-3. The performance characteristics of MACPM have been investigated by Mulligan (1988) for both uncoded and trellis-coded CPM. Of particular interest is the result that trellis-coded CPM with two amplitude levels achieves a gain of 3–4 dB relative to MSK without a significant increase in the signal bandwidth.

5-3-3 Symbol-by-Symbol Detection of CPM Signals

Besides the ML sequence detector, there are other types of detectors that can be used to recover the information sequence in a CPM signal. In this section, we consider symbol-by-symbol detectors. One type of symbol-by-symbol detector is the one described in Section 5-1-5, which exploits the memory of CPM by performing matched filtering or cross-correlation over several signaling intervals. Because of its computational complexity, however, this recursive algorithm has not been directly applied to the detection of CPM. Instead, two similar, albeit suboptimal, symbol-by-symbol detection methods have been described in the papers by deBuda (1972), Osborne and Luntz (1974), and Schonhoff (1976). One of these is functionally equivalent to the algorithm given in Section 5-1-5, and the second is a suboptimum approximation of the first. We shall describe these two methods in the context of demodulation of CPFSK signals, for which these detection algorithms have been applied directly.

To describe these methods, we assume that the signal is observed over the present signaling interval and D signaling intervals into the future in deciding on the information symbol transmitted in the present signaling interval. A

TABLE 5-3-1 MAXIMUM VALUES OF THE UPPER BOUND d_H^2 FOR MULTI-h LINEAR PHASE CPM[a]

M	H	Max d_B^2	dB gain compared with MSK	h_1	h_2	h_3	h_4	$\bar{h}$
2	1	2.43	0.85	0.715				0.715
2	2	4.0	3.0	0.5	0.5			0.5
2	3	4.88	3.87	0.620	0.686	0.714		0.673
2	4	5.69	4.54	0.73	0.55	0.73	0.55	0.64
4	1	4.23	3.25	0.914				0.914
4	2	6.54	5.15	0.772	0.772			0.772
4	3	7.65	5.83	0.795	0.795	0.795		0.795
8	1	6.14	4.87	0.964				0.964
8	2	7.50	5.74	0.883	0.883			0.883
8	3	8.40	6.23	0.879	0.879	0.879		0.879

[a] From Aulin and Sundberg (1982b).

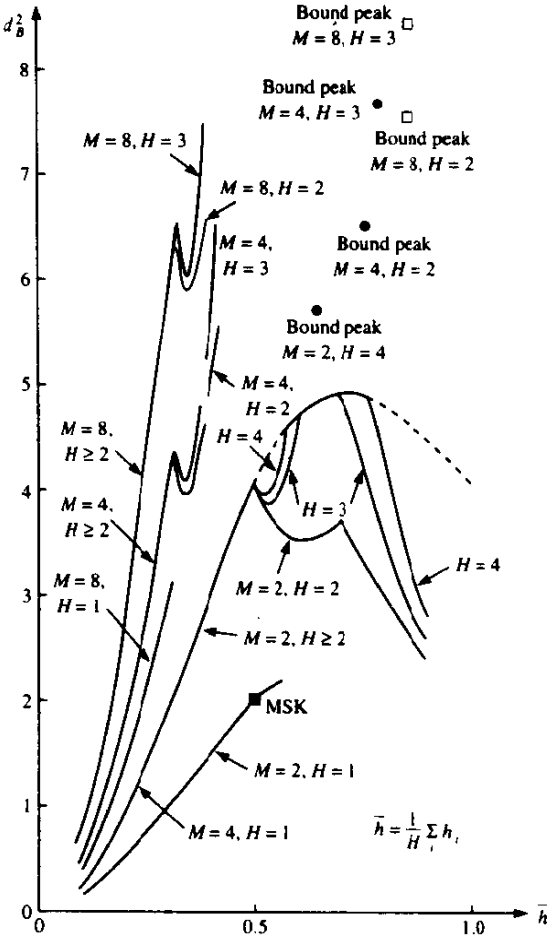

FIGURE 5-3-10 Upper bounds on minimum squared euclidean distance for various M and H values. [*From Aulin and Sundberg (1982b). © 1982 IEEE.*]

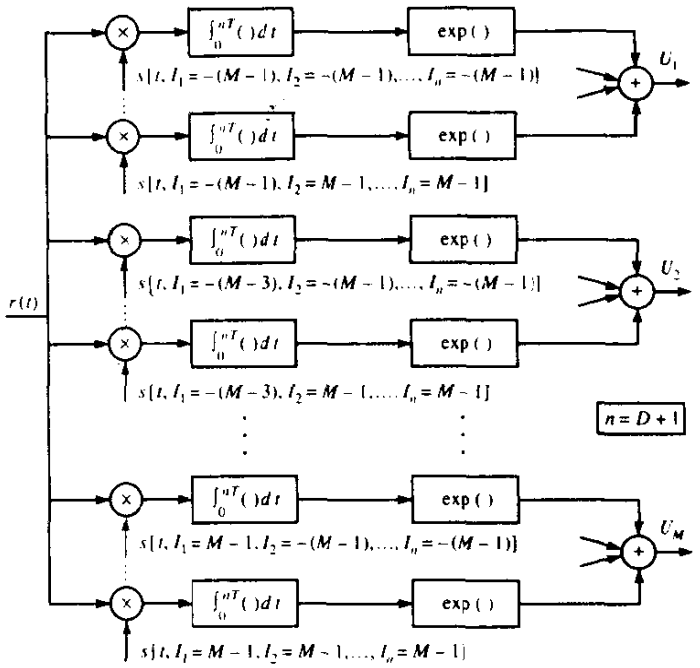

FIGURE 5-3-11 Block diagram of demodulator for detection of CPFSK.

block diagram of the demodulator, implemented as a bank of cross-correlators, is shown in Fig. 5-3-11. Recall that the transmitted CPFSK signal during the nth signaling interval is

$$s(t) = \text{Re}\,[v(t)e^{j2\pi f_c t}]$$

where

$$v(t) = \exp\left\{j\left[\frac{\pi h[t-(n-1)T]I_n}{T} + \pi h\sum_{k=0}^{n-1} I_k + \phi_0\right]\right\}$$

$h = 2f_dT$ is the modulation index, f_d is the peak frequency deviation, and ϕ_0 is the initial phase angle of the carrier.

In detecting the symbol I_1, the cross-correlations shown in Fig. 5-3-11 are performed with the reference signals $s(t, I_1, I_2, \ldots, I_{1+D})$ for all M^{D+1} possible values of the symbols $I_1, I_2, \ldots, I_{1+D}$ transmitted over the $D+1$ signaling intervals. But these correlations in effect generate the variables $r_1, r_2, \ldots, r_{1+D}$, which in turn are the arguments of the exponentials that occur in the pdf

$$p(r_1, r_2, \ldots, r_{1+D} \mid I_1, I_2, \ldots, I_{1+D})$$

Finally, the summations over the M^D possible values of the symbols $I_2, I_3, \ldots, I_{1+D}$ represent the averaging of

$$p(r_1, r_2, \ldots, r_{1+D} \mid I_1, I_2, \ldots, I_{1+D})P(I_1, I_2, \ldots, I_{1+D})$$

over the M^D possible values of these symbols. The M outputs of the demodulator constitute the decision variables from which the largest is selected to form the demodulated symbol. Consequently the metrics generated by the demodulator shown in Fig. 5-3-11 are equivalent to the decision variables given by (5-1-68) on which the decision on I_1 is based.

Signals received in subsequent signaling intervals are demodulated in the same manner. That is, the demodulator cross-correlates the signal received over $D + 1$ signaling intervals with the M^{D+1} possible transmitted signals and forms the decision variables as illustrated in Fig. 5-3-11. Thus the decision made on the mth signaling interval is based on the cross-correlations performed over the signaling intervals $m, m + 1, \ldots, m + D$. The initial phase in the correlation interval of duration $(D + 1)T$ is assumed to be known. On the other hand, the algorithm described by (5-1-76) and (5-1-77) involves an additional averaging operation over the previously detected symbols. In this respect, the demodulator shown in Fig. 5-3-11 differs from the recursive algorithm described above. However, the difference is insignificant.

One suboptimum demodulation method that performs almost as well as the optimum method embodied in Fig. 5-3-11 bases its decision on the largest output from the bank of M^{D+1} cross-correlators. Thus the exponential functions and the summations are eliminated. But this method is equivalent to selecting the symbol I_m for which the probability density function $p(r_m, r_{m+1}, \ldots, r_{m+D} \mid I_m, I_{m+1}, \ldots, I_{m+D})$ is a maximum.

The performance of the detector shown in Fig. 5-3-11 has been upper-bounded and evaluated numerically. Figure 5-3-12 illustrates the performance of binary CPFSK with $n = D + 1$ as a parameter. The modulation index $h = 0.715$ used in generating these results minimizes the probability of error as

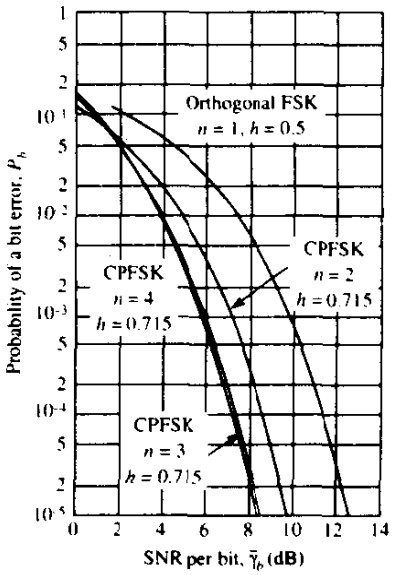

FIGURE 5-3-12 Performance of binary CPFSK with coherent detection.

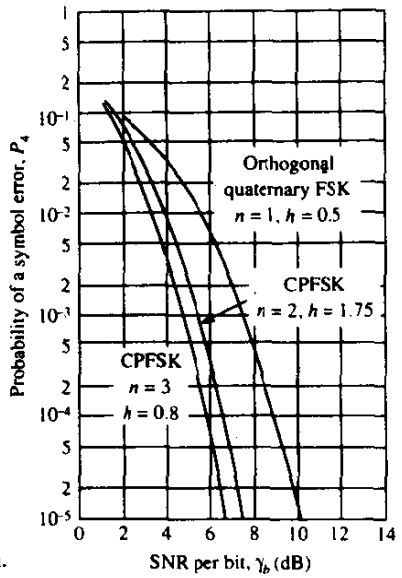

FIGURE 5-3-13 Performance of quaternary CPFSK with coherent detection.

shown by Schonhoff (1976). We note that an improvement of about 2.5 dB is obtained relative to orthogonal FSK ($n = 1$) by a demodulator that cross-correlates over two symbols. An additional gain of approximately 1.5 dB is obtained by extending the correlation time to three symbols. Further extension of the correlation time results in a relatively small additional gain.

Similar results are obtained with larger alphabet sizes. For example, Figs 5-3-13 and 5-3-14 illustrate the performance improvements for quaternary and

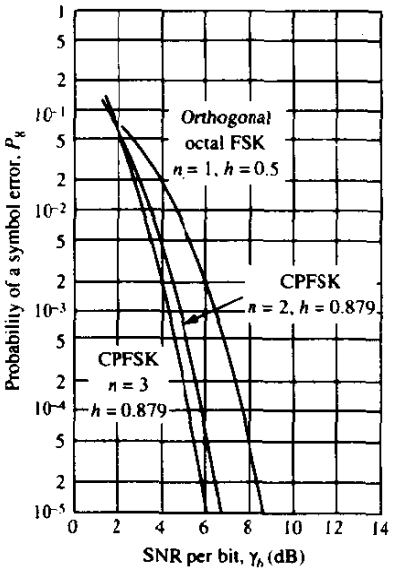

FIGURE 5-3-14 Performance of octal CPFSK with coherent detection.

octal CPFSK, respectively. The modulation indices given in these graphs are the ones that minimize the probability of a symbol error.

Instead of performing coherent detection, which requires knowledge of the carrier phase ϕ_0, we may assume that ϕ_0 is uniformly distributed over the interval 0 to 2π, and average over it in arriving at the decision variables. Thus coherent integration (cross-correlation) is performed over the $n = D + 1$ signaling intervals, but the outputs of the correlators are envelope-detected. This is called *noncoherent detection* of CPFSK. In this detection scheme, performance is optimized by selecting n to be odd and making the decision on the middle symbol in the sequence of n symbols. The numerical results on the probability of error for noncoherent detection of CPFSK are similar to the results illustrated above for coherent detection. That is, a gain of 2–3 dB in performance is achieved by increasing the correlation interval from $n = 1$ to $n = 3$ and to $n = 5$.

5-4 OPTIMUM RECEIVER FOR SIGNALS WITH RANDOM PHASE IN AWGN CHANNEL

In this section, we consider the design of the optimum receiver for carrier modulated signals when the carrier phase is unknown at the receiver and no attempt is made to estimate its value. Uncertainty in the carrier phase of the received signal may be due to one or more of the following reasons: First, the oscillators that are used at the transmitter and the receiver to generate the carrier signals are generally not phase synchronous. Second, the time delay in the propagation of the signal from the transmitter to the receiver is not generally known precisely. To elaborate on this point, a transmitted signal of the form

$$s(t) = \text{Re}\,[g(t)e^{j2\pi f_c t}]$$

that propagates through a channel with delay t_0 will be received as

$$\begin{aligned} s(t - t_0) &= \text{Re}\,[g(t - t_0)e^{j2\pi f_c(t - t_0)}] \\ &= \text{Re}\,[g(t - t_0)e^{-j2\pi f_c t_0}e^{j2\pi f_c t}] \end{aligned}$$

The carrier phase shift due to the propagation delay t_0 is

$$\phi = -2\pi f_c t_0$$

Note that large changes in the carrier phase ϕ can occur due to relatively small changes in the propagation delay. For example, if the carrier frequency $f_c = 1$ MHz, an uncertainty or a change in the propagation delay of 0.5 μs will cause a phase uncertainity of π rad. In some channels (e.g., radio channels) the time delay in the propagation of the signal from the transmitter to the receiver

may change rapidly and in an apparently random manner, so that the carrier phase of the received signal varies in an apparently random fashion.

In the absence of knowledge of the carrier phase, we may treat this signal parameter as a random variable and determine the form of the optimum receiver for recovering the transmitted information from the received signal. First, we treat the case of binary signals and, then, we consider M-ary signals.

5-4-1 Optimum Receiver for Binary Signals

We consider a binary communication system that uses the two carrier modulated signals $s_1(t)$ and $s_2(t)$ to transmit the information, where

$$s_m(t) = \text{Re}\,[s_{lm}(t)e^{j2\pi f_c t}], \quad m = 1, 2, \quad 0 \leq t \leq T \tag{5-4-1}$$

and $s_{lm}(t)$, $m = 1, 2$ are the equivalent lowpass signals. The two signals are assumed to have equal energy

$$\mathscr{E} = \int_0^T s_m^2(t)\,dt = \frac{1}{2}\int_0^T |s_{lm}(t)|^2\,dt \tag{5-4-2}$$

and are characterized by the complex-valued correlation coefficient

$$\rho_{12} \equiv \rho = \frac{1}{\mathscr{E}}\int_0^T s_{l1}^*(t)s_{l2}(t)\,dt \tag{5-4-3}$$

The received signal is assumed to be a phase-shifted version of the transmitted signal and corrupted by the additive noise

$$\begin{aligned} n(t) &= \text{Re}\,\{[n_c(t) + jn_s(t)]e^{j2\pi f_c t}\} \\ &= \text{Re}\,[z(t)e^{j2\pi f_c t}] \end{aligned} \tag{5-4-4}$$

Hence, the received signal may be expressed as

$$r(t) = \text{Re}\,\{[s_{lm}(t)e^{j\phi} + z(t)]e^{j2\pi f_c t}\} \tag{5-4-5}$$

where

$$r_l(t) = s_{lm}(t)e^{j\phi} + z(t), \quad 0 \leq t \leq T \tag{5-4-6}$$

is the equivalent lowpass received signal. This received signal is now passed through a demodulator whose sampled output at $t = T$ is passed to the detector.

The Optimum Demodulator In Section 5-1-1, we demonstrated that if the received signal was correlated with a set of orthonormal functions $\{f_n(t)\}$ that

spanned the signal space, the outputs from the bank of correlators provide a set of sufficient statistics for the detector to make a decision that minimizes the probability of error. We also demonstrated that a bank of matched filters could be substituted for the bank of correlators.

A similar orthonormal decomposition can also be employed for a received signal with an unknown carrier phase. However, it is mathematically convenient to deal with the equivalent lowpass signal and to specify the signal correlators or matched filters in terms of the equivalent lowpass signal waveforms.

To be specific, the impulse response $h_l(t)$ of a filter that is matched to the complex-valued equivalent lowpass signal $s_l(t)$, $0 \leq t \leq T$, is given as (see Problem 5-6)

$$h_l(t) = s_l^*(T - t) \tag{5-4-7}$$

and the output of such a filter at $t = T$ is simply

$$\int_0^T |s_l(t)|^2 \, dt = 2\mathcal{E} \tag{5-4-8}$$

where $\mathcal{E}$ is the signal energy. A similar result is obtained if the signal $s_l(t)$ is correlated with $s_l^*(t)$ and the correlator is sampled at $t = T$. Therefore, the optimum demodulator for the equivalent lowpass received signal $s_l(t)$ given in (5-4-6) may be realized by two matched filters in parallel, one matched to $s_{l1}(t)$ and the other to $s_{l2}(t)$, and shown in Fig. 5-4-1. The output of the matched filters or correlators at the sampling instant are the two complex numbers

$$r_m = r_{mc} + jr_{ms}, \qquad m = 1, 2 \tag{5-4-9}$$

Suppose that the transmitted signal is $s_1(t)$. Then, it is easily shown (see Problem 5-35) that

$$\begin{aligned} r_1 &= 2\mathcal{E}\cos\phi + n_{1c} + j(2\mathcal{E}\sin\phi + n_{1s}) \\ r_2 &= 2\mathcal{E}|\rho|\cos(\phi + \alpha_0) + n_{2c} + j[2\mathcal{E}|\rho|\sin(\phi + \alpha_0) + n_{2s}] \end{aligned} \tag{5-4-10}$$

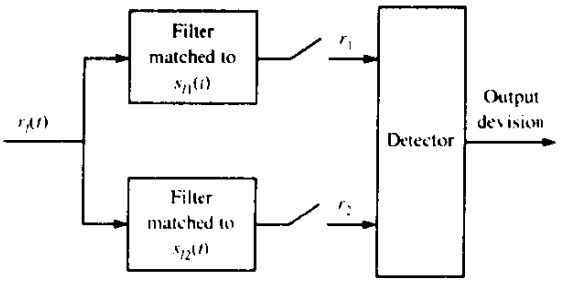

FIGURE 5-4-1 Optimum receiver for binary signals.

where ρ is the complex-valued correlation coefficient of the two signals $s_{l1}(t)$ and $s_{l2}(t)$, which may be expressed as $\rho = |\rho| \exp(\alpha_0)$. The random noise variables n_{1c}, n_{1s}, n_{2c}, and n_{2s} are jointly gaussian, with zero mean and equal variance.

The Optimum Detector The optimum detector observes the random variables $[r_{1c}\ r_{1s}\ r_{2c}\ r_{2s}] = \mathbf{r}$, where $r_1 = r_{1c} + jr_{1s}$ and $r_2 = r_{2c} + jr_{2s}$, and bases its decision on the posterior probabilities $P(\mathbf{s}_m \mid \mathbf{r})$, $m = 1, 2$. These probabilities may be expressed as

$$P(\mathbf{s}_m \mid \mathbf{r}) = \frac{p(\mathbf{r} \mid \mathbf{s}_m)P(\mathbf{s}_m)}{p(\mathbf{r})}, \quad m = 1, 2 \tag{5-4-11}$$

and, hence, the optimum decision rule may be expressed as

$$P(\mathbf{s}_1 \mid \mathbf{r}) \underset{s_2}{\overset{s_1}{\gtrless}} P(\mathbf{s}_2 \mid \mathbf{r})$$

or, equivalently,

$$\frac{p(\mathbf{r} \mid \mathbf{s}_1)}{p(\mathbf{r} \mid \mathbf{s}_2)} \underset{s_2}{\overset{s_1}{\gtrless}} \frac{P(\mathbf{s}_2)}{P(\mathbf{s}_1)} \tag{5-4-12}$$

The ratio of pdfs on the left-hand side of (5-4-12) is the *likelihood ratio*, which we denote as

$$\Lambda(\mathbf{r}) = \frac{p(\mathbf{r} \mid \mathbf{s}_1)}{p(\mathbf{r} \mid \mathbf{s}_2)} \tag{5-4-13}$$

The right-hand side of (5-4-12) is the ratio of the two prior probabilities, which takes the value of unity when the two signals are equally probable.

The probability density functions $p(\mathbf{r} \mid \mathbf{s}_1)$ and $p(\mathbf{r} \mid \mathbf{s}_2)$ can be obtained by averaging the pdfs $p(\mathbf{r} \mid \mathbf{s}_m, \phi)$ over the pdf of the random carrier phase, i.e.,

$$p(\mathbf{r} \mid \mathbf{s}_m) = \int_0^{2\pi} p(\mathbf{r} \mid \mathbf{s}_m, \phi)p(\phi)\, d\phi \tag{5-4-14}$$

We shall perform the integration indicated in (5-4-14) for the special case in which the two signals are orthogonal, i.e., $\rho = 0$. In this case, the outputs of the demodulator are

$$\begin{aligned} r_1 &= r_{1c} + jr_{1s} \\ &= 2\mathscr{E} \cos\phi + n_{1c} + j(2\mathscr{E} \sin\phi + n_{1s}) \\ r_2 &= r_{2c} + jr_{2s} \\ &= n_{2c} + jn_{2s} \end{aligned} \tag{5-4-15}$$

where $(n_{1c}, n_{1s}, n_{2c}, n_{2s})$ are mutually uncorrelated and, hence, statistically independent, zero-mean gaussian random variables (see Problem 5-25). Hence, the joint pdf of $\mathbf{r} = [r_{1c}\ r_{1s}\ r_{2c}\ r_{2s}]$ may be expressed as a product of the marginal pdfs. Consequently,

$$p(r_{1c}, r_{1s} \mid \mathbf{s}_1, \phi) = \frac{1}{2\pi\sigma^2} \exp\left[-\frac{(r_{1c} - 2\mathscr{E}\cos\phi)^2 + (r_{1s} - 2\mathscr{E}\sin\phi)^2}{2\sigma^2}\right]$$
$$p(r_{2c}, r_{2s}) = \frac{1}{2\pi\sigma^2} \exp\left(-\frac{r_{2c}^2 + r_{2s}^2}{2\sigma^2}\right) \tag{5-4-16}$$

where $\sigma^2 = 2\mathscr{E}N_0$.

The uniform pdf for the carrier phase ϕ represents the most ignorance that can be exhibited by the detector. This is called the *least favorable pdf* for ϕ. With $p(\phi) = 1/2\pi$, $0 \leq \phi \leq 2\pi$, substituted into the integral in (5-4-14), we obtain

$$\frac{1}{2\pi}\int_0^{2\pi} p(r_{1c}, r_{1s} \mid \mathbf{s}_1, \phi)\, d\phi$$
$$= \frac{1}{2\pi}\exp\left(-\frac{r_{1c}^2 + r_{1c}^2 + 4\mathscr{E}^2}{2\sigma^2}\right)\frac{1}{2\pi}\int \exp\left[\frac{2\mathscr{E}(r_{1c}\cos\phi + r_{1s}\sin\phi)}{\sigma^2}\right] d\phi \tag{5-4-17}$$

But

$$\frac{1}{2\pi}\int_0^{2\pi} \exp\left[\frac{2\mathscr{E}(r_{1c}\cos\phi + r_{1s}\sin\phi)}{\sigma^2}\right] d\phi = I_0\left(\frac{2\mathscr{E}\sqrt{r_{1c}^2 + r_{1s}^2}}{\sigma^2}\right) \tag{5-4-18}$$

where $I_0(x)$ is the modified Bessel function of zeroth order, defined in (2-1-120).

By performing a similar integration as in (5-4-17) under the assumption that the signal $s_2(t)$ was transmitted, we obtain the result

$$p(r_{2c}, r_{2s} \mid \mathbf{s}_2) = \frac{1}{2\pi}\exp\left(-\frac{r_{2c}^2 + r_{2s}^2 + 4\mathscr{E}^2}{2\sigma^2}\right) I_0\left(\frac{2\mathscr{E}\sqrt{r_{2c}^2 + r_{2s}^2}}{\sigma^2}\right) \tag{5-4-19}$$

When, we substitute these results into the likelihood ratio given by (5-4-13), we obtain the result

$$\Lambda(\mathbf{r}) = \frac{I_0(2\mathscr{E}\sqrt{r_{1c}^2 + r_{1s}^2}/\sigma^2)}{I_0(2\mathscr{E}\sqrt{r_{2c}^2 + r_{2s}^2}/\sigma^2)} \underset{s_2}{\overset{s_1}{\gtrless}} \frac{P(\mathbf{s}_2)}{P(\mathbf{s}_1)} \tag{5-4-20}$$

Thus, the optimum detector computes the two envelopes $\sqrt{r_{1c}^2 + r_{1s}^2}$ and $\sqrt{r_{2c}^2 + r_{2s}^2}$ and the corresponding values of the Bessel function $I_0(2\mathscr{E}\sqrt{r_{1c}^2 + r_{1s}^2}/\sigma^2)$ and $I_0(2\mathscr{E}\sqrt{r_{2c}^2 + r_{2s}^2}/\sigma^2)$ to form the likelihood ratio. We observe that this computation requires knowledge of the noise variance σ^2.

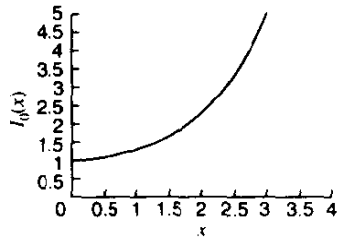

FIGURE 5-4-2 Graph of $I_0(x)$.

The likelihood ratio is then compared with the threshold $P(\mathbf{s}_2)/P(\mathbf{s}_1)$ to determine which signal was transmitted.

A significant simplification in the implementation of the optimum detector occurs when the two signals are equally probable. In such a case the threshold becomes unity, and, due to the monotonicity of the Bessel function shown in Fig. 5-4-2, the optimum detection rule simplifies to

$$\sqrt{r_{1c}^2 + r_{1s}^2} \underset{s_2}{\overset{s_1}{\gtrless}} \sqrt{r_{2c}^2 + r_{2s}^2} \tag{5-4-21}$$

Thus, the optimum detector bases its decision on the two envelopes $\sqrt{r_{1c}^2 + r_{1s}^2}$ and $\sqrt{r_{2c}^2 + r_{2s}^2}$, and, hence, it is called an *envelope detector.*

We observe that the computation of the envelopes of the received signal samples at the output of the demodulator renders the carrier phase irrelevant in the decision as to which signal was transmitted. Equivalently, the decision may be based on the computation of the squared envelopes $r_{1c}^2 + r_{1s}^2$ and $r_{2c}^2 + r_{2s}^2$, in which case the detector is called a *square-law detector.*

Binary FSK signals are an example of binary orthogonal signals. Recall that in binary FSK we employ two different frequencies, say f_1 and $f_2 = f_1 + \Delta f$, to transmit a binary information sequence. The choice of minimum frequency separation $\Delta f = f_2 - f_1$ is considered below. Thus, the signal waveforms may be expressed as

$$\begin{aligned} s_1(t) &= \sqrt{2\mathscr{E}_b/T_b}\cos 2\pi f_1 t, \quad 0 \leq t \leq T_b \\ s_2(t) &= \sqrt{2\mathscr{E}_b/T_b}\cos 2\pi f_2 t, \quad 0 \leq t \leq T_b \end{aligned} \tag{5-4-22}$$

and their equivalent lowpass counterparts are

$$\begin{aligned} s_{l1}(t) &= \sqrt{2\mathscr{E}_b/T_b}, \quad 0 \leq t \leq T_b \\ s_{l2}(t) &= \sqrt{2\mathscr{E}_b/T_b}e^{j2\pi\Delta f t}, \quad 0 \leq t \leq T_b \end{aligned} \tag{5-4-23}$$

The received signal may be expressed as

$$r(t) = \sqrt{\frac{2\mathscr{E}_b}{T_b}}\cos(2\pi f_m t + \phi_m) + n(t) \tag{5-4-24}$$

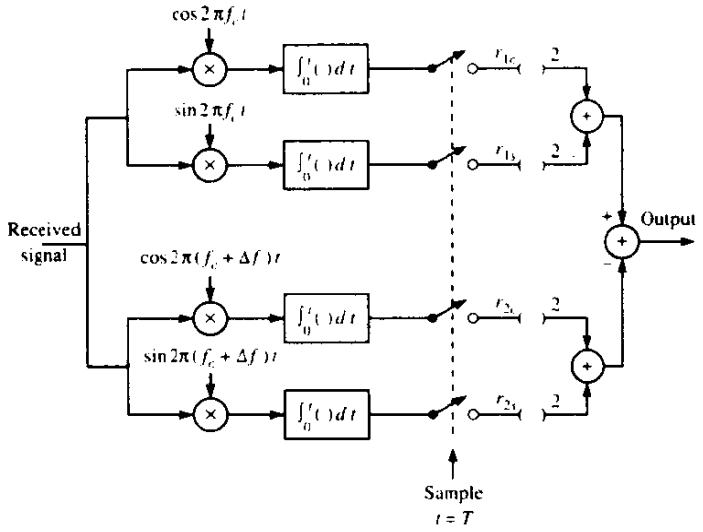

FIGURE 5-4-3 Demodulation and square-law detection of binary FSK signals.

where ϕ_m is the phase of the carrier frequency f_m. The demodulation of the real signal $r(t)$ may be accomplished, as shown in Fig. 5-4-3, by using four correlators with the basis functions

$$f_{1m}(t) = \sqrt{\frac{2}{T_b}} \cos [(2\pi f_1 + 2\pi m\, \Delta f)t], \qquad m = 0, 1$$
$$f_{2m}(t) = \sqrt{\frac{2}{T_b}} \sin [(2\pi f_1 + 2\pi m\, \Delta f)t], \qquad m = 0, 1 \tag{5-4-25}$$

The four outputs of the correlators are sampled at the end of each signal interval and passed to the detector. If the mth signal is transmitted, the four samples at the detector may be expressed as

$$r_{kc} = \sqrt{\mathscr{E}_b}\left[\frac{\sin [2\pi(k-m)\,\Delta f T]}{2\pi(k-m)\,\Delta f T} \cos \phi_m - \frac{\cos [2\pi(k-m)\,\Delta f T] - 1}{2\pi(k-m)\,\Delta f T} \sin \phi_m\right] + n_{kc}, \qquad k, m = 1, 2$$

(5-4-26)

$$r_{ks} = \sqrt{\mathscr{E}_b}\left[\frac{\cos 2\pi(k-m)\,\Delta f T - 1}{2\pi(k-m)\,\Delta f T} \cos \phi_m + \frac{\sin [2\pi(k-m)\,\Delta f T]}{2\pi(k-m)\,\Delta f T} \sin \phi_m\right] + n_{ks}, \qquad k, m = 1, 2$$

where n_{kc} and n_{ks} denote the gaussian noise components in the sampled outputs.

We observe that when $k = m$, the sampled values to the detector are

$$\begin{aligned} r_{mc} &= \sqrt{\mathcal{E}_b}\cos\phi_m + n_{mc} \\ r_{ms} &= \sqrt{\mathcal{E}_b}\sin\phi_m + n_{ms} \end{aligned} \tag{5-4-27}$$

Furthermore, we observe that when $k \neq m$, the signal components in the samples r_{kc} and r_{ks} will vanish, independently of the values of the phase shifts ϕ_k, provided that the frequency separation between successive frequencies is $\Delta f = 1/T$. In such a case, the other two correlator outputs consist of noise only, i.e.,

$$r_{kc} = n_{kc}, \quad r_{ks} = n_{ks}, \quad k \neq m \tag{5-4-28}$$

With a frequency separation of $\Delta f = 1/T$, the relations (5-4-27) and (5-4-28) are consistent with the previous result (5-4-15) for the demodulator outputs. Therefore, we conclude that for envelope or square-law detection of FSK signals, the minimum frequency separation required for orthogonality of the signals is $\Delta f = 1/T$. This separation is twice as large as that required when the detection is phase-coherent.

5-4-2 Optimum Receiver for M-ary Orthogonal Signals

The generalization of the optimum demodulator and detector to the case of M-ary orthogonal signals is straightforward. If the equal energy and equally probable signal waveforms are represented as

$$s_m(t) = \text{Re}\left[s_{lm}(t)e^{j2\pi f_c t}\right], \quad m = 1, 2, \ldots, M, \quad 0 \leq t \leq T \tag{5-4-29}$$

where $s_{lm}(t)$ are the equivalent lowpass signals, the optimum correlation-type or matched-filter-type demodulator produces the M complex-valued random variables

$$r_m = r_{mc} + jr_{ms} = \int_0^T r_l(t)s_{lm}^*(t)\,dt, \quad m = 1, 2, \ldots, M \tag{5-4-30}$$

where $r_l(t)$ is the equivalent lowpass received signal. Then, the optimum detector, based on a random, uniformly distributed carrier phase, computes the M envelopes

$$|r_m| = \sqrt{r_{mc}^2 + r_{ms}^2}, \quad m = 1, 2, \ldots, M \tag{5-4-31}$$

or, equivalently, the squared envelopes $|r_m|^2$, and selects the signal with the largest envelope (or squared envelope).

In the special case of M-ary orthogonal FSK signals, the optimum receiver has the structure illustrated in Fig. 5-4-4. There are $2M$ correlators: two for each possible transmitted frequency. The minimum frequency separation between adjacent frequencies to maintain orthogonality is $\Delta f = 1/T$.

5-4-3 Probability of Error for Envelope Detection of M-ary Orthogonal Signals

Let us consider the transmission of M-ary orthogonal equal energy signals over an AWGN channel, which are envelope-detected at the receiver. We also

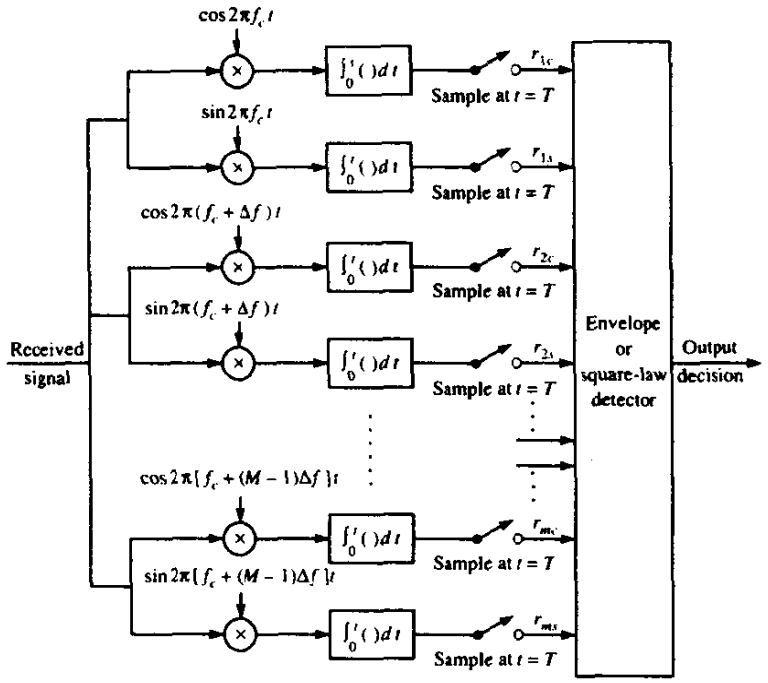

FIGURE 5-4-4 Demodulation of M-ary FSK signals for noncoherent detection.

assume that the M signals are equally probable a priori and that the signal $s_1(t)$ is transmitted in the signal interval $0 \leq t \leq T$.

The M decision metrics at the detector are the M envelopes

$$|\mathbf{r}_m| = \sqrt{r_{mc}^2 + r_{ms}^2}, \qquad m = 1, 2, \ldots, M \tag{5-4-32}$$

where

$$\begin{aligned} r_{1c} &= \sqrt{\mathscr{E}_s}\cos\phi_1 + n_{1c} \\ r_{1s} &= \sqrt{\mathscr{E}_s}\sin\phi_1 + n_{1s} \end{aligned} \tag{5-4-33}$$

and

$$r_{mc} = n_{mc}, \qquad r_{ms} = n_{ms}, \qquad m = 2, 3, \ldots, M \tag{5-4-34}$$

The additive noise components $\{n_{mc}\}$ and $\{n_{ms}\}$ are mutually statistically independent zero-mean gaussian variables with equal variance $\sigma^2 = \frac{1}{2}N_0$. Thus the pdfs of the random variables at the input to the detector are

$$p_{\mathbf{r}_1}(r_{1c}, r_{1s}) = \frac{1}{2\pi\sigma^2}\exp\left(-\frac{r_{1c}^2 + r_{1s}^2 + \mathscr{E}_s}{2\sigma^2}\right) I_0\left(\frac{\sqrt{\mathscr{E}_s(r_{1c}^2 + r_{1s}^2)}}{\sigma^2}\right) \tag{5-4-35}$$

$$p_{\mathbf{r}_m}(r_{mc}, r_{ms}) = \frac{1}{2\pi\sigma^2}\exp\left(-\frac{r_{mc}^2 + r_{ms}^2}{2\sigma^2}\right), \qquad m = 2, 3, \ldots, M \tag{5-4-36}$$

Let us make a change in variables in the joint pdfs given by (5-4-35) and (5-4-36). We define the normalized variables

$$R_m = \frac{\sqrt{r_{mc}^2 + r_{ms}^2}}{\sigma}$$
$$\Theta_m = \tan^{-1}\frac{r_{ms}}{r_{mc}} \tag{5-4-37}$$

Clearly, $r_{mc} = \sigma R_m \cos\Theta_m$ and $r_{ms} = \sigma R_m \sin\Theta_m$. The Jacobian of this transformation is

$$|\mathbf{J}| = \begin{vmatrix} \sigma\cos\Theta_m & \sigma\sin\Theta_m \\ -\sigma R_m \sin\Theta_m & \sigma R_m \cos\Theta_m \end{vmatrix} = \sigma^2 R_m \tag{5-4-38}$$

Consequently,

$$p(R_1, \Theta_1) = \frac{R_1}{2\pi}\exp\left[-\frac{1}{2}\left(R_1^2 + \frac{2\mathscr{E}_s}{N_0}\right)\right] I_0\left(\sqrt{\frac{2\mathscr{E}_s}{N_0}}\,R_1\right) \tag{5-4-39}$$

$$p(R_m, \Theta_m) = \frac{R_m}{2\pi}\exp\left(-\tfrac{1}{2}R_m^2\right), \qquad m = 2, 3, \ldots, M \tag{5-4-40}$$

Finally, by averaging $p(R_m, \Theta_m)$ over Θ_m, the factor of 2π is eliminated from (5-4-39) and (5-4-40). Thus, we find that R_1 has a Rice probability distribution and R_m, $m = 2, 3, \ldots, M$, are each Rayleigh-distributed.

The probability of a correct decision is simply the probability that $R_1 > R_2$, and $R_1 > R_3, \ldots$, and $R_1 > R_M$. Hence,

$$\begin{aligned} P_c &= P(R_2 < R_1, R_3 < R_1, \ldots, R_M < R_1) \\ &= \int_0^\infty P(R_2 < R_1, R_3 < R_1, \ldots, R_M < R_1 \mid R_1 = x) p_{R_1}(x)\, dx \end{aligned} \tag{5-4-41}$$

Because the random variables R_m, $m = 2, 3, \ldots, M$, are statistically iid, the joint probability in (5-4-41) conditioned on R_1 factors into a product of $M - 1$ identical terms. Thus,

$$P_c = \int_0^\infty [P(R_2 < R_1 \mid R_1 = x)]^{M-1} p_{R_1}(x)\, dx \tag{5-4-42}$$

where

$$\begin{aligned} P(R_2 < R_1 \mid R_1 = x) &= \int_0^x p_{R_2}(r_2)\, dr_2 \\ &= 1 - e^{-x^2/2} \end{aligned} \tag{5-4-43}$$

The $(M-1)$th power of (5-4-43) may be expressed as

$$(1 - e^{-x^2/2})^{M-1} = \sum_{n=0}^{M-1} (-1)^n \binom{M-1}{n} e^{-nx^2/2} \tag{5-4-44}$$

Substitution of this result into (5-4-42) and integration over x yields the probability of a correct decision as

$$P_C = \sum_{n=0}^{M-1} (-1)^n \binom{M-1}{n} \frac{1}{n+1} \exp\left[-\frac{n\mathscr{E}_s}{(n+1)N_0}\right] \tag{5-4-45}$$

where $\mathscr{E}_s/N_0$ is the SNR per symbol. Then, the probability of a symbol error, which is $P_M = 1 - P_C$, becomes

$$P_M = \sum_{n=1}^{M-1} (-1)^{n+1} \binom{M-1}{n} \frac{1}{n+1} \exp\left[-\frac{nk\mathscr{E}_b}{(n+1)N_0}\right] \tag{5-4-46}$$

where $\mathscr{E}_b/N_0$ is the SNR per bit.

For binary orthogonal signals ($M = 2$), (5-4-46) reduces to the simple form

$$P_2 = \tfrac{1}{2} e^{-\mathscr{E}_b/2N_0} \tag{5-4-47}$$

For $M > 2$, we may compute the probability of a bit error by making use of the relationship

$$P_b = \frac{2^{k-1}}{2^k - 1} P_M \tag{5-4-48}$$

which was established in Section 5-2. Figure 5-4-5 shows the bit-error probability as a function of the SNR per bit γ_b for $M = 2$, 4, 8, 16, and 32. Just as in the case of coherent detection of M-ary orthogonal signals (see Section 5-2-2), we observe that for any given bit-error probability, the SNR per bit decreases as M increases. It will be shown in Chapter 7 that, in the limit as $M \to \infty$ (or $k = \log_2 M \to \infty$), the probability of a bit error P_b can be made

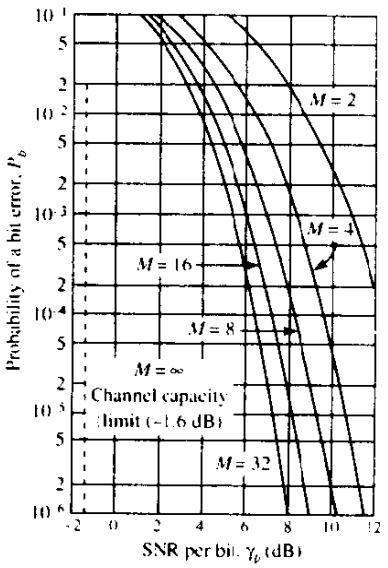

FIGURE 5-4-5 Probability of a bit error for noncoherent detection of orthogonal signals.

arbitrarily small provided that the SNR per bit is greater than the Shannon limit of -1.6 dB. The cost for increasing M is the bandwidth required to transmit the signals. For M-ary FSK, the frequency separation between adjacent frequencies is $\Delta f = 1/T$ for signal orthogonality. The bandwidth required for the M signals is $W = M\,\Delta f = M/T$. Also, the bit rate is $R = k/T$, where $k = \log_2 M$. Therefore, the bit-rate-to-bandwidth ratio is

$$\frac{R}{W} = \frac{\log_2 M}{M} \tag{5-4-49}$$

5-4-4 Probability of Error for Envelope Detection of Correlated Binary Signals

In this section, we consider the performance of the envelope detector for binary, equal-energy correlated signals. When the two signals are correlated, the input to the detector are the complex-valued random variables given by (5-4-10). We assume that the detector bases its decision on the envelopes $|r_1|$ and $|r_2|$, which are correlated (statistically dependent). The marginal pdfs of $R_1 = |r_1|$ and $R_2 = |r_2|$ are Ricean distributed, and may be expressed as

$$p(R_m) = \begin{cases} \dfrac{R_m}{2\mathscr{E}N_0} \exp\left(-\dfrac{R_m^2 + \beta_m^2}{4\mathscr{E}N_0}\right) I_0\left(\dfrac{\beta_m R_m}{2\mathscr{E}N_0}\right) & (R_m > 0) \\ 0 & (R_m < 0) \end{cases} \tag{5-4-50}$$

$m = 1, 2$, where $\beta_1 = 2\mathscr{E}$ and $\beta_2 = 2\mathscr{E}|\rho|$, based on the assumption that signal $s_1(t)$ was transmitted.

Since R_1 and R_2 are statistically dependent as a consequence of the nonorthogonality of the signals, the probability of error may be obtained by evaluating the double integral

$$P_b = P(R_2 > R_1) = \int_0^\infty \int_{x_1}^\infty p(x_1, x_2)\, dx_1\, dx_2 \tag{5-4-51}$$

where $p(x_1, x_2)$ is the joint pdf of the envelopes R_1 and R_2. This approach was first used by Helstrom (1955), who determined the joint pdf of R_1 and R_2 and evaluated the double integral in (5-4-51).

An alternative approach is based on the observation that the probability of error may also be expressed as

$$P_b = P(R_2 > R_1) = P(R_2^2 > R_1^2) = P(R_2^2 - R_1^2 > 0) \tag{5-4-52}$$

But $R_2^2 - R_1^2$ is a special case of a general quadratic form in complex-valued gaussian random variables, treated later in Appendix B. For the special case under consideration, the derivation yields the error probability in the form

$$P_b = Q_1(a, b) - \tfrac{1}{2} e^{-(a^2+b^2)/2} I_0(ab) \tag{5-4-53}$$

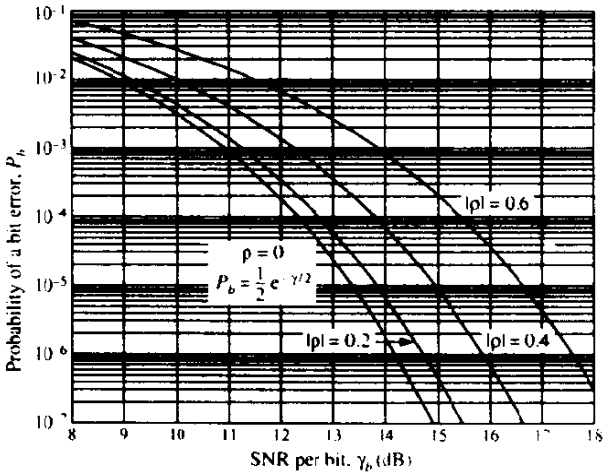

FIGURE 5-4-6 Probability of error for noncoherent detection.

where

$$a = \sqrt{\frac{\mathscr{E}_b}{2N_0}(1 - \sqrt{1 - |\rho|^2})}$$
$$b = \sqrt{\frac{\mathscr{E}_b}{2N_0}(1 + \sqrt{1 - |\rho|^2})} \tag{5-4-54}$$

$Q_1(a, b)$ is the Q function defined in (2-1-123) and $I_0(x)$ is the modified Bessel function of order zero.

The error probability P_b is illustrated in Fig. 5-4-6 for several values of $|\rho|$. P_b is minimized when $\rho = 0$; that is, when the signals are orthogonal. For this case, $a = 0$, $b = \sqrt{\mathscr{E}_b/N_0}$, and (5-4-53) reduces to

$$P_b = Q\left(0, \sqrt{\frac{\mathscr{E}_b}{N_0}}\right) - \tfrac{1}{2}e^{-\mathscr{E}_b/2N_0} \tag{5-4-55}$$

From the definition of $Q_1(a, b)$ in (2-1-123), it follows that

$$Q_1\left(0, \sqrt{\frac{\mathscr{E}_b}{N_0}}\right) = e^{-\mathscr{E}_b/2N_0}$$

Substitution of these relations into (5-4-55) yields the desired result given previously in (5-4-47). On the other hand, when $|\rho| = 1$, the error probability in (5-4-53) becomes $P_b = \frac{1}{2}$, as expected.

5-5 REGENERATIVE REPEATERS AND LINK BUDGET ANALYSIS

In the transmission of digital signals through an AWGN channel, we have observed that the performance of the communication system, measured in terms of the probability of error, depends solely on the received SNR, $\mathscr{E}_b/N_0$.

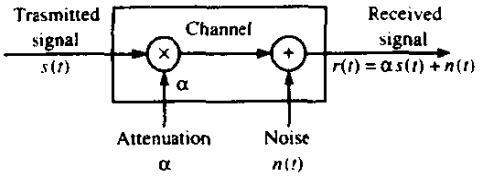

FIGURE 5-5-1 Mathematical model of channel with attenuation and additive noise.

where $\mathscr{E}_b$ is the transmitted energy per bit and $\frac{1}{2}N_0$ is the power spectral density of the additive noise. Hence, the additive noise ultimately limits the performance of the communication system.

In addition to the additive noise, another factor that affects the performance of a communication system is channel attenuation. All physical channels, including wire lines and radio channels, are lossy. Hence, the signal is attenuated as it travels through the channel. The simple mathematical model for the attenuation shown in Fig. 5-5-1 may be used for the channel. Consequently, if the transmitted signal is $s(t)$, the received signal, with $0 < \alpha \leq 1$ is

$$r(t) = \alpha s(t) + n(t) \tag{5-5-1}$$

Then, if the energy in the transmitted signal is $\mathscr{E}_b$, the energy in the received signal is $\alpha^2\mathscr{E}_b$. Consequently, the received signal has an SNR $\alpha^2\mathscr{E}_b/N_0$. Hence, the effect of signal attenuation is to reduce the energy in the received signal and thus to render the communication system more vulnerable to additive noise.

In analog communication systems, amplifiers called repeaters are used to periodically boost the signal strength in transmission through the channel. However, each amplifier also boosts the noise in the system. In contrast, digital communication systems allow us to detect and regenerate a clean (noise-free) signal in a transmission channel. Such devices, called *regenerative repeaters*, are frequently used in wireline and fiber optic communication channels.

5-5-1 Regenerative Repeaters

The front end of each regenerative repeater consists of a demodulator/detector that demodulates and detects the transmitted digital information sequence sent by the preceding repeater. Once detected, the sequence is passed to the transmitter side of the repeater, which maps the sequence into signal waveforms that are transmitted to the next repeater. This type of repeater is called a regenerative repeater.

Since a noise-free signal is regenerated at each repeater, the additive noise does not accumulate. However, when errors occur in the detector of a repeater, the errors are propagated forward to the following repeaters in the channel. To evaluate the effect of errors on the performance of the overall system, suppose that the modulation is binary PAM, so that the probability of

a bit error for one hop (signal transmission from one repeater to the next repeater in the chain) is

$$P_b = Q\left(\sqrt{\frac{2\mathscr{E}_b}{N_0}}\right)$$

Since errors occur with low probability, we may ignore the probability that any one bit will be detected incorrectly more than once in transmission through a channel with K repeaters. Consequently, the number of errors will increase linearly with the number of regenerative repeaters in the channel, and therefore, the overall probability of error may be approximated as

$$P_b \approx KQ\left(\sqrt{\frac{2\mathscr{E}_b}{N_0}}\right) \tag{5-5-2}$$

In contrast, the use of K analog repeaters in the channel reduces the received SNR by K, and hence, the bit error probability is

$$P_b \approx Q\left(\sqrt{\frac{2\mathscr{E}_b}{KN_0}}\right) \tag{5-5-3}$$

Clearly, for the same probability of error performance, the use of regenerative repeaters results in a significant saving in transmitter power compared with analog repeaters. Hence, in digital communication systems, regenerative repeaters are preferable. However, in wireline telephone channels that are used to transmit both analog and digital signals, analog repeaters are generally employed.

Example 5-5-1

A binary digital communication system transmits data over a wireline channel of length 1000 km. Repeaters are used every 10 km to offset the effect of channel attenuation. Let us determine the $\mathscr{E}_b/N_0$ that is required to achieve a probability of a bit error of 10^{-5} if (a) analog repeaters are employed, and (b) regenerative repeaters are employed.

The number of repeaters used in the system is $K = 100$. If regenerative repeaters are used, the $\mathscr{E}_b/N_0$ obtained from (5-5-2) is

$$10^{-5} = 100Q\left(\sqrt{\frac{2\mathscr{E}_b}{N_0}}\right)$$

$$10^{-7} = Q\left(\sqrt{\frac{2\mathscr{E}_b}{N_0}}\right)$$

which yields approximately 11.3 dB. If analog repeaters are used, the $\mathscr{E}_b/N_0$ obtained from (5-5-3) is

$$10^{-5} = Q\left(\sqrt{\frac{2\mathscr{E}_b}{100N_0}}\right)$$

which yields $\mathscr{E}_b/N_0 \approx 29.6$ dB. Hence, the difference in the required SNR is

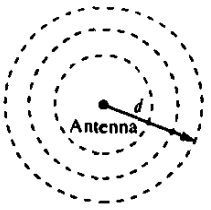

FIGURE 5-5-2 Isotropically radiating antenna.

about 18.3 dB, or approximately 70 times the transmitter power of the digital communication system.

5-5-2 Communication Link Budget Analysis

In the design of radio communications systems that transmit over line-of-sight microwave channels and satellite channels, the system designer must specify the size of the transmit and receive antennas, the transmitted power, and the SNR required to achieve a given level of performance at some desired data rate. The system design procedure is relatively straightforward and is outlined below.

Let us begin with a transmit antenna that radiates isotropically in free space at a power level of P_T watts as shown in Fig. 5-5-2. The power density at a distance d from the antenna is $P_T/4\pi d^2$ W/m^2. If the transmitting antenna has some directivity in a particular direction, the power density in that direction is increased by a factor called the antenna gain and denoted by G_T. In such a case, the power density at distance d is $P_T G_T/4\pi d^2$ W/m^2. The product $P_T G_T$ is usually called the *effective radiated power* (ERP or EIRP), which is basically the radiated power relative to an isotropic antenna, for which $G_T = 1$.

A receiving antenna pointed in the direction of the radiated power gathers a portion of the power that is proportional to its cross-sectional area. Hence, the received power extracted by the antenna may be expressed as

$$P_R = \frac{P_T G_T A_R}{4\pi d^2} \tag{5-5-4}$$

where A_R is the *effective area of the antenna.* From electromagnetic field theory, we obtain the basic relationship between the gain G_R of an antenna and its effective area as

$$A_R = \frac{G_R \lambda^2}{4\pi} \text{ m}^2 \tag{5-5-5}$$

where $\lambda = c/f$ is the wavelength of the transmitted signal, c is the speed of light (3×10^8 m/s), and f is the frequency of the transmitted signal.

If we substitute (5-5-5) for A_R into (5-5-4), we obtain an expression for the received power in the form

$$P_R = \frac{P_T G_T G_R}{(4\pi d/\lambda)^2} \tag{5-5-6}$$

The factor

$$L_s = \left(\frac{\lambda}{4\pi d}\right)^2 \tag{5-5-7}$$

is called the *free-space path loss*. If other losses, such as atmospheric losses, are encountered in the transmission of the signal, they may be accounted for by introducing an additional loss factor, say L_a. Therefore, the received power may be written in general as

$$P_R = P_T G_T G_R L_s L_a \tag{5-5-8}$$

As indicated above, the important characteristics of an antenna are its gain and its effective area. These generally depend on the wavelength of the radiated power and the physical dimensions of the antenna. For example, a parabolic (dish) antenna of diameter D has an effective area

$$A_R = \tfrac{1}{4}\pi D^2 \eta \tag{5-5-9}$$

where $\frac{1}{4}\pi D^2$ is the physical area and η is the *illumination efficiency factor*, which falls in the range $0.5 \leq \eta \leq 0.6$. Hence, the antenna gain for a parabolic antenna of diameter D is

$$G_R = \eta\left(\frac{\pi D}{\lambda}\right)^2 \tag{5-5-10}$$

As a second example, a horn antenna of physical area A has an efficiency factor of 0.8, an effective area of $A_R = 0.8A$, and an antenna gain of

$$G_R = \frac{10A}{\lambda^2} \tag{5-5-11}$$

Another parameter that is related to the gain (directivity) of an antenna is its beamwidth, which we denote as Θ_B and which is illustrated graphically in Fig. 5-5-3. Usually, the beamwidth is measured as the -3 dB width of the

FIGURE 5-5-3 Antenna beamwidth and pattern.

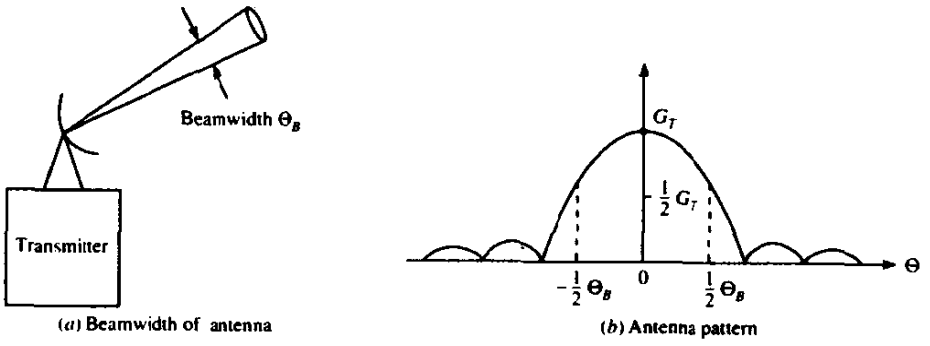

(*a*) Beamwidth of antenna

(*b*) Antenna pattern

antenna pattern. For example, the -3 dB beamwidth of a parabolic antenna is approximately

$$\Theta_B = 70(\lambda/D)^\circ \tag{5-5-12}$$

so that G_T is inversely proportional to Θ_B^2. That is, a decrease of the beamwidth by a factor of two, which is obtained by doubling the diameter D, increases the antenna gain by a factor of four (6 dB).

Based on the general relationship for the received signal power given by (5-5-8), the system designer can compute P_R from a specification of the antenna gains and the distance between the transmitter and the receiver. Such computations are usually done on a power basis, so that

$$(P_R)_{\text{dB}} = (P_T)_{\text{dB}} + (G_T)_{\text{dB}} + (G_R)_{\text{dB}} + (L_s)_{\text{dB}} + (L_a)_{\text{dB}} \tag{5-5-13}$$

Example 5-5-2

Suppose that we have a satellite in geosynchronous orbit (36 000 km above the earth's surface) that radiates 100 W of power, i.e., 20 dB above 1 W (20 dBW). The transmit antenna has a gain of 17 dB, so that the ERP = 37 dBW. Also, suppose that the earth station employs a 3 m parabolic antenna and that the downlink is operating at a frequency of 4 GHz. The efficiency factor is $\eta = 0.5$. By substituting these numbers into (5-5-10), we obtain the value of the antenna gain as 39 dB. The free-space path loss is

$$L_s = 195.6 \text{ dB}$$

No other losses are assumed. Therefore, the received signal power is

$$\begin{aligned}(P_R)_{\text{dB}} &= 20 + 17 + 39 - 195.6 \\ &= -119.6 \text{ dBW}\end{aligned}$$

or, equivalently,

$$P_R = 1.1 \times 10^{-12} \text{ W}$$

To complete the link budget computation, we must also consider the effect of the additive noise at the receiver front end. Thermal noise that arises at the receiver front end has a relatively flat power density spectrum up to about 10^{12} Hz, and is given as

$$N_0 = k_B T_0 \text{ W/Hz} \tag{5-5-14}$$

where k_B is Boltzmann's constant (1.38×10^{-23} W s/K) and T_0 is the noise temperature in Kelvin. Therefore, the total noise power in the signal bandwidth W is $N_0 W$.

The performance of the digital communications system is specified by the $\mathscr{E}_b/N_0$ required to keep the error rate performance below some given value. Since

$$\frac{\mathscr{E}_b}{N_0} = \frac{T_b P_R}{N_0} = \frac{1}{R}\frac{P_R}{N_0} \tag{5-5-15}$$

it follows that

$$\frac{P_R}{N_0} = R\left(\frac{\mathscr{E}_b}{N_0}\right)_{\text{req}} \tag{5-5-16}$$

where $(\mathscr{E}_b/N_0)_{\text{req}}$ is the required SNR per bit. Hence, if we have P_R/N_0 and the required SNR per bit, we can determine the maximum data rate that is possible.

Example 5-5-3

For the link considered in Example 5-5-2, the received signal power is

$$P_R = 1.1 \times 10^{-12}\,\text{W} \quad (-119.6\,\text{dBW})$$

Now, suppose the receiver front end has a noise temperature of 300 K, which is typical for receiver in the 4 GHz range. Then

$$N_0 = 4.1 \times 10^{-21}\,\text{W/Hz}$$

or, equivalently, −203.9 dBW/Hz. Therefore,

$$\frac{P_R}{N_0} = -119.6 + 203.9 = 84.3\,\text{dB Hz}$$

If the required SNR per bit is 10 dB then, from (5-5-16), we have the available rate as

$$\begin{aligned} R_{\text{dB}} &= 84.3 - 10 \\ &= 74.3\,\text{dB} \quad \text{(with respect to 1 bit/s)} \end{aligned}$$

This corresponds to a rate of 26.9 megabits/s, which is equivalent to about 420 PCM channels, each operating at 64 000 bits/s.

It is a good idea to introduce some safety margin, which we shall call the *link margin* M_{dB}, in the above computations for the capacity of the communication link. Typically, this may be selected as $M_{\text{dB}} = 6$ dB. Then, the link budget computation for the link capacity may be expressed in the simple form

$$\begin{aligned} R_{\text{dB}} &= \left(\frac{P_R}{N_0}\right)_{\text{dB Hz}} - \left(\frac{\mathscr{E}_b}{N_0}\right)_{\text{req}} - M_{\text{dB}} \\ &= (P_T)_{\text{dBW}} + (G_T)_{\text{dB}} + (G_R)_{\text{dB}} \\ &\quad + (L_a)_{\text{dB}} + (L_s)_{\text{dB}} - \left(\frac{\mathscr{E}_b}{N_0}\right)_{\text{req}} - M_{\text{db}} \end{aligned} \tag{5-5-17}$$

BIBLIOGRAPHICAL NOTES AND REFERENCES

In the derivation of the optimum demodulator for a signal corrupted by AWGN, we applied mathematical techniques that were originally used in deriving optimum receiver structures for radar signals. For example, the

matched filter was first proposed by North (1943) for use in radar detection, and is sometimes called the North filter. An alternative method for deriving the optimum demodulator and detector is the Karhunen–Loeve expansion, which is described in the classical texts by Davenport and Root (1958), Helstrom (1968), and Van Trees (1968). Its use in radar detection theory is described in the paper by Kelly *et al.* (1960). These detection methods are based on the hypothesis testing methods developed by statisticians, e.g., Neyman and Pearson (1933) and Wald (1947).

The geometric approach to signal design and detection, which was presented in the context of digital modulation and which has its roots in Shannon's original work, is conceptually appealing and is now widely used since its introduction in the text by Wozencraft and Jacobs (1965).

Design and analysis of signal constellations for the AWGN channel have received considerable attention in the technical literature. Of particular significance is the performance analysis of two-dimensional (QAM) signal constellations that has been treated in the papers of Cahn (1960), Hancock and Lucky (1960), Campopiano and Glazer (1962), Lucky and Hancock (1962), Salz *et al.* (1971), Simon and Smith (1973), Thomas *et al.* (1974), and Foschini *et al.* (1974). Signal design based on multidimensional signal constellations has been described and analyzed in the paper by Gersho and Lawrence (1984).

The Viterbi algorithm was devised by Viterbi (1967) for the purpose of decoding convolutional codes. Its use as the optimal maximum-likelihood sequence detection algorithm for signals with memory was described by Forney (1972) and Omura (1971). Its use for carrier modulated signals was considered by Ungerboeck (1974) and MacKenchnie (1973). It was subsequently applied to the demodulation of CPM by Aulin and Sundberg (1981a, b) and others.

PROBLEMS

5-1 A matched filter has the frequency response

$$H(f) = \frac{1 - e^{-j2\pi fT}}{j2\pi f}$$

a Determine the impulse response $h(t)$ corresponding to $H(f)$.
b Determine the signal waveform to which the filter characteristic is matched.

5-2 Consider the signal

$$s(t) = \begin{cases} (A/T)t \cos 2\pi f_c t & (0 \leq t \leq T) \\ 0 & \text{(otherwise)} \end{cases}$$

a Determine the impulse response of the matched filter for the signal.
b Determine the output of the matched filter at $t = T$.
c Suppose the signal $s(t)$ is passed through a correlator that correlates the input $s(t)$ with $s(t)$. Determine the value of the correlator output at $t = T$. Compare your result with that in (b).

5-3 This problem deals with the characteristics of a DPSK signal.

a Suppose we wish to transmit the data sequence

$$1\ 1\ 0\ 1\ 0\ 0\ 0\ 1\ 0\ 1\ 1\ 0$$

by binary DPSK Let $s(t) = A\cos(2\pi f_c t + \theta)$ represent the transmitted signal in any signaling interval of duration T. Give the phase of the transmitted signal for the data sequence. Begin with $\theta = 0$ for the phase of the first bit to be transmitted.

b If the data sequence is uncorrelated, determine and sketch the power density spectrum of the signal transmitted by DPSK.

5-4 A binary digital communication system employs the signals

$$s_0(t) = 0, \quad 0 \leq t \leq T$$
$$s_1(t) = A, \quad 0 \leq t \leq T$$

for transmitting the information. This is called *on–off signaling*. The demodulator cross-correlates the received signal $r(t)$ with $s(t)$ and samples the output of the correlator at $t = T$.

a Determine the optimum detector for an AWGN channel and the optimum threshold, assuming that the signals are equally probable.

b Determine the probability of error as a function of the SNR. How does on–off signaling compare with antipodal signaling?

5-5 The correlation metrics given by (5-1-44) are

$$C(\mathbf{r}, \mathbf{s}_m) = 2\sum_{n=1}^{N} r_n s_{mn} - \sum_{n=1}^{N} s_{mn}^2, \quad m = 1, 2, \ldots, M$$

where

$$r_n = \int_0^T r(t) f_n(t)\, dt$$
$$s_{mn} = \int_0^T s_m(t) f_n(t)\, dt$$

Show that the correlation metrics are equivalent to the metrics

$$C(\mathbf{r}, \mathbf{s}_m) = 2\int_0^T r(t) s_m(t)\, dt - \int_0^T s_m^2(t)\, dt$$

5-6 Consider the equivalent lowpass (complex-valued) signal $s_l(t)$, $0 \leq t \leq T$, with energy

$$\mathcal{E} = \frac{1}{2}\int_0^T |s_l(t)|^2\, dt$$

Suppose that this signal is corrupted by AWGN, which is represented by its equivalent lowpass form $z(t)$. Hence, the observed signal is

$$r_l(t) = s_l(t) + z(t), \quad 0 \leq t \leq T$$

The received signal is passed through a filter that has an (equivalent lowpass) impulse response $h_l(t)$. Determine $h_l(t)$ so that the filter maximizes the SNR at its output (at $t = T$).

5-7 Let $z(t) = x(t) + jy(t)$ be a complex-valued, zero-mean white gaussian noise

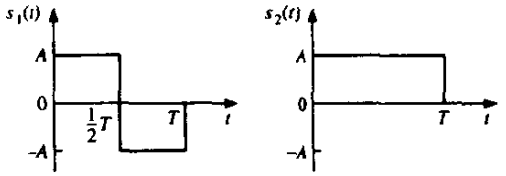

FIGURE P5-8

process with autocorrelation function $\phi_{zz}(\tau) = N_0\delta(\tau)$. Let $f_m(t)$, $m = 1, 2, \ldots, M$, be a set of M orthogonal equivalent lowpass waveforms defined on the interval $0 \leq t \leq T$. Define

$$N_{mr} = \text{Re}\left[\int_0^T z(t)f_m^*(t)\,dt\right], \quad m = 1, 2, \ldots, M$$

a Determine the variance of N_{mr}.
b Show that $E(N_{mr}N_{kr}) = 0$ for $k \neq m$.

5-8 The two equivalent lowpass signals shown in Fig. P5-8 are used to transmit a binary sequence over an additive white gaussian noise channel. The received signal can be expressed as

$$r_i(t) = s_i(t) + z(t), \quad 0 \leq t \leq T, \quad i = 1, 2$$

where $z(t)$ is a zero-mean gaussian noise process with autocorrelation function

$$\phi_{zz}(\tau) = \tfrac{1}{2}E[z^*(t)z(t+\tau)] = N_0\delta(\tau)$$

a Determine the transmitted energy in $s_1(t)$ and $s_2(t)$ and the cross-correlation coefficient ρ_{12}.
b Suppose the receiver is implemented by means of coherent detection using two matched filters, one matched to $s_1(t)$ and the other to $s_2(t)$. Sketch the equivalent lowpass impulse responses of the matched filters.
c Sketch the noise-free response of the two matched filters when the transmitted signal is $s_2(t)$.
d Suppose the receiver is implemented by means of two cross-correlators (multipliers followed by integrators) in parallel. Sketch the output of each integrator as a function of time for the interval $0 \leq t \leq T$ when the transmitted signal is $s_2(t)$.
e Compare the sketches in (c) and (d). Are they the same? Explain briefly.
f From your knowledge of the signal characteristics, give the probability of error for this binary communications system.

5-9 Suppose that we have a complex-valued gaussian random variable $z = x + jy$, where (x, y) are statistically independent variables with zero mean and variance $E(x^2) = E(y^2) = \sigma^2$. Let

$$r = z + m, \quad \text{where } m = m_r + jm_i$$

and define r as

$$r = a + jb$$

Clearly, $a = x + m_r$ and $b = y + m_i$. Determine the following probability density functions:
a $p(a, b)$;

b $p(u, \phi)$, where $u = \sqrt{a^2 + b^2}$ and $\phi = \tan^{-1} b/a$;
c $p(u)$.

Note: In (b) it is convenient to define $\theta = \tan^{-1}(m_i/m_r)$ so that

$$m_i = \sqrt{m_r^2 + m_i^2}\cos\theta, \qquad m_i = \sqrt{m_r^2 + m_i^2}\sin\theta.$$

Furthermore, you must use the relation

$$\frac{1}{2\pi}\int_0^{2\pi} e^{\alpha\cos(\phi-\theta)}\,d\phi = I_0(\alpha) = \sum_{n=0}^{\infty}\frac{\alpha^{2n}}{2^{2n}(n!)^2}$$

where $I_0(\alpha)$ is the modified Bessel function of order zero.

5-10 A ternary communication system transmits one of three signals, $s(t)$, 0, or $-s(t)$, every T seconds. The received signal is either $r_1(t) = s(t) + z(t)$, $r_1(t) = z(t)$, or $r_1(t) = -s(t) + z(t)$, where $z(t)$ is white gaussian noise with $E(z(t)] = 0$ and $\phi_{zz}(\tau) = \frac{1}{2}E[z(t)z^*(\tau)] = N_0\delta(t-\tau)$. The optimum receiver computes the correlation metric

$$U = \mathrm{Re}\left[\int_0^T r(t)s^*(t)\,dt\right]$$

and compares U with a threshold A and a threshold $-A$. If $U > A$, the decision is made that $s(t)$ was sent. If $U < -A$, the decision is made in favor of $-s(t)$. If $-A < U < A$, the decision is made in favor of 0.

a Determine the three conditional probabilities of error, P_e given that $s(t)$ was sent, P_e given that $-s(t)$ was sent, and P_e given that 0 was sent.
b Determine the average probability of error P_e as a function of the threshold A, assuming that the three symbols are equally probable a priori.
c Determine the value of A that minimizes P_e.

5-11 The two equivalent lowpass signals shown in Fig. P5-11 are used to transmit a binary information sequence. The transmitted signals, which are equally probable, are corrupted by additive zero-mean white gaussian noise having an equivalent lowpass representation $z(t)$ with an autocorrelation function

$$\begin{aligned}\phi_{zz}(\tau) &= \tfrac{1}{2}E[z^*(t)z(t+\tau)]\\ &= N_0\delta(\tau)\end{aligned}$$

a What is the transmitted signal energy?
b What is the probability of a binary digit error if coherent detection is employed at the receiver?
c What is the probability of a binary digit error if noncoherent detection is employed at the receiver?

5-12 In Section 4-3-1 it was shown that the minimum frequency separation for orthogonality of binary FSK signals with coherent detection is $\Delta f = 1/2T$.

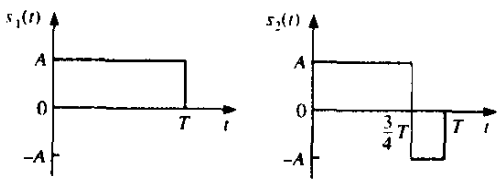

FIGURE P5-11

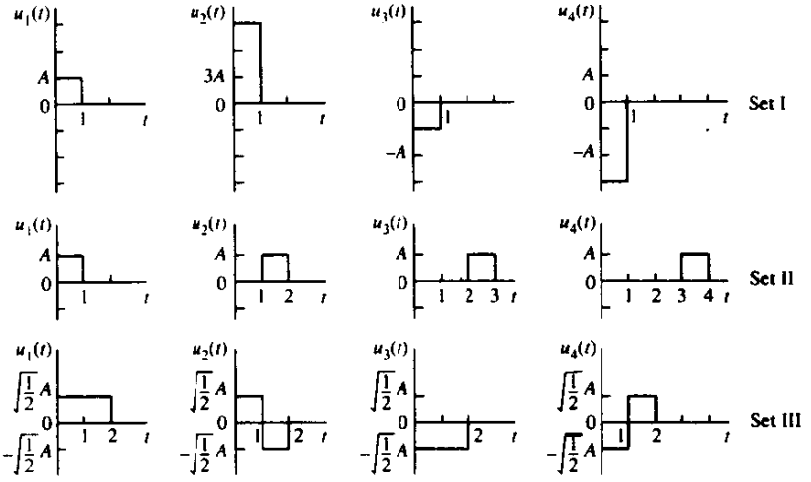

FIGURE P5-13

However, a lower error probability is possible with coherent detection of FSK if Δf is increased beyond $1/2T$. Show that the optimum value of Δf is $0.715/T$ and determine the probability of error for this value of Δf.

5-13 The equivalent lowpass waveforms for three signal sets are shown in Fig. P5-13. Each set may be used to transmit one of four equally probable messages over an additive white gaussian noise channel. The equivalent lowpass noise $z(t)$ has zero mean and autocorrelation function $\phi_{zz}(\tau) = N_0\delta(\tau)$.

- **a** Classify the signal waveforms in sets I, II, and III. In other words, state the category or class to which each signal set belongs.
- **b** What is the *average* transmitted energy for each signal set?
- **c** For signal set I, specify the average probability of error if the signals are detected coherently.
- **d** For signal set II, give a union bound on the probability of a symbol error if the detection is performed (i) coherently and (ii) noncoherently.
- **e** Is it possible to use noncoherent detection on signal set III? Explain.
- **f** Which signal set or signal sets would you select if you wished to achieve a ratio of bit rate to bandwidth (R/W) of at least 2. *Briefly* explain your answer.

5-14 Consider a quaternary ($M = 4$) communication system that transmits, every T seconds, one of four equally probable signals: $s_1(t)$, $-s_1(t)$, $s_2(t)$, $-s_2(t)$. The signals $s_1(t)$ and $s_2(t)$ are orthogonal with equal energy. The additive noise is white gaussian with zero mean and autocorrelation function $\phi_{zz}(\tau) = N_0\delta(\tau)$. The demodulator consists of two filters matched to $s_1(t)$ and $s_2(t)$, and their outputs at the sampling instant are U_1 and U_2. The detector bases its decision on the following rule:

$$U_1 > |U_2| \Rightarrow s_1(t), \qquad U_1 < -|U_2| \Rightarrow -s_1(t)$$
$$U_2 > |U_1| \Rightarrow s_2(t), \qquad U_2 < -|U_1| \Rightarrow -s_2(t)$$

Since the signal set is biorthogonal, the error probability is given by $(1 - P_c)$ where P_c is given by (5-2-34). Express this error probability in terms of a single integral

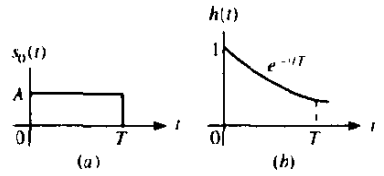

FIGURE P5-15

and, thus, show that the symbol error probability for a biorthogonal signal set with $M = 4$ is identical to that for four-phase PSK. *Hint*: A change in variables from U_1 and U_2 to $W_1 = U_1 + U_2$ and $W_2 = U_1 - U_2$ simplifies the problem.

5-15 The input $s(t)$ to a bandpass filter is

$$s(t) = \text{Re}\,[s_0(t)e^{j2\pi f_c t}]$$

where $s_0(t)$ is a rectangular pulse as shown in Fig. P5-15(a).

a Determine the output $y(t)$ of the bandpass filter for all $t \geq 0$ if the impulse response of the filter is

$$g(t) = \text{Re}\,[2h(t)e^{j2\pi f_c t}]$$

where $h(t)$ is an exponential as shown in Fig. 5-15(b).

b Sketch the *equivalent lowpass output* of the filter.

c When would you sample the output of the filter if you wished to have the maximum output at the sampling instant? What is the value of the maximum output?

d Suppose that in addition to the input signal $s(t)$, there is additive white gaussian noise

$$n(t) = \text{Re}\,[z(t)e^{j2\pi f_c t}]$$

where $\phi_{zz}(\tau) = N_0\delta(\tau)$. At the sampling instant determined in (c), the signal sample is corrupted by an additive gaussian noise term. Determine its mean and variance.

e What is the signal-to-noise ratio γ of the sampled output?

f Determine the signal-to-noise ratio when $h(t)$ is the matched filter to $s(t)$ and compare this result with the value of γ obtained in (e).

5-16 Consider the octal signal point constellations in Fig. P5-16.

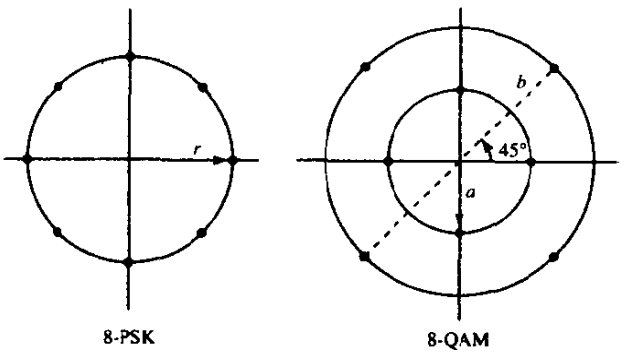

FIGURE P5-16

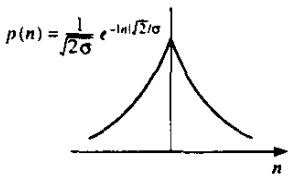

FIGURE P5-19

a The nearest-neighbor signal points in the 8-QAM signal constellation are separated in distance by A units. Determine the radii a and b of the inner and outer circles.

b The adjacent signal points in the 8-PSK are separated by a distance of A units. Determine the radius r of the circle.

c Determine the average transmitter powers for the two signal constellations and compare the two powers. What is the relative power advantage of one constellation over the other? (Assume that all signal points are equally probable.)

5-17 Consider the 8-point QAM signal constellation shown in Fig. P5-16.

a Is it possible to assign three data bits to each point of the signal constellation such that nearest (adjacent) points differ in only one bit position?

b Determine the symbol rate if the desired bit rate is 90 Mbits/s.

5-18 Suppose that binary PSK is used for transmitting information over an AWGN with a power spectral density of $\frac{1}{2}N_0 = 10^{-10}$ W/Hz. The transmitted signal energy is $\mathscr{E}_b = \frac{1}{2}A^2T$, where T is the bit interval and A is the signal amplitude. Determine the signal amplitude required to achieve an error probability of 10^{-6} when the data rate is (a) 10 kbits/s, (b) 100 kbits/s, and (c) 1 Mbit/s.

5-19 Consider a signal detector with an input

$$r = \pm A + n$$

where $+A$ and $-A$ occur with equal probability and the noise variable n is characterized by the (Laplacian) pdf shown in Fig. P5-19.

a Determine the probability of error as a function of the parameters A and σ

b Determine the SNR required to achieve an error probability of 10^{-5}. How does the SNR compare with the result for a Gaussian pdf?

5-20 Consider the two 8-point QAM signal constellations shown in Fig. P5-20. The minimum distance between adjacent points is $2A$. Determine the average transmitted power for each constellation, assuming that the signal points are equally probable. Which constellation is more power-efficient?

5-21 For the QAM signal constellation shown in Fig. P5-21, determine the optimum decision boundaries for the detector, assuming that the SNR is sufficiently high so that errors only occur between adjacent points.

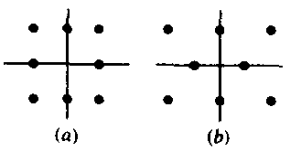

FIGURE P5-20

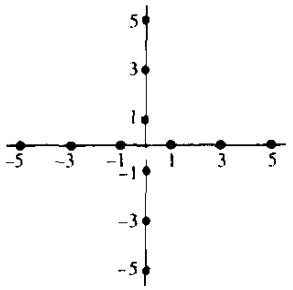

FIGURE P5-21

5-22 Specify a Gray code for the 16-QAM signal constellation shown in Fig. P5-21.

5-23 Two quadrature carriers $\cos 2\pi f_c t$ and $\sin 2\pi f_c t$ are used to transmit digital information through an AWGN channel at two different data rates, 10 kbits/s and 100 kbits/s. Determine the relative amplitudes of the signals for the two carriers so that the $\mathscr{E}_b/N_b$ for the two channels is identical.

5-24 Three messages m_1, m_2, and m_3 are to be transmitted over an AWGN channel with noise power spectral density $\frac{1}{2}N_0$. The messages are

$$s_1(t) = \begin{cases} 1 & (0 \leq t \leq T) \\ 0 & (\text{otherwise}) \end{cases}$$

$$s_2(t) = -s_3(t) = \begin{cases} 1 & (0 \leq t \leq \frac{1}{2}T) \\ -1 & (\frac{1}{2}T \leq 0 \leq T) \\ 0 & (\text{otherwise}) \end{cases}$$

a What is the dimensionality of the signal space?

b Find an appropriate basis for the signal space. [*Hint:* You can find the basis without using the Gram–Schmidt procedure.]

c Draw the signal constellation for this problem.

d Derive and sketch the optimal decision regions R_1, R_2, and R_3.

e Which of the three messages is more vulnerable to errors and why? In other words, which of $P(\text{error} \mid m_i \text{ transmitted})$, $i = 1, 2, 3$, is larger?

5-25 When the additive noise at the input to the demodulator is colored, the filter matched to the signal no longer maximizes the output SNR. In such a case we may consider the use of a prefilter that "whitens" the colored noise. The prefilter is followed by a filter matched to the prefiltered signal. Towards this end, consider the configuration shown in Fig. P5-25.

a Determine the frequency response characteristic of the prefilter that whitens the noise.

FIGURE P5-25

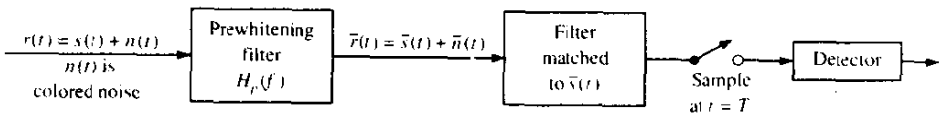

b Determine the frequency response characteristic of the filter matched to $\tilde{s}(t)$.
c Consider the prefilter and the matched filter as a single "generalized matched filter." What is the frequency response characteristic of this filter?
d Determine the SNR at the input to the detector.

5-26 Consider a digital communication system that transmits information via QAM over a voice-band telephone channel at a rate 2400 symbols/s. The additive noise is assumed to be white and gaussian.
a Determine the $\mathscr{E}_b/N_0$ required to achieve an error probability of 10^{-5} at 4800 bits/s.
b Repeat (a) for a rate of 9600 bits/s.
c Repeat (a) for a rate of 19 200 bits/s.
d What conclusions do you reach from these results?

5-27 Consider the four-phase and eight-phase signal constellations shown in Fig. P5-27. Determine the radii r_1 and r_2 of the circles such that the distance between two adjacent points in the two constellations is d. From this result, determine the additional transmitted energy required in the 8-PSK signal to achieve the same error probability as the four-phase signal at high SNR, where the probability of error is determined by errors in selecting adjacent points.

5-28 Digital information is to be transmitted by carrier modulation through an additive gaussian noise channel with a bandwidth of 100 kHz and $N_0 = 10^{-10}$ W/Hz. Determine the maximum rate that can be transmitted through the channel for four-phase PSK, binary FSK, and four-frequency orthogonal FSK, which is detected noncoherently.

5-29 In a MSK signal, the initial state for the phase is either 0 or π rad. Determine the terminal phase state for the following four input pairs of input data: (a) 00; (b) 01; (c) 10; (d) 11.

5-30 A continuous-phase FSK signal with $h = \frac{1}{2}$ is represented as

$$s(t) = \pm\sqrt{\frac{2\mathscr{E}_b}{T_b}}\cos\left(\frac{\pi t}{2T_b}\right)\cos 2\pi f_c t \pm \sqrt{\frac{2\mathscr{E}_b}{T_b}}\sin\left(\frac{\pi t}{2T_b}\right)\sin 2\pi f_c t, \qquad 0 \le t \le 2T_b$$

where the $\pm$ signs depend on the information bits transmitted.
a Show that this signal has constant amplitude.
b Sketch a block diagram of the modulator for synthesizing the signal.
c Sketch a block diagram of the demodulator and detector for recovering the information.

5-31 Sketch the phase tree, the state trellis, and the state diagram for partial-response CPM with $h = \frac{1}{2}$ and

$$u(t) = \begin{cases} 1/4T & (0 \le t \le 2T) \\ 0 & (\text{otherwise}) \end{cases}$$

FIGURE P5-27

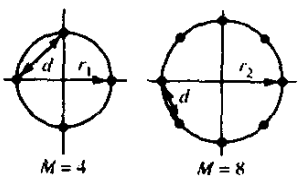

5-32 Determine the number of terminal phase states in the state trellis diagram for (a) a full response binary CPFSK with either $h = \frac{2}{3}$ or $\frac{3}{4}$ and (b) a partial-response $L = 3$ binary CPFSK with either $h = \frac{2}{3}$ or $\frac{3}{4}$.

5-33 Consider a biorthogonal signal set with $M = 8$ signal points. Determine a union bound for the probability of a symbol error as a function of $\mathscr{E}_b/N_0$. The signal points are equally likely a priori.

5-34 Consider an M-ary digital communication system where $M = 2^N$, and N is the dimension of the signal space. Suppose that the M signal vectors lie on the vertices of a hypercube that is centered at the origin. Determine the average probability of a symbol error as a function of $\mathscr{E}_s/N_0$ where $\mathscr{E}_s$ is the energy per symbol, $\frac{1}{2}N_0$ is the power spectral density of the AWGN, and all signal points are equally probable.

5-35 Consider the signal waveform

$$s(t) = \sum_{i=1}^{n} c_i p(t - kT_c)$$

where $p(t)$ is a rectangular pulse of unit amplitude and duration T_c. The $\{c_i\}$ may be viewed as a code vector $\mathbf{C} = [c_1 \ c_2 \ \dots \ c_n]$, where the elements $c_i = \pm 1$. Show that the filter matched to the waveform $s(t)$ may be realized as a cascade of a filter matched to $p(t)$ followed by a discrete-time filter matched to the vector $\mathbf{C}$. Determine the value of the output of the matched filter at the sampling instant $t = nT_c$.

5-36 A speech signal is sampled at a rate of 8 kHz, logarithmically compressed and encoded into a PCM format using 8 bits/sample. The PCM data is transmitted through an AWGN baseband channel via M-level PAM. Determine the bandwidth required for transmission when (a) $M = 4$, (b) $M = 8$, and (c) $M = 16$.

5-37 A Hadamard matrix is defined as a matrix whose elements are ± 1 and whose row vectors are pairwise orthogonal. In the case when n is a power of 2, an $n \times n$ Hadamard matrix is constructed by means of the recursion

$$\mathbf{H}_2 = \begin{bmatrix} 1 & 1 \\ 1 & -1 \end{bmatrix}, \quad \mathbf{H}_{2n} = \begin{bmatrix} \mathbf{H}_n & \mathbf{H}_n \\ \mathbf{H}_n & -\mathbf{H}_n \end{bmatrix}$$

a Let $\mathbf{C}_i$ denote the ith row of an $n \times n$ Hadamard matrix as defined above. Show that the waveforms constructed as

$$s_i(t) = \sum_{k=1}^{n} c_{ik} p(t - kT_c), \quad i = 1, 2, \dots, n$$

are orthogonal, where $p(t)$ is an arbitrary pulse confined to the time interval $0 \le t \le T_c$.

b Show that the matched filters (or cross-correlators) for the n waveforms $\{s_i(t)\}$ can be realized by a single filter (or correlator) matched to the pulse $p(t)$ followed by a set of n cross-correlators using the code words $\{\mathbf{C}_i\}$.

5-38 The discrete sequence

$$r_k = \sqrt{\mathscr{E}_b} c_k + n_k, \quad k = 1, 2, \dots, n$$

represents the output sequence of samples from a demodulator, where $c_k = \pm 1$ are elements of one of two possible code words, $\mathbf{C}_1 = [1 \ 1 \ \dots \ 1]$ and $\mathbf{C}_2 = [1 \ 1 \ \dots \ 1 \ -1 \ \dots \ -1]$. The code word $\mathbf{C}_2$ has w elements that are $+1$ and $n - w$

elements that are -1, where w is some positive integer. The noise sequence $\{n_k\}$ is white gaussian with variance σ^2.

a What is the optimum maximum likelihood detector for the two possible transmitted signals?

b Determine the probability of error as a function of the parameters (σ^2, $\mathscr{E}_b$, w).

c What is the value of w that minimizes the error probability?

5-39 Derive the outputs r_1 and r_2 of the two correlators shown in Fig. 5-4-1. Assume that a signal $s_{l1}(t)$ is transmitted and that

$$r_l(t) = s_{l1}(t)e^{j\phi} + z(t)$$

where $z(t) = n_c(t) + jn_s(t)$ is the additive gaussian noise.

5-40 Determine the covariances and variances of the gaussian random noise variables n_{1c}, n_{2c}, n_{1s}, and n_{2s} in (5-4-15) and the joint pdf.

5-41 Derive the matched filter outputs given by (5-4-10).

5-42 In on–off keying of a carrier-modulated signal, the two possible signals are

$$s_0(t) = 0, \quad 0 \le t \le T_b$$

$$s_1(t) = \sqrt{\frac{2\mathscr{E}_b}{T_b}} \cos 2\pi f_c t, \quad 0 \le t \le T_b$$

The corresponding received signals are

$$r(t) = n(t), \quad 0 \le t \le T_b$$

$$r(t) = \sqrt{\frac{2\mathscr{E}_b}{T_b}} \cos (2\pi f_c t + \phi) + n(t), \quad 0 \le t \le T_b$$

where ϕ is the carrier phase and $n(t)$ is AWGN.

a Sketch a block diagram of the receiver (demodulator and detector) that employs noncoherent (envelope) detection.

b Determine the pdfs for the two possible decision variables at the detector corresponding to the two possible received signals.

c Derive the probability of error for the detector.

5-43 In two-phase DPSK, the received signal in one signaling interval is used as a phase reference for the received signal in the following signaling interval. The decision variable is

$$D = \operatorname{Re}(V_m V_{m-1}^*) \underset{\text{"0"}}{\overset{\text{"1"}}{\gtrless}} 0$$

$$V_k = 2\alpha\mathscr{E}e^{j(\theta_k - \phi)} + N_k$$

represents the complex-valued output of the filter matched to the transmitted signal $u(t)$. N_k is a complex-valued gaussian variable having zero mean and statistically independent components.

a Writing $V_k = X_k + jY_k$, show that D is equivalent to

$$d = [\tfrac{1}{2}(X_m + X_{m-1})]^2 + [\tfrac{1}{2}(Y_m + Y_{m-1})]^2 - [\tfrac{1}{2}(X_m - X_{m-1})]^2 - [\tfrac{1}{2}(Y_m - Y_{m-1})]^2$$

b For mathematical convenience; suppose that $\theta_k = \theta_{k-1}$. Show that the random variables U_1, U_2, U_3, and U_4 are statistically independent gaussian variables, where $U_1 = \frac{1}{2}(X_m + X_{m-1})$, $U_2 = \frac{1}{2}(Y_m + Y_{m-1})$, $U_3 = \frac{1}{2}(X_m - X_{m-1})$, and $U_4 = \frac{1}{2}(Y_m - Y_{m-1})$.

c Define the random variables $W_1 = U_1^2 + U_2^2$ and $W_2 = U_3^2 + U_4^2$. Then

$$D = W_1 - W_2 \gtrless 0$$

Determine the probability density functions for W_1 and W_2.

d Determine the probability of error P_b, where

$$P_b = P(D < 0) = P(W_1 - W_2 < 0) = \int_0^\infty P(W_2 > w_1 \mid w_1) p(w_1)\, dw_1$$

5-44 Recall that MSK can be represented as a four-phase offset PSK modulation having the lowpass equivalent form

$$v(t) = \sum_k [I_k u(t - 2kT_b) + jJ_k u(t - 2kT_b - T_b)]$$

where

$$u(t) = \begin{cases} \sin(\pi t/2T_b) & (0 \leq t \leq 2T_b) \\ 0 & (\text{otherwise}) \end{cases}$$

and $\{I_k\}$ and $\{J_k\}$ are sequences of information symbols (± 1).

a Sketch the block diagram of an MSK demodulator for offset QPSK.

b Evaluate the performance of the four-phase demodulator for AWGN if no account is taken of the memory in the modulation.

c Compare the performance obtained in (b) with that for Viterbi decoding of the MSK signal.

d The MSK signal is also equivalent to binary FSK. Determine the performance of noncoherent detection of the MSK signal. Compare your result with (b) and (c).

5-45 Consider a transmission line channel that employs $n - 1$ regenerative repeaters plus the terminal receiver in the transmission of binary information. Assume that the probability or error at the detector of each receiver is p and that errors among repeaters are statistically independent.

a Show that the binary error probability at the terminal receiver is

$$P_n = \tfrac{1}{2}[1 - (1 - 2p)^n]$$

b If $p = 10^{-6}$ and $n = 100$, determine an approximate value of P_n.

5-46 A digital communication system consists of a transmission line with 100 digital (regenerative) repeaters. Binary antipodal signals are used for transmitting the information. If the overall end-to-end error probability is 10^{-6}, determine the probability of error for each repeater and the required $\mathscr{E}_b/N_0$ to achieve this performance in AWGN.

5-47 A radio transmitter has a power output of $P_T = 1$ W at a frequency of 1 GHz. The transmitting and receiving antennas are parabolic dishes with diameter $D = 3$ m.

a Determine the antenna gains.

b Determine the EIRP for the transmitter.

c The distance (free space) between the transmitting and receiving antennas is 20 km. Determine the signal power at the output of the receiving antenna in dBm.

5-48 A radio communication system transmits at a power level of 0.1 W at 1 GHz. The transmitting and receiving antennas are parabolic, each having a diameter of 1 m. The receiver is located 30 km from the transmitter.
- **a** Determine the gains of the transmitting and receiving antennas.
- **b** Determine the EIRP of the transmitted signal.
- **c** Determine the signal power from the receiving antenna.

5-49 A satellite in synchronous orbit is used to communicate with an earth station at a distance of 40 000 km. The satellite has an antenna with a gain of 15 dB and a transmitter power of 3 W. The earth station uses a 10 m parabolic antenna with an efficiency of 0.6. The frequency band is at $f = 10$ GHz. Determine the received power level at the output of the receiver antenna.

5-50 A spacecraft located 100 000 km from the earth is sending data at a rate of R bits/s. The frequency band is centered at 2 GHz and the transmitted power is 10 W. The earth station uses a parabolic antenna, 50 m in diameter, and the spacecraft has an antenna with a gain of 10 dB. The noise temperature of the receiver front end is $T_0 = 300$ K.
- **a** Determine the received power level.
- **b** If the desired $\mathscr{E}_b/N_0 = 10$ dB, determine the maximum bit rate that the spacecraft can transmit.

5-51 A satellite in geosynchronous orbit is used as a regenerative repeater in a digital communication system. Consider the satellite-to-earth link in which the satellite antenna has a gain of 6 dB and the earth station antenna has a gain of 50 dB. The downlink is operated at a center frequency of 4 GHz, and the signal bandwidth is 1 MHz. If the required $\mathscr{E}_b/N_0$ for reliable communication is 15 dB, determine the transmitted power for the satellite downlink. Assume that $N_0 = 4.1 \times 10^{-21}$ W/Hz.